



Vrije Universiteit Brussel



FACULTY OF ENGINEERING

# Adaptation of continuous descent and climb operational techniques at Brussels Airport aiming at cost efficiency.

---

Author: Sam Peeters

---



Academic year 2012-2013

Master's thesis submitted under the supervision of Prof. Ir. Jean-Jacques Speyer, the co-supervision of Prof. Dr. Ir. Patrick Hendrick, in order to be awarded the Master's Degree of Applied Sciences and Engineering: Electro-Mechanical Engineering: Aeronautics



## Preface

First, I would like to thank Prof. Ir. Jean-Jacques Speyer (Airbus-retired) and Prof. Dr. Ir. Patrick Hendrick for providing this interesting Master thesis subject because air traffic management and all related subjects fascinate me. The continuous follow-up and extensive communication with Prof. Speyer was a great help to bring this Master thesis to a good end. I have also had a lot of help from people of the aviation industry. Many thanks go to Liesbeth Peeters, Paul Hopff and Carlo Vandersmissen of Belgocontrol for the good information, data and cooperation on several occasions. Thanks to the efforts of Carl-Philippe Combès and Tom Vaes of Thomas Cook Airlines, Rudolf Christen, CEO Aviaso and André Berger, Brecht Lievrouw and Laurens Wielfaert of Jetairfly, I could check my calculations against real flight data so again thank you for that. I have also very much appreciated the remarks and comments of Elmar Recker of the RMA and Capt. Peter Griffiths (EasyJet-retired) and Guglielmo Guastalla of Eurocontrol who have contributed to this work in a very positive way.

Last but not least, I thank my family for supporting me during this whole period and especially my girlfriend Kathleen for her patience and good care.

## **Legal notice**

This documentation, material or product has been created by using the V-PAT tool, makes reference to the V-PAT tool or contains software parts of the V-PAT tool. The V-PAT tool has been created and made available by the European Organisation for the Safety of Air Navigation (EUROCONTROL). EUROCONTROL is the exclusive owner of the V-PAT tool. All Rights reserved.

## Summaries

### English summary

This Master thesis: "Adaptation of continuous descent and climb operational techniques at Brussels Airport aiming at cost efficiency" was written by Sam Peeters in the academic year 2012-2013 in order to be awarded the Master's Degree of Applied Sciences and Engineering: Electro-Mechanical Engineering: Aeronautics.

Keywords:

Continuous descent operations, continuous climb operations, cost index, dynamic trajectory allocation, energy management

Abstract:

Continuous descent and climb operations aim at reducing the fuel burn and emissions during respectively the descent and climb phases. In this Master thesis, the optimal descent and climb profiles, based on the aircraft performance and the restrictions in the Belgian airspace, are calculated using the BADA database of Eurocontrol.

The optimal descent profiles are calculated by determining the ideal descent angle at every moment during the descent. The optimal climb profiles are retrieved using the specific excess power and fuel specific energy. The optimal profile depends on the cost index which reflects the ratio of cost of time and cost of fuel. In this work, the profiles for minimum fuel burn (cost index equal to zero) and for minimum time (cost index maximum) are calculated. The calculated profiles are then compared to profiles retrieved from real flight data. For the climb profiles, this reveals that for the real flights around 306 to 390kg of extra fuel is used, 2.7 to 3.4 minutes of extra time are needed and 3.4 to 17.2NM of extra track distances until the top of climb are flown, compared to the calculated climb profiles. The parameters of the real descent profiles are corresponding quite well to the calculated ones.

To account for a multiple aircraft situation for continuous descents, a simulation is performed. This is done by discretizing the airspace around Brussels Airport and determining the optimal trajectories. The simulation uses the traffic situation of September 2012 to have a realistic situation.

Overall, it can be seen that there is still some margin to save on flight costs but this will only be possible through close and unconditional coordination between airlines and air traffic management services.

## Nederlandse samenvatting

Deze Master thesis: "Adaptation of continuous descent and climb operational techniques at Brussels Airport aiming at cost efficiency" is geschreven door Sam Peeters in het academiejaar 2012-2013 voor het behalen van de graad Master of Applied Sciences and Engineering: Electro-Mechanical Engineering: Aeronautics.

Trefwoorden:

Continuous descent operations, continuous climb operations, cost index, dynamische trajecttoewijzing, energiemanagement

Abstract:

Procedures voor een ononderbroken klim en daling hebben als doel het verminderen van het brandstofverbruik en de emissies, respectievelijk tijdens de klim- en dalingsfase van de vlucht. De optimale klim- en daalprofielen worden in deze Master thesis berekend, gebaseerd op de prestaties van het vliegtuig en de beperkingen in het Belgische luchtruim. Dit wordt gedaan aan de hand van de BADA database van Eurocontrol.

De optimale daalprofielen zijn berekend door op elk moment van de daling de ideale daalhoek te bepalen. De optimale klimprofielen zijn bepaald door gebruik te maken van het specifiek resterend vermogen en specifieke energie van de brandstof. De optimale profielen hangen van de cost index af die de verhouding van de tijdkost tot de brandstofkost weerspiegelt. In dit werk worden de profielen voor minimum brandstofverbruik (cost index gelijk aan nul) en voor minimum tijd (maximale cost index) berekend. De berekende profielen worden dan vergeleken met profielen afkomstig van echte vluchtdaten. Bij de klimprofielen ziet men dat de echte vluchten 306 tot 390kg extra brandstof verbruiken, 2,7 tot 3,4 minuten extra vluchttijd nodig hebben en 3,4 tot 17,2NM extra afstand vliegen tot het einde van de klim, vergeleken met de berekende profielen. De parameters van de reële daalprofielen vertonen een goede overeenkomst met de berekende parameters.

Om rekening te houden met een situatie met verschillende vliegtuigen, wordt er een simulatie gedaan. Hierbij wordt het luchtruim rond Brussels Airport gediscretiseerd en wordt het optimale traject bepaald voor elk vliegtuig. De simulatie maakt gebruik van de verkeerssituatie van september 2012 om een realistische situatie te simuleren.

Over het algemeen kan besloten worden dat er nog steeds marge bestaat om vluchtkosten verder te reduceren, maar dit zal enkel mogelijk worden door een nauwe en onvoorwaardelijke samenwerking tussen luchtvaartmaatschappijen en de luchtverkeersleiding.

## Résumé français

Cette thèse: "Adaptation of continuous descent and climb operational techniques at Brussels Airport aiming at cost efficiency" a été écrite par Sam Peeters à l'année académique 2012-2013 afin d'obtenir le grade de Master of Applied Sciences and Engineering: Electro-Mechanical Engineering: Aeronautics.

Mots clé:

Continuous descent operations, continuous climb operations, cost index, allocation dynamique de la trajectoire, gestion de l'énergie

Abstrait:

Les procédures des montées et descentes non-interrompues sont effectuées afin de réduire la consommation de carburant et les émissions pendant la montée comme pendant la descente. Dans cette thèse, les descentes et les montées optimales, sur base des performances avions et des limitations de l'espace aérien Belge, sont calculées à l'aide de la base de données BADA de Eurocontrol.

Les profils des descentes optimales sont calculés en déterminant la pente idéale à chaque moment pendant la descente. Les profils des montées optimales sont déterminés en utilisant la poussée en excès spécifique et l'énergie du carburant spécifique. Le profile optimal dépend du cost index qui est le ratio des couts du temps et des couts de carburant. Dans cette thèse, les profils de consommation minimale (cost index égal à zéro) et de temps minimal (cost index maximal) sont calculés. Ensuite, les profils calculés sont comparées avec des profiles réels. Pour les profils de montées, on remarque que les vols réels ont besoin de 306 à 390kg de carburant en plus, de 2,7 à 3,4 minutes en plus et de 3,4 à 17,2NM en distance supplémentaire jusqu'à la fin de la montée. Les paramètres pour les descentes réelles sont en bonne correspondance avec les paramètres calculés.

Pour considérer une situation de trafic avec plusieurs avions en descente, une simulation a été effectuée. A cette fin, une discréétisation de l'espace aérien autour de l'Aéroport de Bruxelles est réalisée et les trajectoires optimales sont ainsi déterminées. La simulation utilise le trafic aérien de Septembre 2012 pour obtenir une situation réelle et représentative.

On peut finalement conclure qu'il y a encore de la marge pour réduire les coûts opérationnels des vols mais cela ne sera possible qu'au moyen d'une adéquate et inconditionnelle coordination entre les compagnies aériennes et les services de contrôle aérien.

## Table of Contents

Preface.....	3
Legal notice .....	4
Summaries.....	5
English summary .....	5
Nederlandse samenvatting.....	6
Résumé français.....	7
List of symbols and abbreviations .....	11
List of figures .....	12
List of tables .....	15
1. Introduction.....	17
2. Current ATM provisions.....	18
2.1. Continuous descent operations .....	18
2.2. Continuous climb operations .....	19
2.3. SESAR.....	19
2.4. Point merge method .....	21
2.5. Other initiatives and possible solutions .....	22
2.6. Airspace situation around Brussels Airport.....	23
2.7. Cost index .....	26
2.7.1. Impact on descent profiles.....	27
2.7.2. Impact on climb profiles.....	27
2.7.3. Climb and descent overview .....	28
2.7.4. Impact of deviations from the optimal profile .....	28
2.7.5. Influence of different cost indices.....	29
3. Software tools.....	30
3.1. BADA.....	30
3.1.1. Drag calculation.....	30
3.1.2. Thrust calculation [22].....	30
3.1.3. Fuel burn calculation [22].....	31
3.2. V-PAT .....	32
3.2.1. CCO analysis for Brussels Airport .....	32
3.3. Flight data management tools .....	40
4. Descent and climb profiles .....	41
4.1. Atmospheric model .....	41
4.1.1. Temperature model .....	41
4.1.2. Pressure model.....	41
4.1.3. Density model.....	42
4.2. Governing equations for performance calculations.....	43

4.3. Performance during climb.....	44
4.3.1. Initial developments.....	44
4.3.2. Time to climb.....	45
4.3.3. Fuel used during the climb .....	47
4.3.4. Current climb procedures.....	49
4.3.5. Comparison of the optimal climb profiles.....	55
4.3.6. Comparison with flight data .....	56
4.4. Performance during descent.....	60
4.4.1. Initial developments.....	60
4.4.2. Descent profile for minimal time to descent .....	60
4.4.3. Descent profile for minimal fuel burn .....	62
4.4.4. Restrictions to the descent profiles.....	65
4.4.5. Comparison of the optimal descent profiles.....	68
4.4.6. Comparison with flight data .....	69
4.4.7. Influence of the crossover altitude .....	72
4.5. Optimal climb versus optimal descent.....	73
5. Dynamic CDO.....	75
5.1. Concept .....	75
5.2. Implementation.....	75
5.2.1. Discretization of the airspace.....	75
5.2.2. Determination of the optimal trajectory.....	76
5.2.3. Multiple aircraft scenario .....	77
5.3. Results .....	78
6. Future perspectives .....	82
6.1. Cost reduction tool.....	82
6.1.1. Taxi in/out .....	82
6.1.2. Takeoff.....	82
6.1.3. Climb and descent .....	82
6.1.4. Cruise.....	82
6.2. Point merge .....	83
6.3. Dynamic CDO.....	83
7. Conclusions.....	84
8. References .....	86
9. Appendix.....	89
A. Airspace structure in the Brussels FIR .....	89
B. Results of the climb analyses .....	90
C. Profiles of departing traffic .....	93
a. Friday 14/09/2012.....	93

b.	Sunday 23/09/2012.....	96
D.	ILS chart runway 25L .....	100
E.	Distribution of aircraft types at Brussels airport.....	101
F.	Matlab code.....	102
a.	Temperature model .....	102
b.	Pressure model.....	102
c.	Density model.....	102
d.	Profile for minimum climb time .....	102
e.	Profile for minimum climb fuel .....	105
f.	Profile for minimum descent time .....	108
g.	Profile for minimum descent fuel .....	111
h.	Dynamic CDO simulation.....	114

## List of symbols and abbreviations

P	Pressure (Pa)
T	Temperature (K or °C)
$\rho$	Density (kg/m <sup>3</sup> )
R	Universal gas constant (287 J/kg/K)
g	Gravitational acceleration (9.81 m/s <sup>2</sup> )
h	Altitude (m or ft)
W	Aircraft weight (N)
V	True airspeed (m/s or ft/s)
S	Reference wing surface (m <sup>2</sup> )
$C_D$	Drag coefficient (-)
$F_A$	Available thrust (N)
$C_{SF}$	Side force coefficient (-)
$C_L$	Lift coefficient (-)
R/C	Rate of climb (m/s or ft/s)
D	Drag (N)
E	Energy (J)
$E_p$	Potential energy (J)
$E_k$	Kinetic energy (J)
m	Mass (kg)
$E_s$	Specific energy (m or ft)
M	Mach number (-)
$P_s$	Specific excess power (m/s or ft/s)
$h_e$	Energy height (m or ft)
$P_A$	Available power (W)
$P_R$	Required power (W)
$f_s$	Fuel specific energy (m/N)
$W_f$	Fuel weight (N)
FF	Fuel flow (kg/s)
TSFC	Thrust specific fuel consumption (kg/daN/h)
$V_z$	Vertical speed (m/s or ft/s)
ATM	Air Traffic Management
$C_{D0}$	Zero lift drag coefficient

## List of figures

Figure 1: Non-CDO and CDO approach profiles .....	18
Figure 2: Overview of the functional airspace blocks [10] .....	21
Figure 3: Point merge system with two arrival flows [11] .....	22
Figure 4: CDA Map Tool of Eurocontrol depicting the status of CDO around Europe [13].....	24
Figure 5: Airspace requirements to enable CDO at the major airports in Western Europe [14].....	25
Figure 6: Possible point merge system for aircraft landing on runway 25L [2] .....	26
Figure 7: Influence of the cost index on the descent profile [20] .....	27
Figure 8: Influence of the cost index on the climb profile [20] .....	27
Figure 9: Overview of the influence of the cost index on the flight profile .....	28
Figure 10: Exit sectors with their respective limits (departures from runways 25 within a radius of 75NM).....	35
Figure 11: Exit sectors with their respective limits (departures from runways 07 within a radius of 75NM).....	35
Figure 12: Scatter plot of the exit bearings .....	36
Figure 13: Horizontal profiles of the flights leaving to the East and Southeast on 14/09/2012.....	37
Figure 14: Vertical profiles of the flights leaving to the East and Southeast on 14/09/2012 .....	37
Figure 15: Horizontal profiles of the flights with a level part leaving to the East and Southeast on 14/09/2012.....	38
Figure 16: Vertical profiles of the flights with a level part leaving to the East and Southeast on 14/09/2012.....	38
Figure 17: Illustration for the bad fuel results in V-PAT .....	39
Figure 18: Temperature evolution in ISA conditions.....	41
Figure 19: Pressure evolution in ISA conditions.....	42
Figure 20: Density evolution in ISA conditions.....	43
Figure 21: Constant energy height lines with respect to the Mach number .....	45
Figure 22: Ideal climb profile with minimal time to climb .....	46
Figure 23: Zoom of the final part of the climb (lowest time to climb).....	47
Figure 24: Ideal climb profile with minimal fuel to climb .....	48
Figure 25: Zoom of the final part of the climb (minimum fuel to climb) .....	49
Figure 26: Dependence of the crossover altitude on the cost index for Airbus aircraft [18] .....	51
Figure 27: Adapted profile for minimal climb time with respect to noise abatement procedures .....	52
Figure 28: Reference profile for minimal climb time .....	53
Figure 29: Ideal climb profile for minimal time to climb as a function of the distance from the airport .....	53
Figure 30: Adapted profile for minimal climb fuel with respect to noise abatement procedures .....	54
Figure 31: Reference profile for minimal climb fuel .....	54
Figure 32: Ideal climb profile for minimal fuel to climb as a function of the distance from the airport .....	55
Figure 33: Overlay of the two climb profiles with the extra cruise segment.....	56
Figure 34: Comparison between real flight profiles and the reference profiles.....	58
Figure 35: Comparison between real flight profiles and the reference profiles.....	58
Figure 36: Comparison between real flight profiles and the reference profiles corrected with the average winds.....	59
Figure 37: Ideal descent profile for minimal time to descent .....	61
Figure 38: Ideal descent profile for minimal time to descent as a function of the Mach number .....	62
Figure 39: Ideal descent profile for minimal time to descent as a function of the distance from the final approach fix.....	62
Figure 40: Ideal descent profile for minimal fuel to descent .....	63
Figure 41: Ideal descent profile for minimal fuel to descent as a function of the Mach number .....	64

Figure 42: Ideal descent profile for minimal fuel to descent as a function of the distance from the final approach fix.....	64
Figure 43: Flight trajectories of some representative flights towards Brussels Airport (chart from [27]) .....	65
Figure 44: Vertical profiles of representative flights coming from France .....	66
Figure 45: Vertical profiles of representative flights coming from Germany .....	66
Figure 46: Overlay of the ideal profile for minimum fuel burn with and without the handover constraint .....	67
Figure 47: Overlay of the ideal profile for minimum descent time with and without the handover constraint .....	67
Figure 48: Overlay of the two profiles with the extra cruise segment .....	68
Figure 49: Comparison between real flight profiles and the reference profiles.....	71
Figure 50: Comparison between real flight profiles and the reference profiles.....	72
Figure 51: Overlay of simple CDO and CCO profiles.....	74
Figure 52: Discretized airspace around Brussels Airport .....	76
Figure 53: Waypoints in TSA26A at 24,000ft highlighted in yellow .....	76
Figure 54: Possible transitions for the Airbus 320 between the 5 most inner rings.....	77
Figure 55: Horizontal trajectories of the two first aircraft in the simulation sequence .....	79
Figure 56: Optimal trajectories of flights coming from France and Germany (chart from [27]) <sup>1</sup> .....	80
Figure 57: Radar image from Belgocontrol highlighting the main traffic flows from France and Germany.....	81
Figure 58: Chart of the airspaces in the Belgian Flight Information Region .....	89
Figure 59: Horizontal profiles of the flights leaving to the North .....	93
Figure 60: Horizontal profiles of the flights with a level part leaving to the North .....	93
Figure 61: Vertical profiles of the flights leaving to the North.....	93
Figure 62: Vertical profiles of the flights with a level part leaving to the North.....	93
Figure 63: Horizontal profiles of the flights leaving to the Southwest .....	94
Figure 64: Horizontal profiles of the flights with a level part leaving to the Southwest .....	94
Figure 65: Vertical profiles of the flights leaving to the Southwest.....	94
Figure 66: Vertical profiles of the flights with a level part leaving to the Southwest .....	94
Figure 67: Horizontal profiles of the flights leaving to the West Northwest .....	95
Figure 68: Horizontal profiles of the flights with a level part leaving to the West Northwest .....	95
Figure 69: Vertical profiles of the flights leaving to the West Northwest.....	95
Figure 70: Vertical profiles of the flights with a level part leaving to the West Northwest.....	95
Figure 71: Horizontal profiles of the flights leaving to the North .....	96
Figure 72: Horizontal profiles of the flights with a level part leaving to the North .....	96
Figure 73: Vertical profiles of the flights leaving to the North.....	96
Figure 74: Vertical profiles of the flights with a level part leaving to the North.....	96
Figure 75: Horizontal profiles of the flights leaving to the East and Southeast.....	97
Figure 76: Horizontal profiles of the flights with a level part leaving to the East and Southeast.....	97
Figure 77: Vertical profiles of the flights leaving to the East and Southeast .....	97
Figure 78: Vertical profiles of the flights with a level part leaving to the East and Southeast .....	97
Figure 79: Horizontal profiles of the flights leaving to the Southwest .....	98
Figure 80: Horizontal profiles of the flights with a level part leaving to the Southwest .....	98
Figure 81: Vertical profiles of the flights leaving to the Southwest .....	98
Figure 82: Vertical profiles of the flights with a level part leaving to the Southwest.....	98
Figure 83: Horizontal profiles of the flights leaving to the West Northwest .....	99
Figure 84: Horizontal profiles of the flights with a level part leaving to the West Northwest .....	99
Figure 85: Vertical profiles of the flights leaving to the West Northwest.....	99
Figure 86: Vertical profiles of the flights with a level part leaving to the West Northwest.....	99
Figure 87: ILS approach chart for runway 25L at Brussels Airport [27] .....	100



## List of tables

Table 1: Overview of the V-PAT parameters.....	32
Table 2: Bearing intervals of the exit sectors .....	36
Table 3: Noise abatement procedures for takeoff.....	50
Table 4: Overview of the climb results.....	55
Table 5: Average climb values of the flight data .....	57
Table 6: Comparison of the flight data with the calculated values for the climb phase.....	57
Table 7: Reference climb parameters after correction .....	57
Table 8: Fuel burn and descent time for the possible trajectories .....	68
Table 9: Fuel burn and descent time for the possible trajectories (extra cruise segment considered)	69
Table 10: Average descent values of the flight data .....	69
Table 11: Comparison of the flight data with the calculated values for the descent phase.....	70
Table 12: Reference descent parameters after correction .....	70
Table 13: Average descent values of the considered flights coming from Germany.....	71
Table 14: Percentages of flights per aircraft category .....	73
Table 15: Aircraft types with their respective cost indices for the simulation .....	77
Table 16: Standard separation minima for aircraft flying at the same altitude.....	78
Table 17: Simulation sequence (aircraft type and initiation time) .....	78
Table 18: Results of the simulation .....	79



## **1. Introduction**

Transportation is responsible for a big part of air pollution and so is the aviation industry. Everywhere in the world, people are looking for methods to reduce this pollution. The vision for 2020 is to accomplish a reduction of 50% of the CO<sub>2</sub> emissions of which 5 to 10% should come from air traffic management by RNAV/RNP, ADS-B, ATOP, ASPIRE, ADAR,... [1]. Nevertheless, what is important for airlines and air traffic services providers is a reduction of the costs. Indeed, airlines don't only have fuel costs but also time related costs which have to be taken into account. However, since the price of fuel is quite high, the overall costs are dominated by the fuel costs. Various solutions that can have a big impact for the cost reduction problem already exist. 4D flight planning, optimal routes and continuous descent operations are difficult to achieve while pilot technique, fuel management and climb at reduced power are easier [1].

This Master thesis is focused on the possible cost reductions of continuous climb operations (CCO) and descent operations (CDO). Initially, the current air traffic management provisions are summarized to get a general idea about the current situation. Here, also the cost index, which is reflecting the relative costs of fuel and time, is explained. The current situation for the descents towards Brussels Airport is already analysed in [2] but this hasn't been done for the climbs so a small analysis is done in this work. Initially, the general principle of continuous descents and climbs is outlined and ideal descent and climb profiles are calculated. In a next step, the operational restrictions are considered for descents and climbs towards and from Brussels Airport to obtain profiles that are adapted to the Belgian airspace and its regulations. The optimal profiles are calculated for two situations: one where the time to descent or climb is minimized and one with a minimal descent or climb fuel. The fuel consumption and flight time of these profiles is then compared to real flight data to see how much the costs could be reduced using these profiles. Since a lot of aircraft are flying around, they have to be separated which can mean that the optimal profile can't be flown. To see the impact of this problem, a simulation is made in which the optimal descent profile is calculated for every aircraft, taking into account the actual traffic situation. This method is called dynamic CDO because it's calculating the best trajectory for every aircraft in the always changing traffic situation.

The completion of this Master thesis was made possible by the cooperation of the people of Belgocontrol, Eurocontrol, Thomas Cook and Jetairfly.

## 2. Current ATM provisions

### 2.1. Continuous descent operations

Continuous descent operations (CDO) is a method to lower the fuel burn and emissions of aircraft in the descent phase towards the airport. The official definition given by Eurocontrol is: "Continuous Descent Approach is an aircraft operating technique in which an arriving aircraft descends from an optimal position with minimum thrust and avoids level flight to the extent permitted by the safe operation of the aircraft and compliance with published procedures and ATC instructions" [3].

Another definition is given by ICAO<sup>1</sup> in Document 9931: "An aircraft operating technique aided by appropriate airspace and procedure design and appropriate ATC clearances enabling the execution of a flight profile optimized to the operating capability of the aircraft, with low engine thrust settings and, where possible, a low drag configuration, thereby reducing fuel burn and emissions during descent. The optimum vertical profile takes the form of a continuously descending path, with a minimum of level flight segments only as needed to decelerate and configure the aircraft or to establish on a landing guidance system (e.g. ILS<sup>2</sup>)."

So the main target is to reduce the fuel burn and emissions without compromising the safety. Mainly the vertical descent profile is taken into consideration to examine the influence of the CDO method. Nowadays, a staircase-like descent is seen to be the commonly used method to approach an airport. An example can be seen in Figure 1.

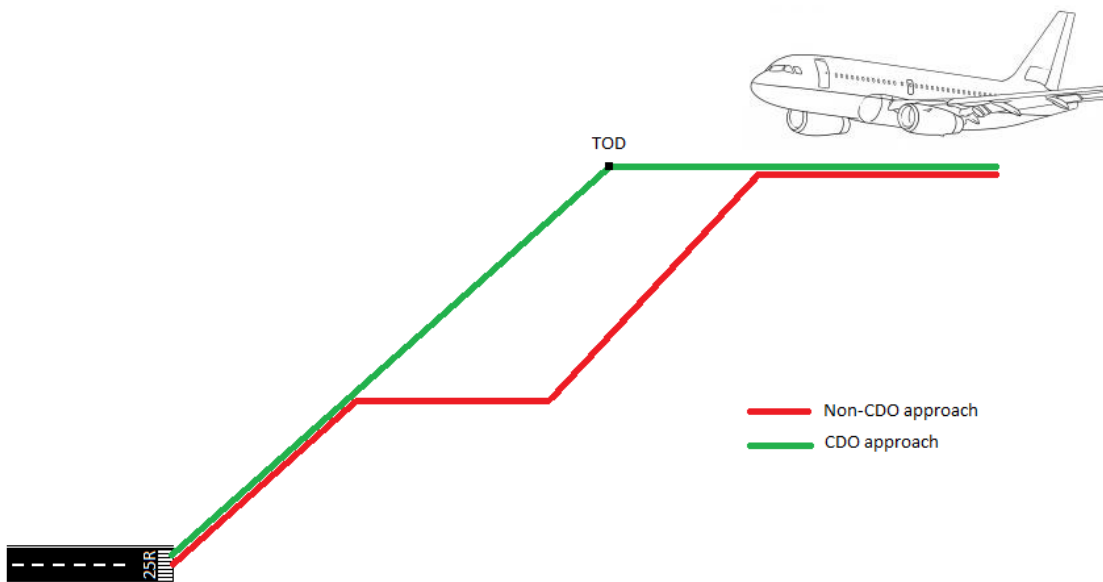


Figure 1: Non-CDO and CDO approach profiles

In Figure 1 only one intermediate level in the descent is shown but there can be a lot more level parts during the descent.

The ideal CDO starts at the top of descent (TOD) and ends when the ILS glide slope is intercepted. This will only be possible if there are no constraints imposed due to airspace boundaries, speed

<sup>1</sup> ICAO: International Civil Aviation Organization: Agency of the United Nations promoting the development of international civil aviation and setting standards and regulations to ensure aviation safety, security, efficiency and regularity.

<sup>2</sup> ILS: Instrument Landing System: Radio navigation system enabling precision approaches by providing the offset from the runway centerline and from the ideal descent angle.

limitations, traffic limits, operational limits,... Nevertheless, even if not the complete descent is considered CDO, there will be some benefit for the airline and the environment by doing descents which are partially CDO.

The advantages of applying continuous descents are multiple: most importantly, the fuel burn can be reduced which has a direct influence on the emission of exhaust gases. Additionally, because the airplanes doing a CDO fly higher than with a conventional descent during the largest part of the approach, the noise level perceived on the ground is lower. This is in turn advantageous for people living near an airport [4]. So while the airlines are saving on their fuel cost, the environment also takes advantage of it. The CDO method can reduce the workload of the air traffic control officers because there are fewer interventions with altitude instructions needed. However, the planning of these flights will be more time-consuming. The workload of the pilots will be reduced when the CDO procedure can be more automated using the FMC<sup>3</sup> onboard the aircraft.

## 2.2. Continuous climb operations

Continuous climb operations (CCO) or uninterrupted climb operations is similarly to CDO a technique of performing the climb without any level parts. This will again reduce the fuel burn, the emissions and the noise perceived on the ground. ICAO defines continuous climb operations as: "CCO is an aircraft operating technique enabled by airspace design, procedure design and facilitation by ATC, enabling the execution of a flight profile optimized to the performance of the aircraft." [5].

There is less attention given to CCO and consequently, there is less information available on this method. It is sometimes said that CCO has more potential for fuel reductions because the climb is a high energy phase. Whether this statement is correct will be examined in 4.5. In addition, the current situation of the climbs out of Brussels Airport is analysed in 3.2.1.

## 2.3. SESAR

In 2004, the initial steps were taken to implement the Single European Sky by dismantling the borders in the sky. Later the Single European Sky ATM Research (SESAR) programme was founded by Eurocontrol and the European Union to design, develop and implement all operational and technical elements. The general goal is to create the future ATM system that will be used as from 2020.

The objective is to design a system with high performance requirements which will be progressively introduced. The final goal is to accommodate three times as much traffic with an individual safety risk that is decreased with a factor of three, to reduce the environmental impact of each flight by 10% and to reduce the ATM cost of every flight with 50%. Furthermore, SESAR aims to reduce the flight time on average with 8 to 14 minutes, the fuel burn with 300 to 500kg per flight and consequently the emission of CO<sub>2</sub> with 948 to 1575kg per flight.

The environmental objectives are further specified: the noise should be minimised, local air quality around airports has to be improved and the fight against climate change due to aircraft emissions has to be continued. Therefore SESAR aims to reduce CO<sub>2</sub> emissions by 10% per flight, to manage noise emissions by optimising the climb and descent solutions and to improve ATM to comply with local regulations and aircraft restrictions.

To accomplish all these objectives, different work packages were started which all have their specific area in which they try to find solutions to achieve the goals. More specifically, the work packages address amongst others the green departures, green cruise and green approaches.

---

<sup>3</sup> FMC: Flight Management Computer

The green departures ask for a continuous climb so a climb without any level segment until the top of climb to make the most efficient use of fuel. A level part in the climb phase is neither efficient nor environmentally friendly. Demonstrations and flight trials have already been done to investigate the possible profits of continuous climb operations in Paris [6].

The green cruise initiatives try to enable aircraft to fly at their optimal altitude and speed depending on weight, airframe design, weather, airspace,... This is done by direct routing, better lateral and vertical profiles and choosing the correct cost index (see 2.7). Demonstrations have been done using for example ADS-B<sup>4</sup> [7].

The objective for a green approach is to start at the top of descent. The descent planning should be made in order to use the available potential energy of the aircraft to perform a descent with idle thrust setting. At landing, idle thrust reversing can help to achieve the reduction of emissions and fuel burn. Several tests have been performed in Stockholm and Madrid [8], [9].

The tests and flight trials are done within the scope of AIRE (Atlantic Interoperability Initiative to Reduce Emissions) which tries to reduce emissions without or with little research and development. SESAR has been tasked to develop the required technology to create one single European sky over the European Union. This is of course not possible in one step so as an intermediate step, the so called functional airspace blocks (FABs) are created. The 67 airspace blocks based on the national boundaries are combined into 9 functional airspace blocks (Figure 2). This will improve safety and capacity and lower the costs. The Belgian airspace is now integrated in the FABEC (Functional Airspace Block Europe Central) together with the airspaces of France, Germany, the Netherlands, Luxembourg and Switzerland. 55% of all European air traffic passes every year through this airspace which shows that this is a very crowded airspace.

---

<sup>4</sup> ADS-B: Automatic Dependant Surveillance-Broadcast: Surveillance technology to track aircraft and receive and transmit certain information. The aircraft's position and speed are transmitted every second to air traffic control which allows it to replace radar.

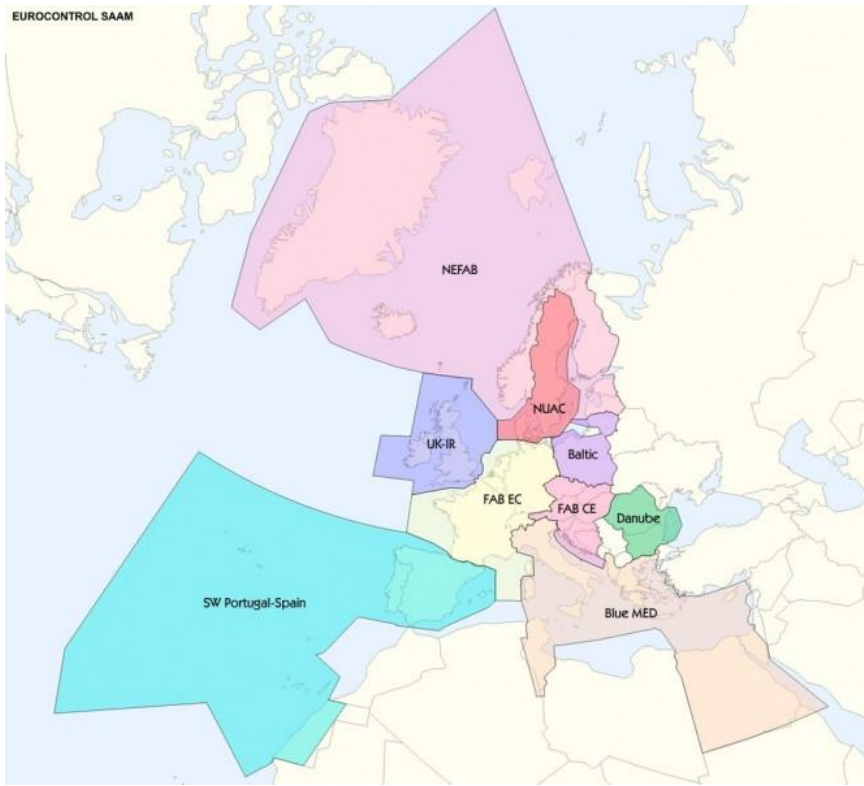


Figure 2: Overview of the functional airspace blocks<sup>5</sup> [10]

In the United States, the FAA<sup>6</sup> is doing a similar project: the Next Generation Air Transportation System (NextGen). It has nearly the same goals as SESAR to accommodate for future needs of the air traffic. Several initiatives are developed to reduce the fuel burn, emissions and noise pollution. One of the initiatives is to join the airspaces above their major airports in order to provide precise patterns for the air traffic. The big advantage in the United States is that in general a lot more airspace is available which is absolutely not the case in Europe.

#### 2.4. Point merge method

The point merge method uses the RNAV<sup>7</sup> routing system to decrease the workload of the air traffic controllers, increase the predictability of the trajectories during the approach and minimize the environmental impact. Nowadays, the radar controllers have to give heading and altitude instructions to sequence the aircraft approaching the airport. With point merge, the workload and stress are significantly reduced. The area which is flown over is also smaller with respect to approaches with radar vectoring so the impacted area of the arrivals is reduced. Nevertheless, the area which is still flown over will suffer from more noise exposure. To realize this concept, a number of pre-defined points are to be followed to approach the airport. The principal point is the merge point. From this point on, the aircraft are sequenced and sufficiently separated. In front of the merge point, a number of sequencing legs are provided to allow the air traffic controller to sequence the approaching aircraft. Generally, these legs are made of concentric circles with the merge point as centre since they provide equidistant points from the merge point. A nice advantage of this method is that it enables continuous descent operations from the moment the controller instructs the

<sup>5</sup> Eurocontrol, "FABs," 2011. [Online]. Available: [www.eurocontrol.int](http://www.eurocontrol.int). [Accessed 21 April 2013].

<sup>6</sup> FAA: Federal Aviation Administration

<sup>7</sup> RNAV: Area Navigation: a method to perform a navigation using predefined waypoints. The advantage is that ground based navigation aids don't have to be flown over.

aircraft to turn towards the merge point. The cockpit crew then has an exact idea of the distance from touchdown which is very useful to plan the continuous descent. Another advantage is that point merge doesn't require any additional equipment in aircraft or on the ground if an AMAN<sup>8</sup> system is already present. The workload of the air traffic controller is decreased since fewer instructions have to be given to the aircraft. As a consequence the radio frequency is more often free for transmissions. Figure 3 shows an example of a standard point merge design with two arrival flows.

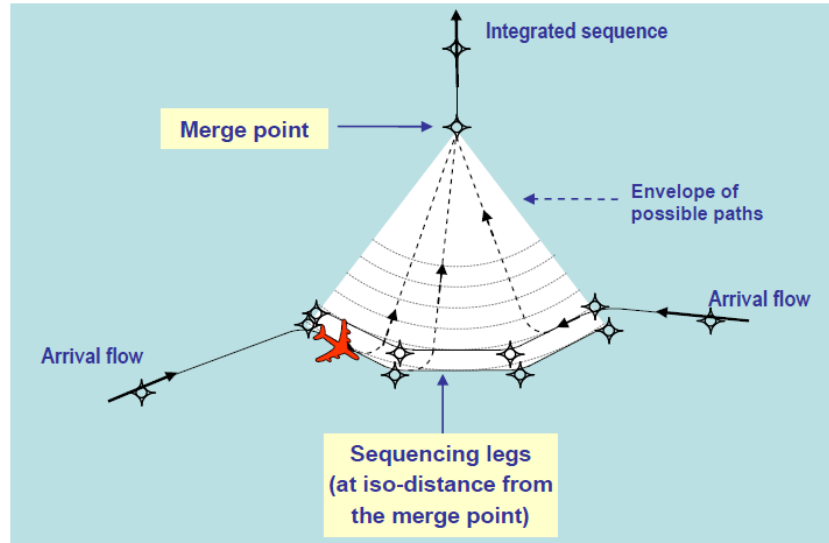


Figure 3: Point merge system with two arrival flows<sup>9</sup> [11]

The first time the point merge method was used, was for the airport of Oslo. The researchers found that a reduction of the fuel burn by 300kg per flight could be achieved. However the airspace around Oslo is not as complex as around Brussels and is much larger so the implementation was much easier than it would be for Brussels or other airports in Europe. The French air navigation service provider DSNA has conducted some successful trials with arriving traffic for Paris-Charles De Gaulle Airport. Especially the controllers were very pleased about the new method. In December 2012, the Irish Aviation Authority has implemented point merge for runway 28 at Dublin. Here as well, the comments of airlines and air traffic control are very positive [12].

Although it is generally said that point merge would reduce the fuel burn, one could think that it could even increase the fuel burn when an aircraft has to fly the complete sequencing leg before it can turn towards the merge point. Moreover, when aircraft are flying to an airport that uses point merge, they always have to take enough fuel to be able to fly the complete sequencing leg. This additional fuel increases the overall fuel burn because of the extra weight.

Thus, additional investigation about this topic is required. Since point merge is still in development, there is little information available, so the point merge method is not considered here.

## 2.5. Other initiatives and possible solutions

As said before, the airspace above Western Europe is pretty congested. Several solutions are brought forward to improve the situation while trying to incorporate the goals of SESAR.

A big milestone is the first test flight of 4D flights. The four dimensions are the position in latitude, longitude, altitude and time (or speed) so that the trajectories or parts thereof are completely

<sup>8</sup> AMAN: Arrival manager: Tools to assist air navigation service providers with aircraft arrivals.

<sup>9</sup> Eurocontrol, "Point merge: a more efficient way of sequencing arrivals," 2011.

determined in advance: the aircraft should be at certain fixed positions within certain time frames. The aim is to get more predictable flights, smooth sequencing towards a runway, to reduce conflicts along the trajectories and eliminate holdings so less fuel is used and less noise and emissions are produced. To mutually determine the flight trajectory, a data exchange between the FMC and the ground automation systems is foreseen through data link. Using this technology, the capacity of airports and airspace will become greater and better planning will enable environmentally friendly flights. During the first flight trial the decision on the arrival trajectory and the time at the merge point was determined 40 minutes before the landing. This was done taking into account the weather and atmospheric conditions during the descent. This trajectory was then inserted in the FMC which conducted the descent appropriately. The actual time at the merge point differed only some seconds from the predicted time. Thus, the trial demonstrated that the technology is able to perform these flights and that it is operationally feasible when there is close collaboration between all related parties.

In the United States a different approach is used: the airspace structure is adapted to provide the best solutions for the major airports only. This means that smaller, regional airports are more or less neglected. Using this method, a large part of the flights can be accommodated with better airspace provisions. The big advantage in the United States is that there is a lot more airspace available which makes it easier to redesign the airspace structures to introduce new methodologies.

## 2.6. Airspace situation around Brussels Airport

Belgium has one of the most congested and complicated airspaces in Europe. This is due to the presence of 5 civil and 4 military airfields on a rather small area and due to the central location of Belgium in between some major airports (London, Amsterdam, Paris, Frankfurt,...). To illustrate the complexity of the airspace structure in Belgium, the chart of the Brussels FIR is provided in Appendix A. This is one of the big hurdles to take for the implementation of CDO.

The opportunity to visit the CANAC 2 centre at Belgocontrol clarified a lot concerning the problems which are present when speaking about continuous descents and climbs. As said before, the complexity and the lack of space in the Belgian airspace is the major issue. If one would try to foresee a route or procedure to enable continuous descents for example, the impact would be enormous on all the other traffic so that it would even be possible that the overall traffic situation would deteriorate heavily. For example: when the approaching traffic from the southeast would be provided with a corridor or airspace configuration exclusively intended for performing CDO arrivals, this would mean that the Letter of Agreement<sup>10</sup> should be changed to enable the arriving aircraft to perform the ideal descent profile which will probably start from a higher altitude than the altitude which is used nowadays. So the altitude of the handover will not be fixed anymore which again implies that the departing traffic to the southeast will not have a fixed altitude under which they have to stay since they have to pass below the arriving traffic. This will make it complicated for the air traffic controllers because the situation then changes continuously because every aircraft will perform a different CDO considering the airline policy, type of aircraft, weight,... The situation is even nearly impracticable if we further consider the traffic departing from Dusseldorf which has to climb above the arriving traffic towards Brussels. This means that the arriving traffic cannot start its descent too high because otherwise the traffic coming from Dusseldorf will not be able to be above the arriving traffic. This is a nice example of the complexity of the airspace in and around Belgium. It

---

<sup>10</sup> Letter of Agreement: Agreement between neighbouring countries which specifies the altitudes at which aircraft are handed over from one controlling agency to the other.

is clear that any change of airspace structure has wide-ranging consequences and is also impacting to a large extent the whole European airspace. It can be seen as a kind of snowball effect.

The large amount of variables is a big problem in the implementation of CDO. From the air traffic control's point of view the differences between aircraft types and airline policies form a big issue. These differences result in different speeds of the aircraft during the descent and climb phases. Estimating the speed of an aircraft is not easy in the first place but sequencing and separating aircraft flying at different speeds (horizontal, vertical, yet angular) is certainly very difficult. A standardization of the aircraft would be a solution but this is far from being realistic. Considering this, the air traffic controllers would be continuously puzzling to get all aircraft on the ground in as safe, orderly and expeditious way. This would be very demanding and actually impossible. Air traffic controllers should be able to fall back on 3 to 4 different scenarios to control the traffic so that every controller knows what is happening at that moment and there is no confusion about the situation. This pertains to the human factors embedded in this subject but falls outside the scope of this work.

From the above discussion it is clear that a nice implementation of CDO is not for the near future in the Belgian and even European airspace. Nevertheless, there are some projects running that are investigating the subject to create a “single sky” over Europe. It would be a big step forward to create one large airspace without any internal borders. This would enable the creation of routes intended to give the opportunity to fly CDO procedures but that project is still in development.

Despite the various difficulties concerning CDO, there are already quite some airports which facilitate CDO in some way. This can be seen in Figure 4 which comes from the CDA Map Tool of Eurocontrol [13]:

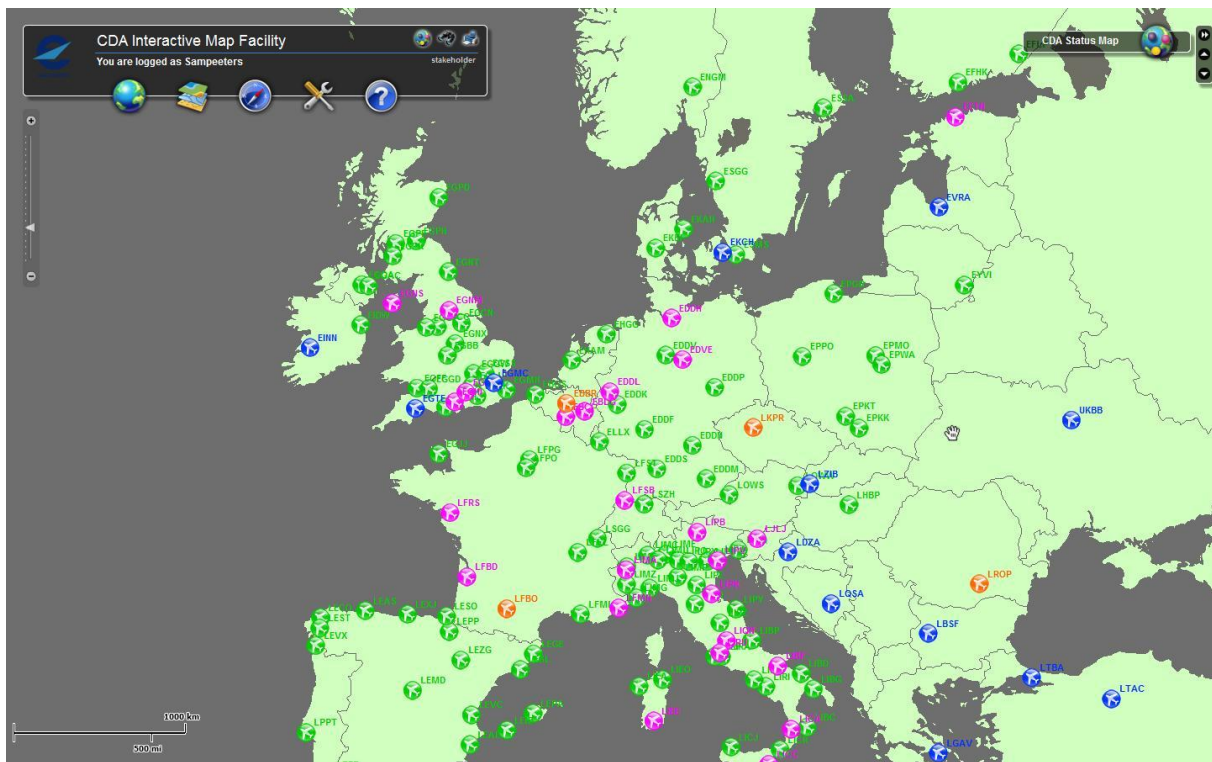


Figure 4: CDA Map Tool of Eurocontrol depicting the status of CDO around Europe<sup>11</sup> [13]

Figure 4 shows the major airports in Europe with a specific colour. Green means that CDO is implemented, pink airports have committed to investigate CDO feasibility, orange airports are doing

<sup>11</sup> Eurocontrol, "CDA Map Tool," 2010. [Online]. Available: <http://extranet.eurocontrol.int>. [Accessed 10 April 2013].

trials and blue airports were visited by the CDA implementation team of Eurocontrol but there is no intention to facilitate CDO nor has any progress been made until now.

The feasibility study for implementing the point merge method for Brussels Airport was investigated by Belgocontrol as well. Due to the limited airspace around Brussels Airport, the point merge method would be useful to arrange the traffic flows. Some preliminary designs for Brussels Airport were proposed in the past but this project was not continued. The big disadvantage of the point merge method is that it needs a large amount of airspace, especially for the sequencing legs. If point merge would be introduced for Brussels Airport, some airspace in France and the Netherlands would be needed. This would mean that the airspace above and around Belgium should be revised. Of course the same amounts of airspace would have to be foreseen for the surrounding major airports like Paris, Amsterdam, London, Frankfurt,... Unfortunately these airspaces would overlap each other which can be seen in Figure 5:

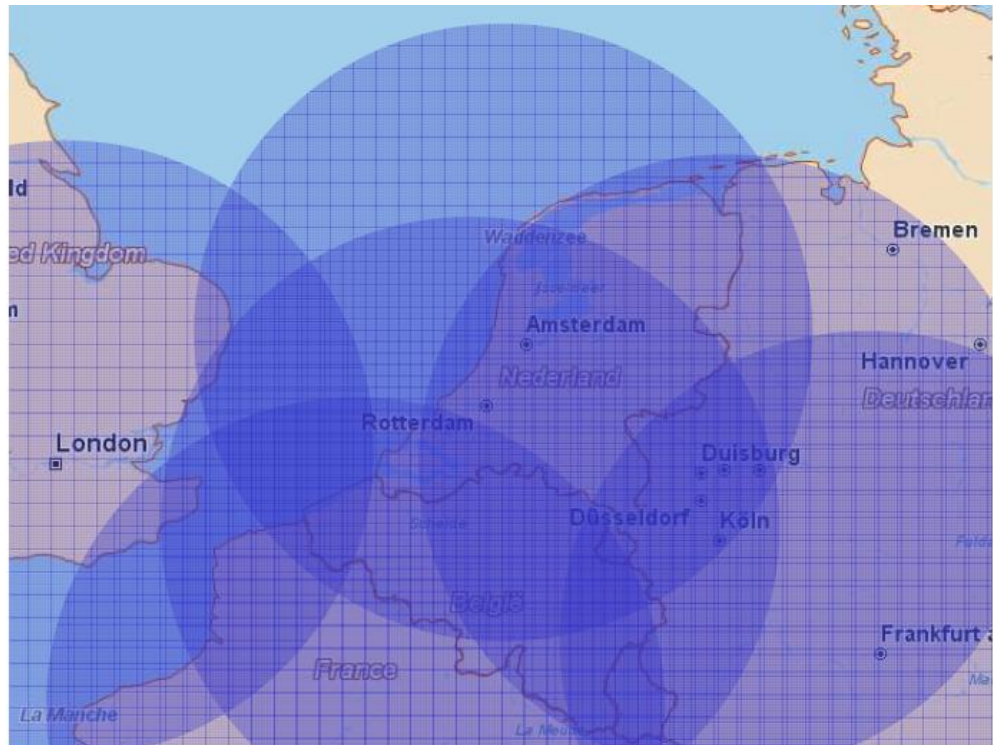


Figure 5: Airspace requirements to enable CDO at the major airports in Western Europe<sup>12</sup> [14]

It is clear that it is impossible to accommodate every airport with enough airspace to provide continuous descents and climbs. But another possible way of solving this issue is to set up a system which designates airspace to a certain airport during a certain time period to allow continuous descents and climbs to and from that airport. After that time period, the control of the airspace can be transferred to another airport. This procedure could be applied so that airspace is alternately designated to one airport when some airports are close together.

A possible design of the point merge method for Brussels Airport is given in Figure 6 for landings on runway 25L. One can see that two merge points are used to provide an approach from every direction towards Brussels Airport. This is a bit more difficult because the air traffic controller has to do the sequencing of aircraft coming from the two merge points. However, this can't be a problem because a similar sequencing is already done nowadays.

---

<sup>12</sup> R. De Muynck, S. Raynaud and B. Korn, "Optimal User Forum: Session 1 - Continuous descent approach," 2008.

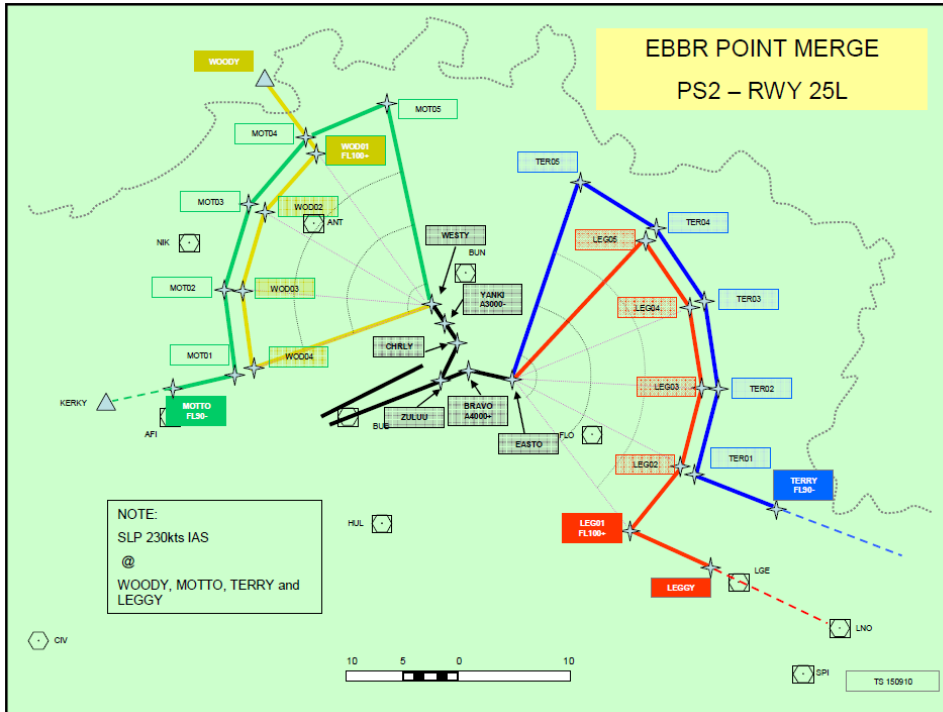


Figure 6: Possible point merge system for aircraft landing on runway 25L<sup>13</sup> [2]

## 2.7. Cost index

The total costs of a flight are made up of variable and fixed costs:

$$C = C_F \cdot \Delta F + C_T \cdot \Delta T + C_C \quad (2.1)$$

With:  $C$ : Total flight cost

$C_F$ : Cost of the fuel per kg

$\Delta F$ : Trip fuel (kg)

$C_T$ : Cost related to time per minute of flight

$\Delta T$ : Trip time (min)

$C_C$ : Fixed costs

The variable costs are the costs of time and the costs of fuel. So to minimize the flight cost, we have to minimize these variable costs. To achieve this, a trade off between the fuel costs and the time costs is made which is reflected in the cost index [15]. The cost index (CI) is a parameter used by aircraft operators to have an idea of the importance of fuel cost with respect to the cost of time. The time related costs include the crew salaries, aircraft leasing costs, maintenance costs, depreciation costs, delay costs,... The cost index is defined as follows:

$$\text{Cost index} = \frac{\text{Time cost } [\text{€}/\text{min}]}{\text{Fuel cost } [\text{€}/\text{kg}]} \quad (2.2)$$

This value is entered in the Flight Management Computer onboard the aircraft which will calculate the economy cruise, climb and descent speeds. The cost index value can be different for every flight, for every company and for every route depending on numerous factors [16]. The cost index is a parameter which is a variable. If the cost of fuel changes, the cost index should be adapted

<sup>13</sup> B3 SESAR JU Project, "Phase two report," 2012.

accordingly to keep minimizing the costs. The same is valid for the cost of time. If the cost index wouldn't be changed, the total cost will be higher than before, whether the fuel price decreases or increases. Moreover the cost of time can vary as well, it depends of the cost of maintenance as well as of the cost of flight/cabin crew which in the end are variables as well [17], [18], [19].

### 2.7.1. Impact on descent profiles

Depending on the outcome of the cost calculation in the airline, the cost index is determined which will influence the profile of the descent. Figure 7 shows that flying on a cost index of zero will result in a top of descent which is further away from the airport than when the cost index is higher. Consequently, the higher the cost index, the steeper the descent path and the shorter the descent distance is. The profile with cost index equal to zero represents the profile for minimum fuel consumption and the profile with maximum cost index is the one for minimum descent time.

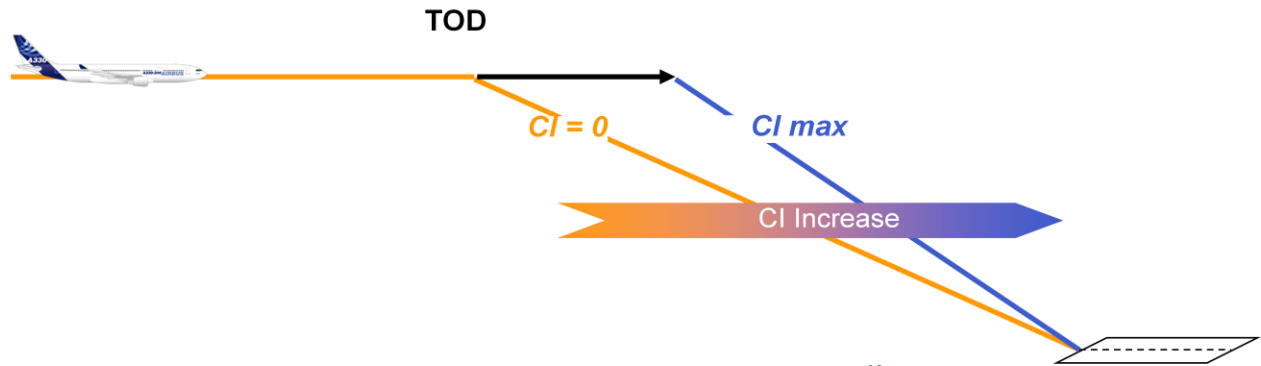


Figure 7: Influence of the cost index on the descent profile<sup>14</sup> [20]

### 2.7.2. Impact on climb profiles

Similar to the descent profile, the climb profile is depending on the cost index. However, in this case the influence on the path angle and the climb distance is different: a cost index of zero will cause a top of climb which is closer to the airport than with a maximum cost index. So, for higher cost indices, the climb path will be shallower and the climb distance will be longer (Figure 8). The maximum cost index will result in flying the climb at the highest allowed speed so the time to climb will be minimal. To the contrary, a low speed will be used when the cost index is zero. This results in a profile with minimal fuel consumption.

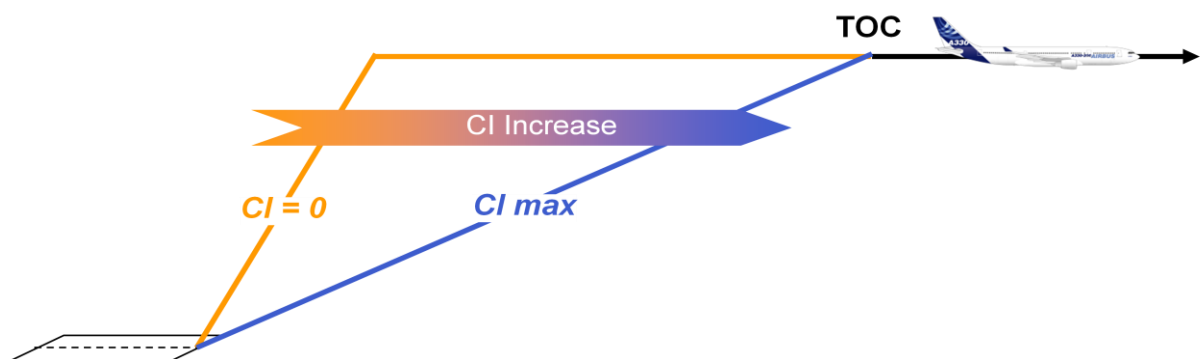


Figure 8: Influence of the cost index on the climb profile<sup>15</sup> [20]

<sup>14</sup> Airbus, "Airbus views on fuel economy," in 15th Performance & Operations conference, Puerto Vallarta, 2007.

<sup>15</sup> Airbus, "Airbus views on fuel economy," in 15th Performance & Operations conference, Puerto Vallarta, 2007.

### 2.7.3. Climb and descent overview

Combining the climb and descent profiles depending on the cost index, we can come up with an overview of the complete flight profile as shown in Figure 9:

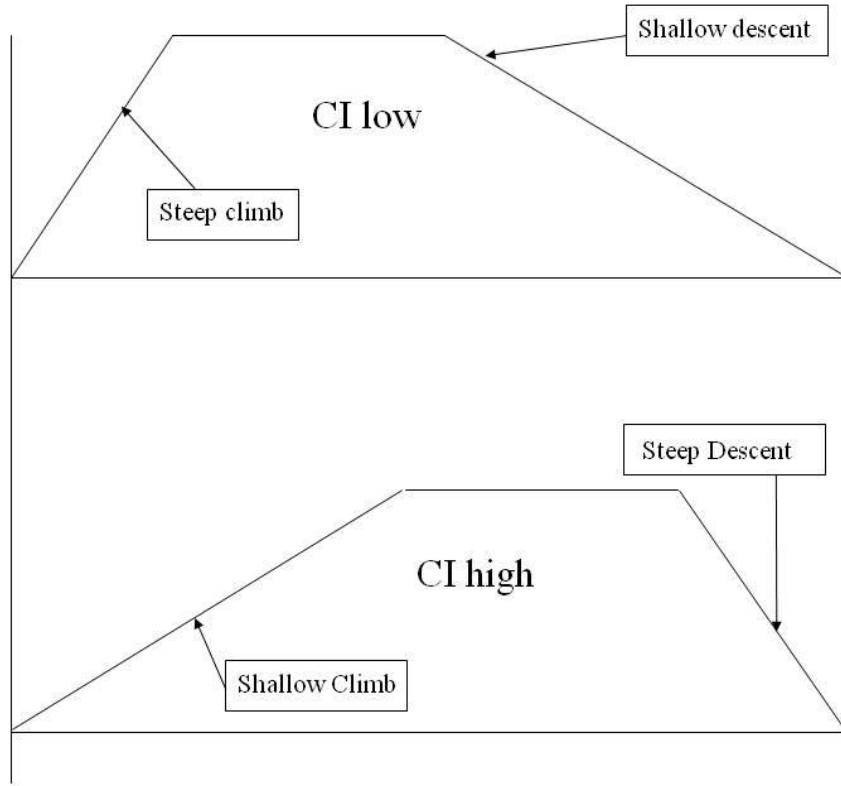


Figure 9: Overview of the influence of the cost index on the flight profile

Figure 9 clearly shows that the cost index has an influence on the climb and descent profiles which shouldn't be ignored. This is especially important when several aircraft are flying with different cost indices. This is precisely one of the difficulties for air traffic control. Several conflicts may be encountered: for example, if an aircraft with a low cost index is descending in front of an aircraft with a higher cost index, the second aircraft will be catching up with the first one because it is flying faster. This situation can be resolved by air traffic control by giving a speed restriction or a lateral deviation to the second aircraft. But this will mean that the second aircraft is not flying at its optimal speed. Consequently, there will be a higher cost for the second aircraft (higher time cost which can't be compensated by the lower fuel cost by flying slower).

### 2.7.4. Impact of deviations from the optimal profile

Using the cost index the optimal profile is determined but due to several reasons, the aircraft could be located above or below the optimal profile. These two cases will result in a higher cost. For example, when an aircraft descending towards the airport is above its optimal path, it will have burnt more fuel during extra level segments (for example when the aircraft has to stay longer on its cruise level). When the aircraft is below its optimal path, there will be more time needed for the descent when it is flown in idle operation. It could also result in a fuel burn increment when thrust is used (for example when a level part is flown). This could happen when the aircraft had to descent before the optimal top of descent.

### **2.7.5. Influence of different cost indices**

When all airlines are using different cost indices, all aircraft are flying at a different speed. This is very hard for air traffic control because additional interventions are needed to keep aircraft separated. This is for example the case when low cost airlines are flying at a very low cost index. They are consequently flying at low speeds, which has consequences for all following aircraft. Indeed, the aircraft flying behind a slower aircraft can get a speed restriction to maintain the required separation. This would mean that the following aircraft can't fly on its desired cost index anymore which results in a higher cost. To counteract this phenomenon, the European Commission and Eurocontrol are considering a system that improves the harmonization of the air traffic [21]. This could be done by setting a range of cost indices that can be used by the airlines. If an airline decides to use a cost index outside the range, a cost penalty will be given. In fact, this extra cost should then be added as an additional factor in the calculation of the cost index. This should encourage airlines to use a cost index in the prescribed range so that a more harmonized air traffic is obtained.

## 3. Software tools

### 3.1. BADA

The Base of Aircraft Data (BADA) version 3.9 is an aircraft performance model which provides a database of files with performance coefficients for 338 different aircraft types. These coefficients can be used to calculate for example thrust, drag, fuel flow and reference speeds during different flight phases. The BADA User manual provides the theoretical background and the expressions to calculate the different performance parameters. The information in the files is intended to be used in trajectory simulations to validate and analyse new ATM concepts or ATC procedures, for prediction algorithms, to plan traffic flows, for environmental studies with respect to aircraft emission,...

Several types of files are provided of which the most important are:

- Operations performance files: files containing the performance parameters for a particular aircraft type.
- Performance table files: files which summarize performance characteristics such as true air speed, rates of climb and descent and fuel flow at different flight levels for a specific aircraft type.
- Performance table data: similar to the Performance table files but with more detailed performance data.

The data which are available in the different files are intended to be used in several equations and models which are described in [22]. The atmospheric model (see 4.1) and the total energy model (see 4.2) are the most important ones and will also be used in this work. The principle data that are used from the files are thrust, drag and fuel flow coefficients and typical weights.

#### 3.1.1. Drag calculation

The drag is calculated using the well known relations [22]:

$$C_L = \frac{2mg}{\rho V^2 S \cos \phi} \quad (3.1)$$

$$C_D = C_{D0} + C_{D2} \cdot (C_L)^2 \quad (3.2)$$

$C_{D2}$  is the coefficient that is more commonly written as k. This notation is used to be coherent with the BADA database.

$$D = \frac{C_D \cdot \rho \cdot V^2 \cdot S}{2} \quad (3.3)$$

#### 3.1.2. Thrust calculation [22]

Thrust determination is done depending on the phase of flight, the type of engines, the pressure altitude h and the true airspeed V. The maximum climb and takeoff thrust is calculated as follows:

Jets: 
$$F_{A,\text{max climb}} = C_{Tc,1} \cdot \left( 1 - \frac{h}{C_{Tc,2}} + C_{Tc,3} \cdot h^2 \right) \quad (3.4)$$

Turboprops: 
$$F_{A,\text{max climb}} = \frac{C_{Tc,1}}{V} \cdot \left( 1 - \frac{h}{C_{Tc,2}} \right) + C_{Tc,3} \quad (3.5)$$

With:  $F_A$ : Thrust (Newton)  
 $C_{Tc,1}, C_{Tc,2}, C_{Tc,3}$ : Coefficients provided by BADA

(3.4) shows that the thrust of jet powered aircraft is assumed to be constant at a particular altitude, so it is independent of the velocity.

In normal operations, the maximum climb power isn't used to save on maintenance costs and extend the engine life time. A factor is used to come up with the reduced climb power:

$$C_{pow,red} = 1 - C_{red} \frac{m_{\text{max}} - m_{\text{act}}}{m_{\text{max}} - m_{\text{min}}} \quad (3.6)$$

With:  $C_{pow,red}$ : Coefficient to be used in the rate of climb or descent calculation

$C_{red}$ : Coefficient provided by BADA

$m_{\text{max}}$ : Maximum aircraft weight

$m_{\text{act}}$ : Actual aircraft weight

$m_{\text{min}}$ : Minimum aircraft weight

$C_{pow,red}$  must then be added as a factor in the equation to calculate the rate of climb or descent.

The cruise and descent thrust is calculated using a factor provided in the data files:

$$F_{A,\text{cruise max}} = C_{Tcr} \cdot F_{A,\text{max climb}} \quad (3.7)$$

$$F_{A,\text{descent}} = C_{Tdes} \cdot F_{A,\text{max climb}} \quad (3.8)$$

There are different coefficients for the descent thrust depending on the altitude and on the configuration of the aircraft.

### 3.1.3. Fuel burn calculation [22]

Finally, the fuel consumption is determined by first calculating the thrust specific fuel consumption (TSFC):

Jets: 
$$TSFC = C_{f1} \cdot \left( 1 + \frac{V}{C_{f2}} \right) \quad (3.9)$$

Turboprops: 
$$TSFC = C_{f1} \cdot \left( 1 - \frac{V}{C_{f2}} \right) \cdot \left( \frac{V}{1000} \right) \quad (3.10)$$

The nominal fuel flow can then be determined:

$$f_{\text{nom}} = TSFC \cdot F_A \quad (3.11)$$

To determine the fuel flow during a descent with the engine in idle thrust, coefficients for the minimum fuel flow are provided:

$$f_{\text{min}} = C_{f3} \left( 1 - \frac{h}{C_{f4}} \right) \quad (3.12)$$

There is another coefficient for the fuel consumption in cruise:

$$f_{cr} = TSFC \cdot F_A \cdot C_{fr} \quad (3.13)$$

### 3.2. V-PAT

The V-PAT tool, previously called EFICAT tool, from Eurocontrol was conceived to analyse the departure and arrival trajectories of aircraft. Initially the tool was designed to assess the descent profiles and how good aircraft were adhering to a continuous descent approach. The main interest is to determine the amount of level flight and where that level part has taken place during the arrival of each aircraft. By analyzing the flights arriving at a particular airport, we can look for positions and time periods where level parts are observed regularly. A similar analysis can be done for the departing aircraft to evaluate level parts during the climb.

#### 3.2.1. CCO analysis for Brussels Airport

##### 3.2.1.1. Scope of the analysis

In the past, descents into Brussels Airport were already examined by Belgocontrol in the B3 project [2] but there are no figures or analyses yet for departing traffic. So as a part of this Master thesis, an evaluation of the trajectories of the departing aircraft was made. For this, the flights which took off from Brussels Airport in September 2012 were analysed.

##### 3.2.1.2. Analysis parameters

V-PAT allows to filter the available radar data so that only the data, in which we are interested, are being displayed. The parameters as used during the analyses are shown in Table 1:

Table 1: Overview of the V-PAT parameters

Parameter	Setting
Above/Below Altitude Cut-Off	25,000 feet
Flight Level Tolerance	300 ft/min
Radius from ADEP	75NM
Last Plot Maximum Distance to ADEP	2 NM
Minimum Altitude Plot Cut-Off	0 feet
Optimum Climb Angle	3°
Shallow Climb Angle	2°
Use Shallow Angle in Algorithms	No
Noise Delta Altitude #1	10,000 feet
Noise Delta Altitude #2	4,000 feet
Ignore Flights Cruise Below	5,000 feet
Minimum Level Distance Above Altitude	0 NM
Minimum Level Distance Below Altitude	0 NM
Minimum Time for Level Plots	20 seconds

The reasoning behind these settings is as follows:

- Above/Below Altitude Cut-Off:

This parameter sets a vertical limit to the airspace in which the analysis is performed. Since data from Belgocontrol are used, the analysis can only be done inside the airspace of Belgocontrol as set by the

agreement with Eurocontrol and Belgocontrol. This airspace goes up to FL245<sup>16</sup> so 25,000 feet was selected as maximum altitude for the analysis since the program allows choosing between multiples of 1,000ft. However, it would be very interesting if the analysis could be performed without this limit.

- Flight Level Tolerance:

To determine when a part of a flight is flown level, the flight level tolerance is set. When the rate of climb between two radar plots is lower than the parameter setting, the flight is considered as flying level between these two plots. This parameter is also used to suppress any faulty results due to small errors of the altitude of the radar plots. The setting is retrieved in an empirical way by manually examining some flights and varying the parameter setting.

- Radius from ADEP:

For the lateral limitation of the airspace, the radius from the departure airport has to be set. The user can choose from a list with multiples of 25NM. For Brussels Airport, 75NM is chosen because this is the best approximation of the Belgian airspace.

- Last Plot Maximum Distance to ADEP:

To be sure that the considered flights have an as complete as possible set of radar plots, this parameter determines how far the first plot of a flight can be from the airport. If the first plot is further away than this distance, the flight is not considered in the analysis. Since the radar data of Belgocontrol are of good quality, a distance of 2 NM around Brussels Airport was chosen.

- Minimum Altitude Plot Cut-Off:

This parameter determines at which altitude the analysis is started. The first radar plots of some flights are at an altitude of 50 feet; so to take into account the complete climb to the maximum extend, this altitude was set to 0 feet.

- Optimum Climb Angle:

The optimum climb angle is not considered in the current study because the calculations are made for a mix of departing aircraft with large differences in optimum climb angle. V-PAT uses the optimum climb angle when the shallow angle algorithm is activated and for the calculation of noise deltas. The shallow angle algorithm is not used and the noise deltas are not considered.

- Shallow Climb Angle:

Default values are kept because the shallow angle algorithm is not used.

- Use Shallow Angle in Algorithms:

This option allows having a correction of the results in case of radar plots with a low resolution. The radar data provided by Belgocontrol contain one plot every 4 seconds. The resolution is very well so there is no need to use the shallow angle algorithm.

---

<sup>16</sup> FL245: Flight level 245 corresponds to an altitude of 24,500ft assuming an altimeter setting of the international standard mean sea level pressure of 1013.25hPa.

- Noise Delta Altitude #1/#2:

Default values are kept because the noise deltas are not considered.

- Ignore Flights Cruise Below:

Flights which have their cruise altitude below this parameter setting will be ignored by the analysis. FL 50 is chosen as the minimum cruise level for the considered flights. This level is pretty low but is used to include also some flights towards nearby airports.

- Minimum Level Distance Above Altitude:

This parameter sets the amount of level flight that can be ignored above the Above/Below Altitude Cut-Off parameter. This parameter was not used since it only influences flights that are outside the Belgian airspace (above FL245).

- Minimum Level Distance Below Altitude:

Analogous to the previous parameter, this parameter sets the amount of level flight that can be ignored but now below the Above/Below Altitude Cut-Off parameter. To get a clear view of the whole distance flown level, this parameter was set to zero. Care must be taken that the ground roll or part of it or taxi plots are not considered as level flight. This has only been seen for a small amount of flights.

- Minimum Time for Level Plots:

To avoid that V-PAT considers a flight segment between 2 plots as level flight due to a limited resolution of the radar data, every level segment of less than 20 seconds is disregarded. This setting resulted from the assessment of several flights.

### ***3.2.1.3. Analysis setup***

To analyse the departing traffic, the flights are divided according to the 4 principal exit directions:

- N
- E-SE
- SW
- WNW

These sectors are represented in Figure 10 and Figure 11 which display all flights on two representative days: respectively 28/09/2012 with departures mainly from runways 25 and 23/09/2012 with departures from runways 07.

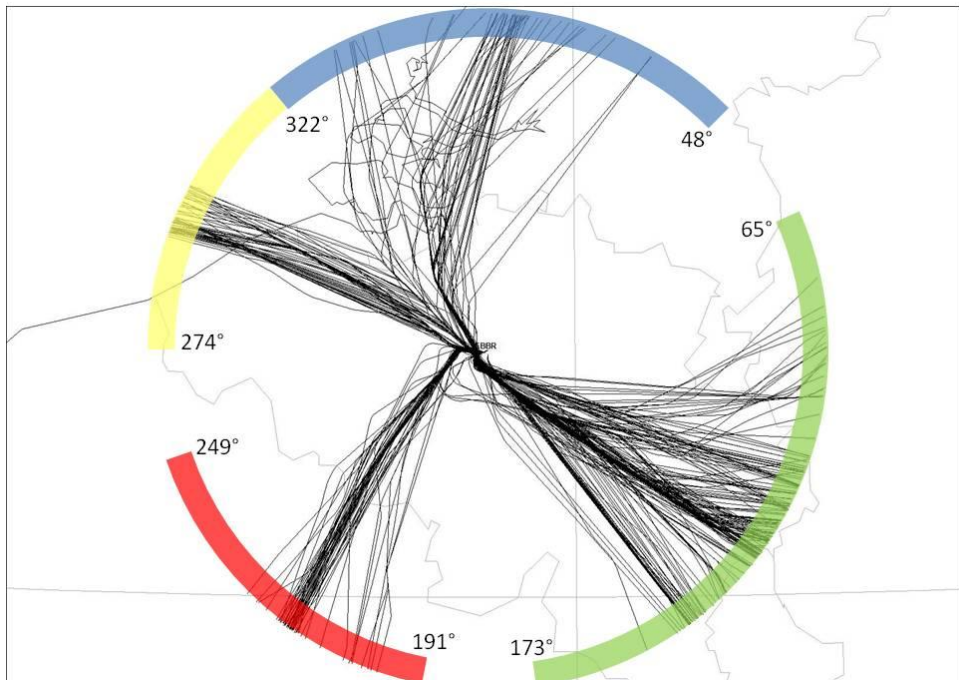


Figure 10: Exit sectors with their respective limits (departures from runways 25 within a radius of 75NM)

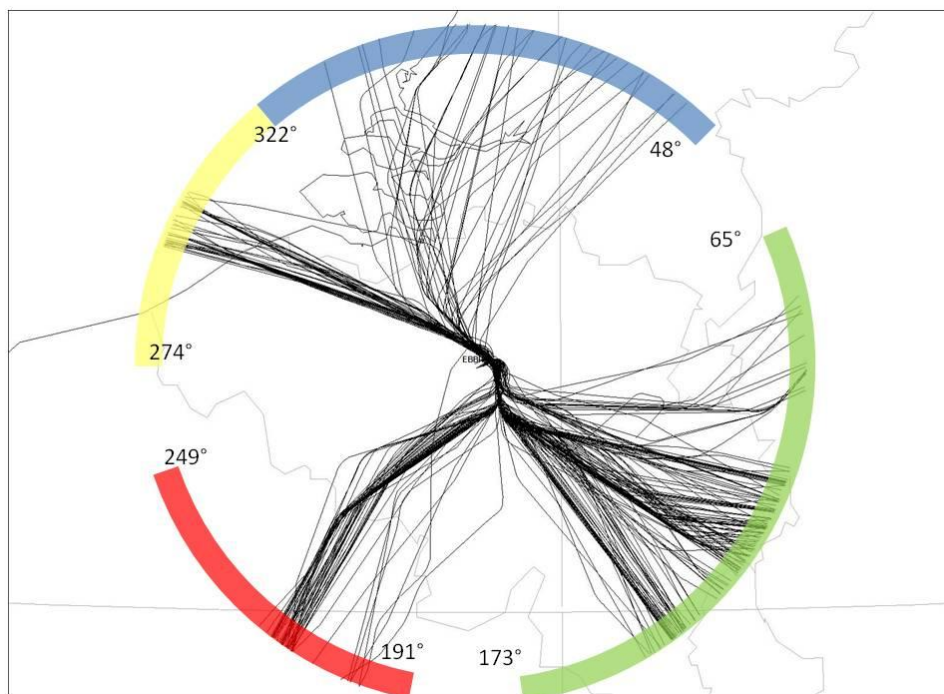
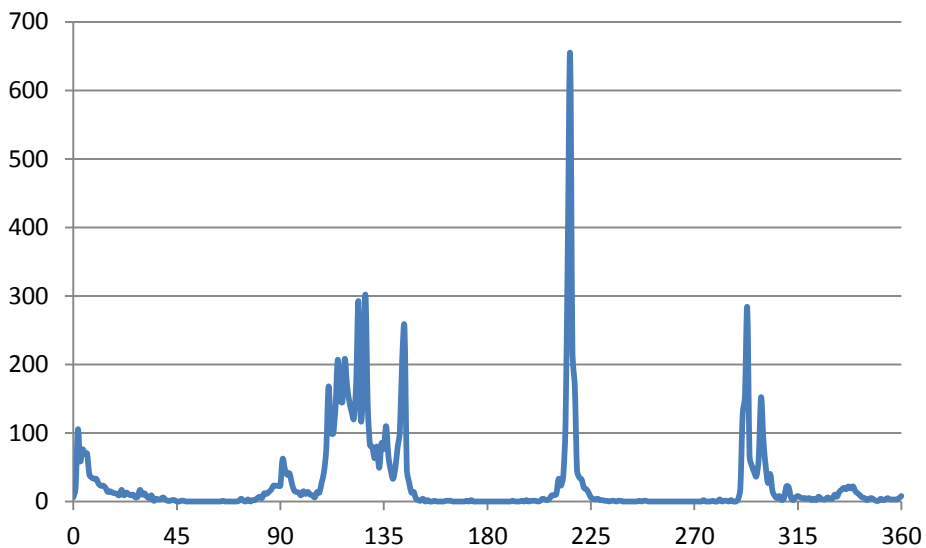


Figure 11: Exit sectors with their respective limits (departures from runways 07 within a radius of 75NM)

The bearing intervals for the different exit directions were determined using a scatter plot (Figure 12). A bearing is the angle between the North-South axis and the line connecting the aerodrome reference point with the exit point. The intervals retrieved from the radar data are presented in Table 2:

**Table 2: Bearing intervals of the exit sectors**

Exit sector	Bearing interval
N	322°-48°
E-SE	65°-173°
SW	191°-249°
WNW	274°-322°



**Figure 12: Scatter plot of the exit bearings**

To see the difference between flights flying at daytime and at night, the analysis is also done for these two time periods. The time period from 04:00 to 20:59 (UTC<sup>17</sup> time) is considered being daytime and night goes from 21:00 to 03:59. The UTC time is used since the radar data are also using the UTC time [23]. The chosen time periods are the same as those used for the preferential runway system at Brussels Airport.

#### **3.2.1.4. Results of the analysis**

The data from V-PAT were subdivided according to their departure runway, exit sector and the departure period of the flight (day or night). To have a global overview of the situation, first all flights are analysed together regardless of their departure time. Then the flights during daytime and night are analysed separately to see any differences between them. The detailed results of the analyses can be found in Results of the climb analyses.

##### **3.2.1.4.1. Analysis of all flights**

This global analysis allows having a first overview of the current situation regarding departing traffic from Brussels Airport. In the available data, from runway 20 there are only 3 flights departing to the North and 6 flights departing to the Southwest. Since these data are statistically irrelevant, these flights are not considered in the analysis.

First the amount of flights that have a level part in their departure profile is examined. The average is around 9.3% of flights with a level part, ranging from 4.3% to 19.2% depending on the exit sector and

<sup>17</sup> UTC: Coordinated Universal Time: Standard time to which many countries define their standard time. For example, Belgium is in the time zone UTC+01:00 (in wintertime).

the departure runway. The flights departing from runway 20 have the lowest average: 4.3%. In September 2012, runway 20 was only used due to the preferential runway use system. This system is used to distribute the noise pollution around Brussels Airport and foresees the use of runway 20 during periods with a low amount of traffic. This can be a reason for the low average. As an example, the horizontal and vertical profiles of the flights leaving to the East and Southeast on 14/09/2012 are respectively shown in Figure 13 and Figure 14. The corresponding profiles of only the flights that have a level part are depicted in Figure 15 and Figure 16. The profiles of the flights leaving to the other exit sectors are shown in Profiles of departing traffic. The same pictures for a typical weekend day are also given in Profiles of departing traffic. The level parts in the climb profiles are only due to traffic separation because there are no procedures containing level-off parts. North of Brussels Airport, departing traffic can initially climb only until FL60 because arriving traffic is flying at FL70 (a standard separation of 1,000ft is applicable). Around 50 to 60NM east of Brussels Airport, there is a similar conflict with aircraft going towards Brussels Airport and aircraft leaving Düsseldorf and Cologne. These are possible reasons for the level parts in the climb profiles and they clearly show the complexity of finding solutions to achieve the goals of SESAR (see 2.3). When one would change something to improve a certain situation, this could have negative consequences for a lot of other situations.

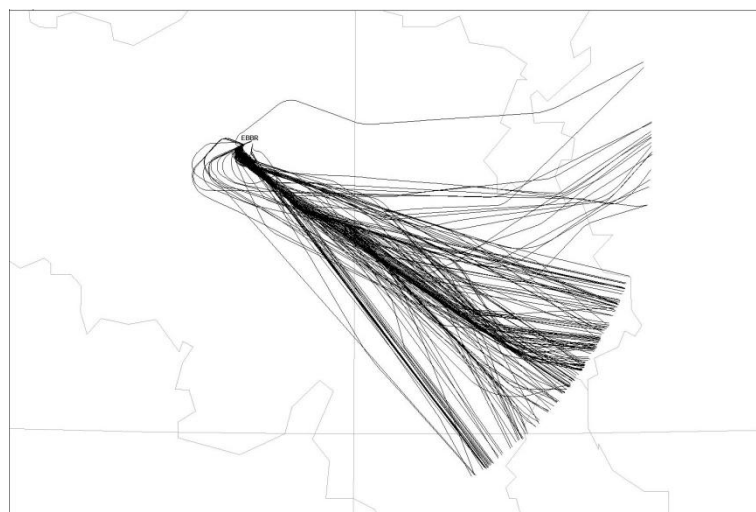


Figure 13: Horizontal profiles of the flights leaving to the East and Southeast on 14/09/2012

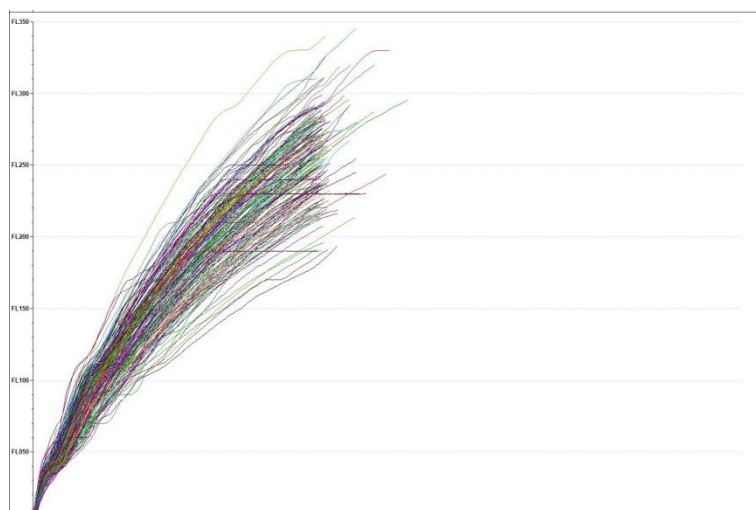


Figure 14: Vertical profiles of the flights leaving to the East and Southeast on 14/09/2012



Figure 15: Horizontal profiles of the flights with a level part leaving to the East and Southeast on 14/09/2012

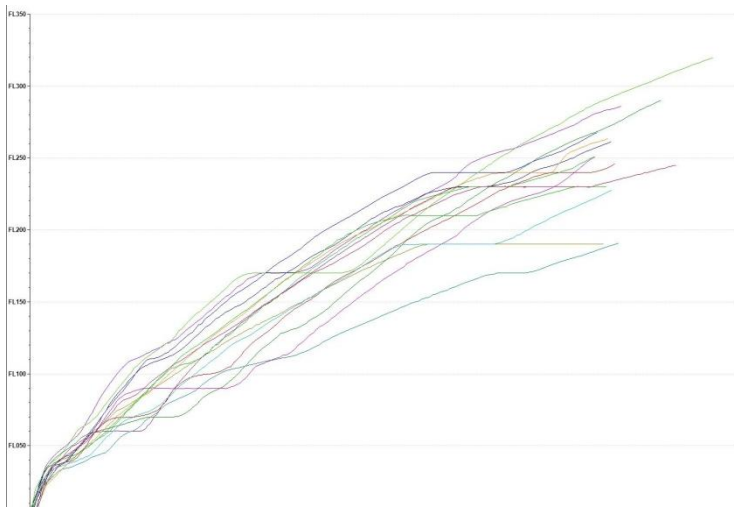


Figure 16: Vertical profiles of the flights with a level part leaving to the East and Southeast on 14/09/2012

The previously mentioned percentages don't take into account the amount of level flight which is of course more important. When looking at the amount of level flight we see that the average distances range from 3.7 NM to 8.4 NM depending on the runway and departure direction. The total distance flown is 63.2NM on average which results in 6.0% to 12.8% of level flight during the climb phase. This can have several reasons: arriving aircraft, overflying aircraft, separation rules, airspace limitations,... Analogously, the average time of level flight is calculated: from 40 to 88 seconds over an average total climb time of about 12 minutes. These results might be a direct consequence of the settings of the analysis parameters. Ideally, every flight should be analysed separately to see the real situation but this is very impractical considering the large amount of flights (9641 departing flights in September 2012 are retrieved from the available data).

From the V-PAT data the average fuel consumption and CO<sub>2</sub> emission is deduced. Unfortunately, these data can't be used to make any conclusions. For example 19.2% of the flights departing from runway 07 to the West Northwest have a level part which is around two times more than the flights leaving to the Southwest. Remarkably the flights to the Southwest would use some 50kg more fuel than the ones leaving to the West Northwest. Normally, one would expect that this would be the other way around. This is due to the way of calculating the fuel consumption in V-PAT. For this, V-PAT uses fixed values for the fuel consumption in level, descending and climbing flight with a higher fuel consumption in climbing flight than in level flight. V-PAT doesn't see whether the flight has already

reached his cruising altitude when going beyond the analysis radius. Indeed, we would expect that an aircraft that has a level part during the climb phase would burn more fuel before reaching his top of climb than an aircraft that can climb uninterruptedly. Figure 17 visualizes the situation where comparing V-PAT results leads to wrong conclusions. The green flight path is an uninterrupted climbing flight and the red flight has a level part in its climb. The red flight will have a shorter cruise part but will have a higher fuel burn until the top of climb because the aircraft is flying level at a lower altitude than the cruise altitude. Aircraft typically burn more fuel at lower altitudes than at cruising altitude. V-PAT will calculate the fuel consumption until the analysis radius so it will give a smaller fuel burn for the red flight due to the level part. More relevant would be to know how much fuel is used until a common point on the cruise profile is reached (e.g. TOC 2 in Figure 17). The V-PAT tool doesn't allow this so a relevant comparison for the fuel consumption is not possible here. The emission of CO<sub>2</sub> is directly linked with the fuel consumption:

$$3,14 * \text{mass fuel burnt (kg)} = \text{mass CO}_2 \text{ emitted (kg)} \quad (3.14)$$

Due to this relation, also no conclusions can be made for the CO<sub>2</sub> emission.

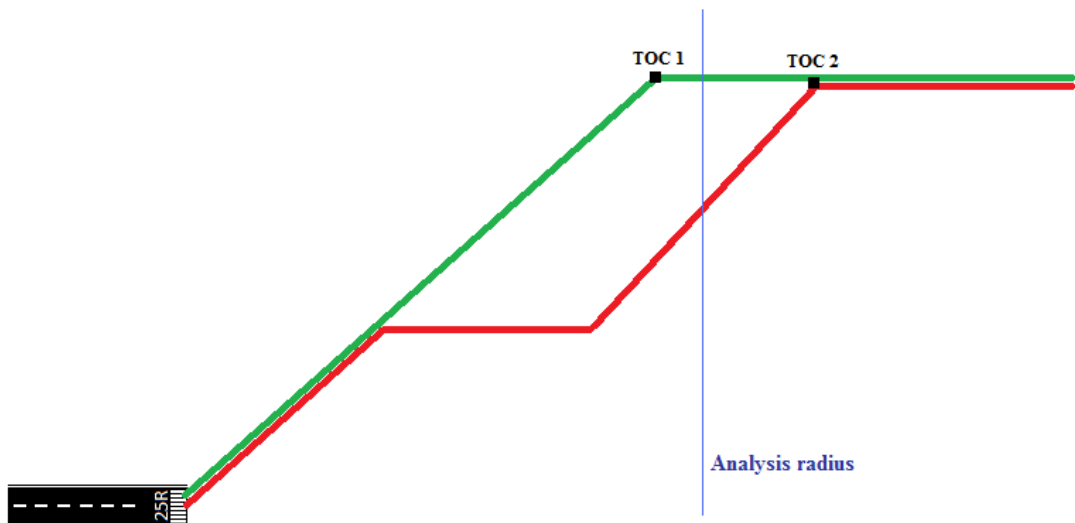


Figure 17: Illustration for the bad fuel results in V-PAT

Additionally, V-PAT provides the average climb angle of every flight. The overall average climb angle is 3.7°.

#### 3.2.1.4.2. Analysis of daytime flights

The data for the daytime flights present approximately the same results as for the analysis of all flights. This is quite normal since 96.4% of the departures take place during daytime. The average values differ only up to 3.1% from the average values of the analysis of all flights so the conclusions made above are valid here as well. Though, there is a large difference of around 14% for the fuel burn and CO<sub>2</sub> emission for flights departing from runway 20. Since the calculations of the fuel burn aren't reliable, these figures are not considered.

#### 3.2.1.4.3. Analysis of night flights

The results of the analysis of the night flights are somewhat different than the results of the previous analyses. This might be, among other reasons, the consequence of the low traffic density during this

time frame. In this analysis there are only few flights departing from runway 07 to all directions and from runway 20 to the North and Southwest so they are not taken into account.

Very remarkable is that the amount of flights that have a level part in their climb is much lower: from 1.8% up to only 6.3% depending on their exit sector. This is around a third of the corresponding results for all flights.

As a direct result of the lower traffic density, the total distance flown is less than during daytime (1 to 6.9 NM less). Some operational reasons might be the cause of this. Another reduction is seen for the amount of level flight: the distance of level flight in the climb (for flights having a level part) appears to be lower than for day flights, except for the flights leaving to the Southwest and West Northwest from runway 25. However, there are very few flights with a level part so these longer level parts could be statistical coincidences.

The time needed for the climb in the Brussels airspace is shortened with 0.5 to 1.5 minutes except again for the flights leaving to the West Northwest from runway 25.

The average climb angles are similar to those of the daytime flights and as before, the results of the fuel consumption and the CO<sub>2</sub> emission are not analysed since they are not calculated in a consistent way.

### **3.3. Flight data management tools**

Flight data from Thomas Cook are made available through the Fuel Efficiency tool from Aviaso [16]. This tool allows to extract specific parameters needed for a certain analysis, follow up certain initiatives and have an overview of the fuel efficiency of the airline. The different data can be exported in a number of graphical presentations which simplifies the assessment of the data. A similar tool was used with the flight data of Jetairfly.

## 4. Descent and climb profiles

### 4.1. Atmospheric model

Aircraft performance is highly depending on the atmospheric conditions in which the flight is undertaken. Since these conditions are continuously changing, a reference situation is taken. Here the general International Standard Atmosphere model is taken as a reference, which is also adopted by ICAO. This standard uses a model for the temperature, pressure and density of the air. The models used in this work are as stated in [22], [24]. The reference temperature at sea level is 15°C ( $T_0$ ) with a pressure of 1013.25 hPa ( $P_0$ ) and an air density of 1.225kg/m<sup>3</sup> ( $\rho_0$ ).

#### 4.1.1. Temperature model

Temperature decreases by -6.5°C/1000m or -1.98°C/1000ft in the troposphere until the tropopause is reached, which has a standard altitude of 11,000m or 36,089ft. Above that altitude, the temperature remains constant at -56.5°C until the stratosphere which starts at an altitude of 20,000m or 65,617ft. This altitude will never be reached by a commercial airliner so only the model for the troposphere and tropopause are used. The following formula will be used in the troposphere:

$$\text{ISA temperature } (\text{°C}) = T_0 - 1.98 \times \frac{\text{altitude (feet)}}{1000} \quad (4.1)$$

Figure 18 shows the temperature evolution according to the altitude:

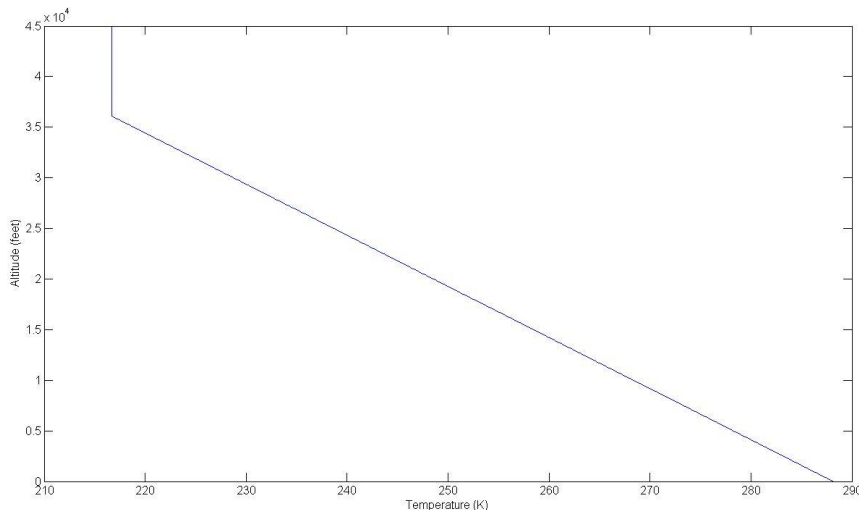


Figure 18: Temperature evolution in ISA conditions

#### 4.1.2. Pressure model

The pressure at a certain altitude is calculated with the assumptions that the temperature is standard at every altitude and that air is a perfect gas. Using the aerostatic equation (4.2) and the perfect gas equation (4.3), an equation to calculate the pressure at a particular altitude in the troposphere is established:

$$dP = -\rho \cdot g \cdot dh \quad (4.2)$$

$$P = \rho \cdot R \cdot T \quad (4.3)$$

$$\frac{dP}{P} = -\frac{g}{R \cdot T} dh \quad (4.4)$$

$$\int_{P_0}^P \frac{dP}{P} = -\frac{g}{R} \int_{h_0=0}^h \frac{dh}{T_0 - \alpha h} \quad (4.5)$$

$$\ln \frac{P}{P_0} = \frac{g}{\alpha R} \ln \left( \frac{h - \frac{T_0}{\alpha}}{-\frac{T_0}{\alpha}} \right) \quad (4.6)$$

$$P = P_0 \left( 1 - \frac{\alpha h}{T_0} \right)^{\frac{g}{\alpha R}} \quad (4.7)$$

With:  $\alpha = 0.0065 \text{ K/m}$

Above the tropopause this becomes:

$$\int_{P_t}^P \frac{dP}{P} = -\frac{g}{R \cdot T_t} \int_{h_t}^h dh \quad (4.8)$$

$$\ln \frac{P}{P_t} = -\frac{g}{R \cdot T_t} (h - h_t) \quad (4.9)$$

$$P = P_t e^{-\frac{g}{R \cdot T_t} (h - h_t)} \quad (4.10)$$

With:  $P_t = 226.15 \text{ hPa}$  (standard pressure at 36,089ft)

$T_t = 216.69 \text{ K}$  (standard temperature at 36,089ft)

Figure 19 shows the pressure evolution with respect to the altitude:

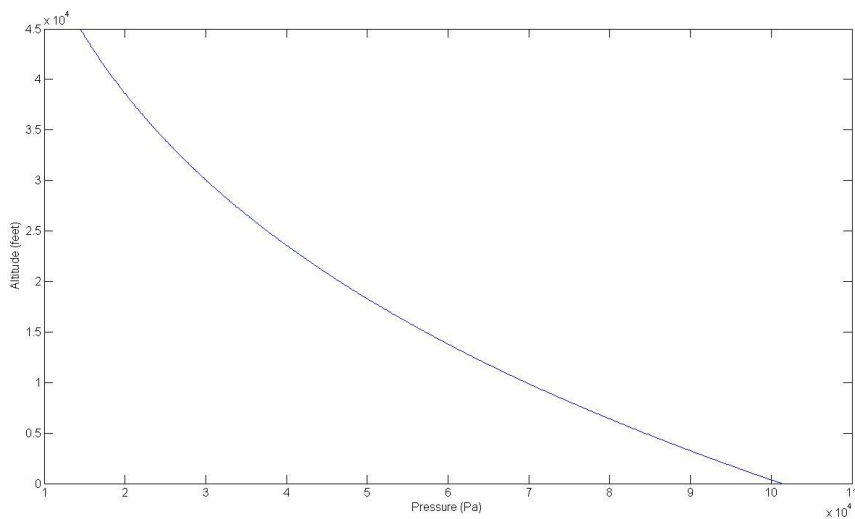


Figure 19: Pressure evolution in ISA conditions

#### 4.1.3. Density model

Since the air is assumed to be a perfect gas, the density is calculated using the perfect gas law (4.3).

Figure 20 shows the evolution of the air density in ISA conditions:

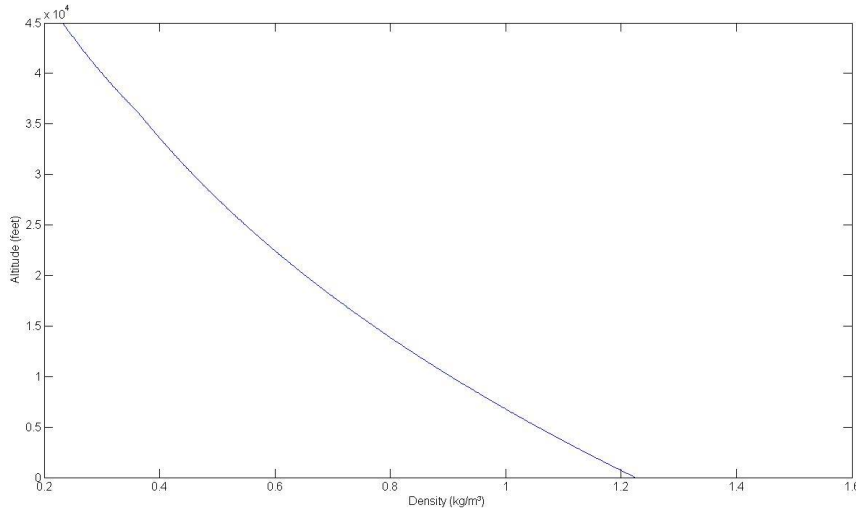


Figure 20: Density evolution in ISA conditions

## 4.2. Governing equations for performance calculations

The equations needed for the calculations are derived from the general governing equations retrieved from [25]:

$$W \left( \frac{\dot{V}}{g} + \sin \gamma \right) = -\frac{1}{2} \rho V^2 S C_D + F_A \cos \varepsilon_F \cos \beta \quad (4.11)$$

$$W \left( \frac{r_{a/e}}{g} \cdot V - \cos \gamma \cdot \sin \mu \right) = \frac{1}{2} \rho V^2 S C_{SF} - F_A \cos \varepsilon_F \sin \beta \quad (4.12)$$

$$W \left( \frac{q_{a/e}}{g} \cdot V + \cos \gamma \cdot \cos \mu \right) = \frac{1}{2} \rho V^2 S C_L + F_A \sin \varepsilon_F \quad (4.13)$$

With:  $\gamma$  = angle between the flight path and the horizontal going through the center of gravity

$\varepsilon_F$  = angle between the thrust vector and the flight path

$\beta$  = sideslip angle (angle between the flight path and the airspeed vector)

$\mu$  = part of the bank angle between the airspeed vector and the horizontal going through the center of gravity

We assume symmetric flight so equations (4.11)-(4.13) respectively become:

$$W \left( \frac{\dot{V}}{g} + \sin \gamma \right) = -\frac{1}{2} \rho V^2 S C_D + F_A \quad (4.14)$$

$$\frac{1}{2} \rho V^2 S C_{SF} = 0 \quad (4.15)$$

$$W \cdot \cos \gamma = \frac{1}{2} \rho V^2 S C_L \quad (4.16)$$

In (4.14)-(4.16) the angle between the thrust vector and the flight path is considered to be negligible. This angle varies between 0° and 5° so it is acceptable to neglect its impact.

### 4.3. Performance during climb

The way of executing the climb phase is depending on the priorities of the aircraft operator. For example, a climb of a military aircraft will differ significantly from the climb of a civil transport aircraft. In the literature, generally two typical climb trajectories are described: one with a minimum fuel burn and one with the shortest time to climb. In reality however, airlines are working with the cost index which is an indicator of the trade-off made between the cost of time and the cost of fuel (see 2.7). A cost index of 0 will provide a climb with minimal fuel usage while a high cost index results in a minimum of time needed for the climb.

#### 4.3.1. Initial developments

The following equations are used to obtain an expression for the rate of climb R/C<sup>18</sup>:

$$\sin \gamma = \frac{R/C}{V} \quad (4.17)$$

$$\dot{V} = \frac{dV}{dt} = \frac{dV}{dz} \cdot \frac{dz}{dt} \quad (4.18)$$

We obtain using (4.14):

$$R/C = \frac{F_A - D}{W \left( \frac{1}{g} \cdot \frac{dV}{dz} + \frac{1}{V} \right)} = \frac{(F_A - D)V}{W} \left( \frac{V}{g} \cdot \frac{dV}{dz} + 1 \right)^{-1} \quad (4.19)$$

The last factor in (4.19) is called the energy share factor which specifies how much of the available power is used for climbing during a climb procedure. The remaining part of the available power is then used for acceleration.

These equations are developed using the forces acting on the aircraft. Since the speed and acceleration during the climb are changing, this has to be accounted for. A different approach is given by the concept of energy height, which considers the changes of energy as presented in [25], [26]. When considering an aircraft at a particular altitude and speed, we can determine its total energy:

$$E = E_p + E_k = mgh + \frac{mV^2}{2} \quad (4.20)$$

The specific energy is then defined as:

$$E_s = \frac{mgh + \frac{mV^2}{2}}{W} = h + \frac{V^2}{2g} \quad (4.21)$$

The specific energy is independent of the aircraft characteristics and is also called the energy height  $h_e$ . This is the altitude that an aircraft can reach when all its kinetic energy is traded for potential energy. The energy height as a function of the Mach number is given in Figure 21. The lines in this figure are lines of constant energy height: 5,000ft for the lower line and 50,000ft for the upper one with an interval of 5,000ft for the intermediate lines.

---

<sup>18</sup>R/C: Rate of climb: the amount of altitude which is gained per unit of time.

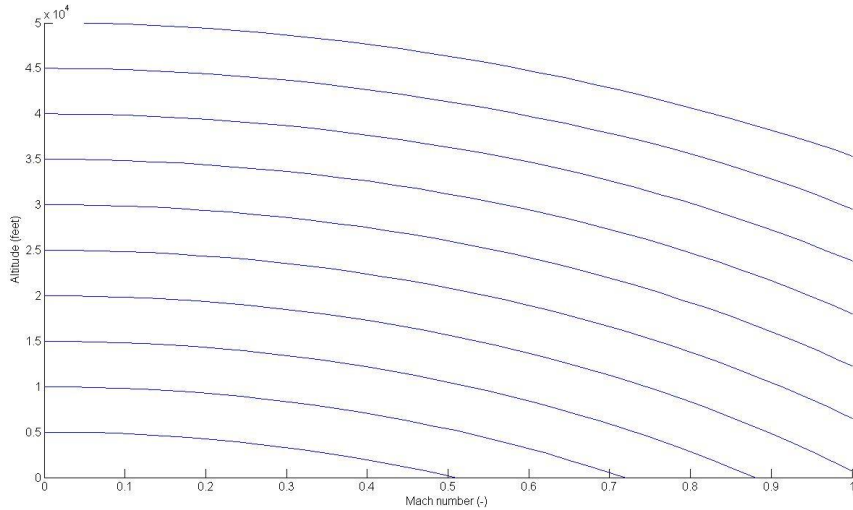


**Figure 21: Constant energy height lines with respect to the Mach number**

The derivative of the energy height with respect to time is the specific (excess) power  $P_s$ :

$$P_s = \frac{dh_e}{dt} = \frac{dh}{dt} + \frac{V}{g} \frac{dV}{dt} \quad (4.22)$$

Considering the force equilibrium (4.14), this can further be rewritten:

$$F_A = D + W \sin \gamma + \frac{W}{g} \frac{dV}{dt} \quad (4.23)$$

$$\sin \gamma = \frac{F_A - D}{W} - \frac{1}{g} \frac{dV}{dt} \quad (4.24)$$

$$V \sin \gamma = \frac{dh}{dt} = \frac{(F_A - D)V}{W} - \frac{V}{g} \frac{dV}{dt} \quad (4.25)$$

Using (4.22), we can come up with the final expression for the specific energy:

$$\frac{dh_e}{dt} = P_s = \frac{(F_A - D)V}{W} \quad (4.26)$$

This expression is used for jet aircraft. For propeller equipped aircraft, this becomes:

$$P_s = \frac{P_A - P_R}{W} \quad (4.27)$$

#### 4.3.2. Time to climb

From (4.22), the time needed to go from one energy height to another can be calculated:

$$dt = \frac{dh_e}{P_s} \quad (4.28)$$

$$\Delta t = \int_{h_{e1}}^{h_{e2}} \frac{1}{P_s} dh_e \quad (4.29)$$

Relation (4.29) shows that the time to climb from one energy height to another is minimized if  $P_s$  is maximal at every energy height which is passed. These points are shown on a chart presenting the

energy height and the specific excess power as a function of the Mach number. If  $P_s$  is maximal for a given energy height, the  $P_s$  curve is tangent to that energy height curve. Connecting all of those points will give the trajectory to climb in the least amount of time.

This procedure is applied for a typical flight climbing to an altitude of 36,000ft (FL360) and a cruise Mach number of 0.78. This situation corresponds to an energy height of 44,867ft. A medium size jet powered aircraft such as the Boeing 737 or the Airbus 320 with a nominal weight is taken as an example because these types of aircraft are most commonly used at Brussels Airport. The data needed for the calculation are taken from the BADA database.

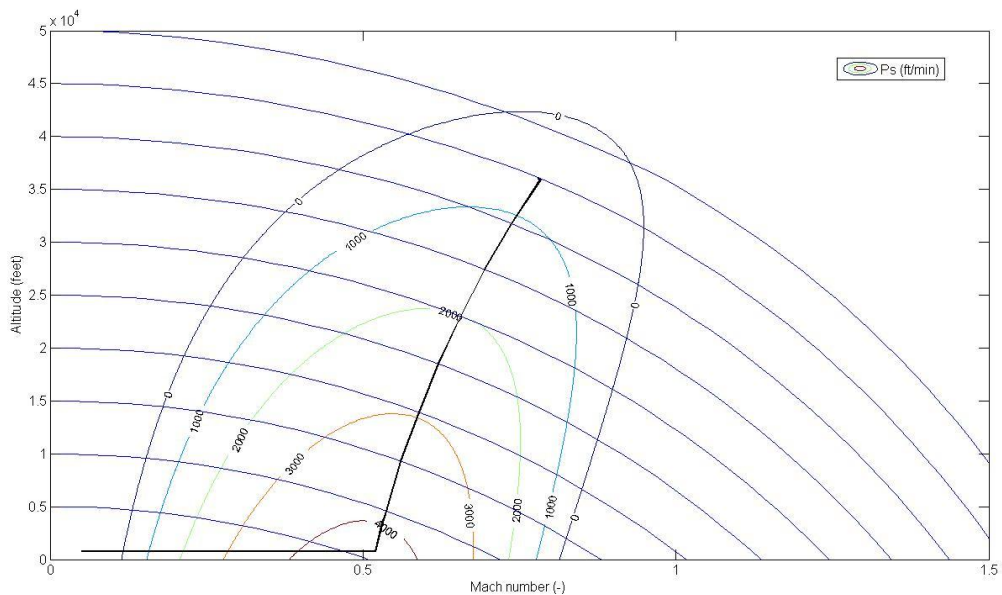


**Figure 22: Ideal climb profile with minimal time to climb**

As can be seen on Figure 22, to climb in the least amount of time possible, the aircraft initially has to accelerate at low level before climbing. Then it continues with a rather steep climb angle on a trajectory which connects points of maximum specific excess power at every energy height. The aircraft comes at an energy height of 44,867ft which corresponds to an altitude of 35,900ft and M0.784. Then the aircraft finishes its climb by remaining on the same energy height, climbing to 36,000ft and decelerating to M0.78. A zoom of this final part is presented in Figure 23.

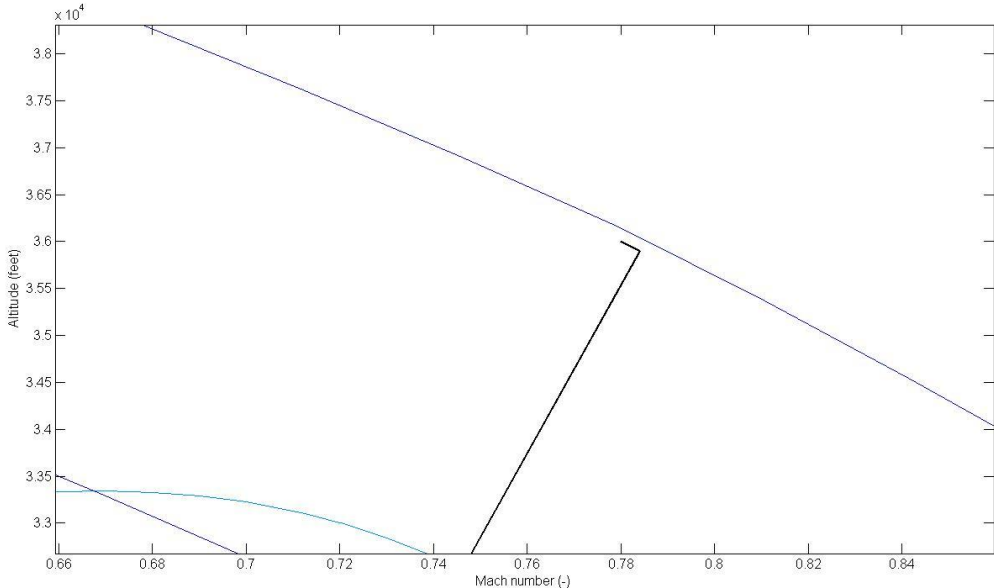


**Figure 23: Zoom of the final part of the climb (lowest time to climb)**

The initial acceleration part as proposed here is of course not feasible because this would mean that the aircraft would fly very low for a rather long time. This would have several disadvantages: noise pollution and high emissions above populated areas which would mean a lot more health issues and complaints from people living in a wide range around the airport. In addition, the aircraft needs to stay in the controlled airspace of Brussels Airport.

The time to climb can be determined numerically by integration. This is approximated by:

$$\Delta t_{h_{e,0}}^{h_{e,n}} = \sum_{i=0}^n \left[ \left( \frac{1}{P_S} \right)_{i,\text{avg}} * (h_{e,i+1} - h_{e,i}) \right] \quad (4.30)$$

With:

$$\left( \frac{1}{P_S} \right)_{i,\text{avg}} = 0.5 * \left( \frac{1}{P_{S,i}} + \frac{1}{P_{S,i+1}} \right) \quad (4.31)$$

This is applied on the example which shows that the aircraft will reach its top of climb after nearly 23 minutes, of which only 114 seconds are taken for the low level acceleration.

### 4.3.3. Fuel used during the climb

When an airline is only interested to fly at a low cost index, so to reduce the cost of the fuel, the trajectory with the least consumption of fuel will be preferred. To calculate the fuel used, the fuel specific energy  $f_s$  is defined:

$$f_s = -\frac{dh_e}{dW_f} = -\frac{dh_e/dt}{dW_f/dt} = -\frac{P_S}{dW_f/dt} \quad (4.32)$$

The rate of weight loss is related to the fuel flow FF:

$$\frac{dW_f}{dt} = -FF \cdot g = -TSFC \cdot F_A \cdot g \quad (4.33)$$

$$f_s = \frac{P_S}{TSFC \cdot F_A \cdot g} \quad (4.34)$$

$$dW_f = -\frac{TSFC \cdot F_A \cdot g}{P_S} dh_e \quad (4.35)$$

Consequently, the total fuel consumed when climbing from energy height  $h_{e1}$  to  $h_{e2}$  is calculated using:

$$\Delta W_f = \int_{h_{e1}}^{h_{e2}} \frac{1}{f_s} dh_e \quad (4.36)$$

This shows that the fuel consumed during the climb is minimal if  $f_s$  is maximum at every energy height which is passed. The trajectory which will consume the least amount of fuel is thus the line which connects all points where the plots of constant  $f_s$  are tangent to the plots of the energy heights.

The same example is taken as in the previous part for the minimum time to climb. Now, lines with constant  $f_s$  are plotted together with the lines of constant energy height (see Figure 24). The climb trajectory is similar to the trajectory for minimal time to climb, except that the climb angle is slightly steeper. This leads to the fact that the aircraft reaches its final energy height at a higher altitude than the requested altitude. This can clearly be seen on Figure 25: the aircraft has to descent again and accelerate further to the final altitude and speed.

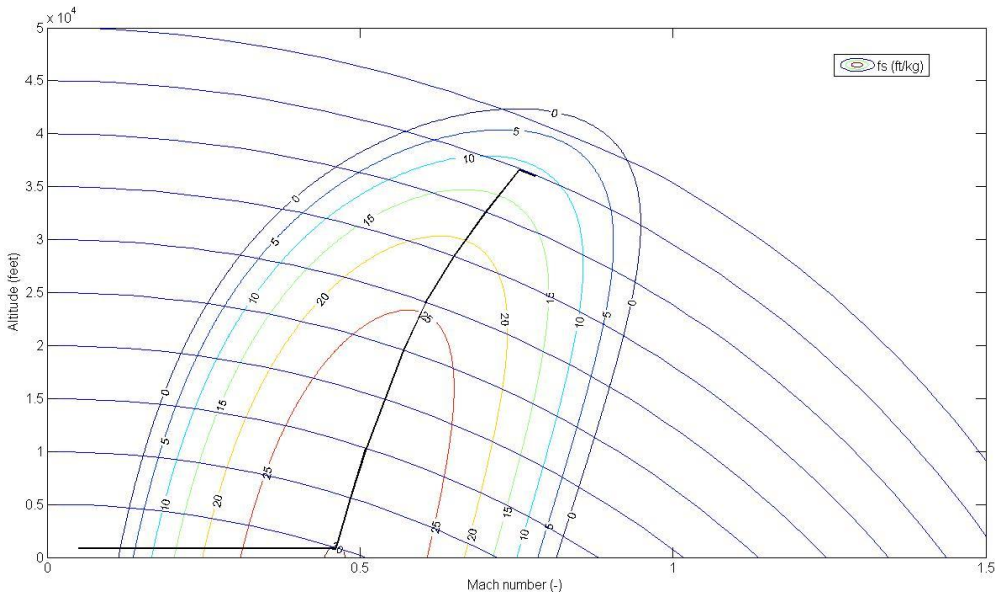


Figure 24: Ideal climb profile with minimal fuel to climb

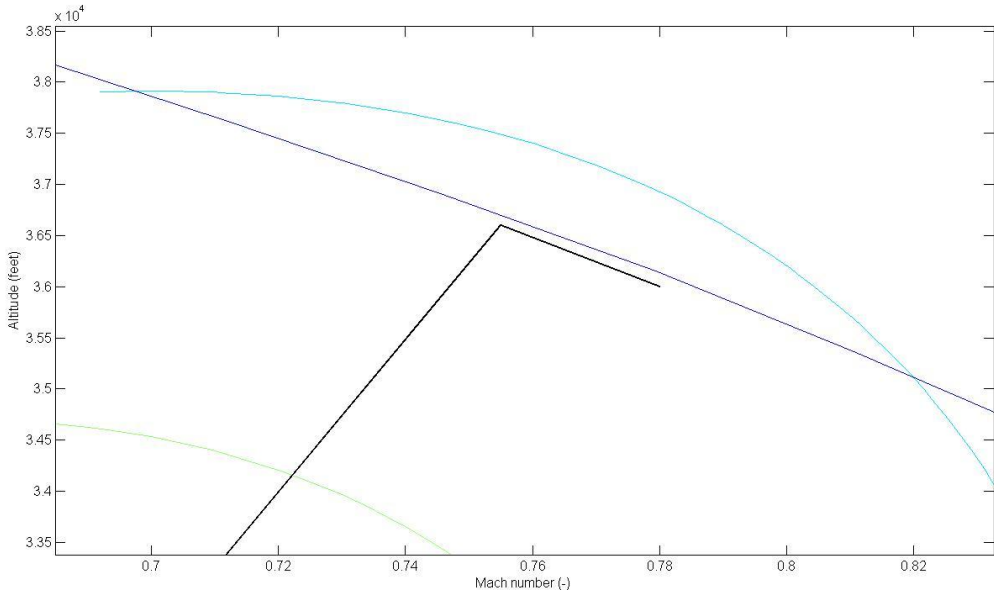


Figure 25: Zoom of the final part of the climb (minimum fuel to climb)

The fuel consumed during the climb is calculated similar to the calculation of the time to climb:

$$\Delta W_f^{h_{e,n}} = \sum_{i=0}^n \left[ \left( \frac{1}{f_S} \right)_{i,avg} * (h_{e,i+1} - h_{e,i}) \right] \quad (4.37)$$

With:

$$\left( \frac{1}{f_S} \right)_{i,avg} = 0.5 * \left( \frac{1}{f_{S,i}} + \frac{1}{f_{S,i+1}} \right) \quad (4.38)$$

This method gives a fuel burn for the climb of 1946kg of which 207kg of fuel is used for the level acceleration part.

#### 4.3.4. Current climb procedures

As stated before, the ideal climb profiles are not really useful and in strong contrast with the current climb procedures from Brussels Airport due to the noise abatement regulations. These procedures are described in the eAIS Package of Belgocontrol [27]. There are several SIDs<sup>19</sup> available depending on the departure runway and the destination of the aircraft.

The prescriptions concerning the climb gradient are the following: in order to minimize noise nuisance and to clear obstacles in the departure area, aircraft have to maintain a net climb gradient of at least 7% until passing 3,200ft. This corresponds to a climb angle of 4°. If unable to comply, pilots have to advise ATS accordingly when requesting start-up clearance.

In addition to all these regulations, there are general noise abatement procedures which are already implemented in the departure procedures. These are depending on the type of propulsion as can be seen in Table 3. The prescriptions for jet aircraft are in accordance with the ICAO-A procedure and the more recent NADP 1 procedure for noise abatement as stated in [28], [29].

---

<sup>19</sup> SID: Standard Instrument Departure: Published flight procedure for departing flights flying IFR (Instrumental Flight Rules)

Table 3: Noise abatement procedures for takeoff

	Turbojet aircraft	Propeller aircraft
From takeoff to 1,700ft	<ul style="list-style-type: none"> <li>• Takeoff power</li> <li>• Takeoff flaps</li> <li>• Climb to <math>V2^{20}+10</math> or 20kt or as limited by body angle.</li> </ul>	<ul style="list-style-type: none"> <li>• Takeoff power</li> <li>• Climb at maximum gradient compatible with safety</li> <li>• Speed not less than single engine climb speed, nor higher than best rate of climb speed.</li> </ul>
At 1,700ft	Reduce thrust to not less than climb thrust.	Reduce power to the maximum normal operating power (if this power has been used for showing compliance with the noise certification requirements) or to the maximum climb power.
From 1,700ft to 3,200ft	Climb at $V2+10$ or 20kt.	Climb at the maximum gradient with reduced power, maintaining constant speed.
At 3,200ft	Accelerate smoothly to en-route climb speed with flaps retraction.	Accelerate smoothly to en-route climb speed.

After consulting some airlines for their typical climb procedures, we see that the noise abatement procedures are adhered to. When reaching 3,200ft, acceleration is performed to 250kts below 10,000ft. After that the flight accelerates to the optimum climb speed and Mach number until the top of climb.

The switch between flying on an indicated airspeed (IAS) and flying at a specific Mach number is done at the crossover altitude. This altitude is depending on the cost index since the cost index is influencing the optimum climb and descent speeds. Figure 26 [18] shows the variation of the crossover altitudes depending on the cost index value for several Airbus aircraft families.

---

<sup>20</sup> V2: Takeoff safety speed. Flying at V2 ensures that the required climb gradient can be achieved in case of an engine failure during takeoff.

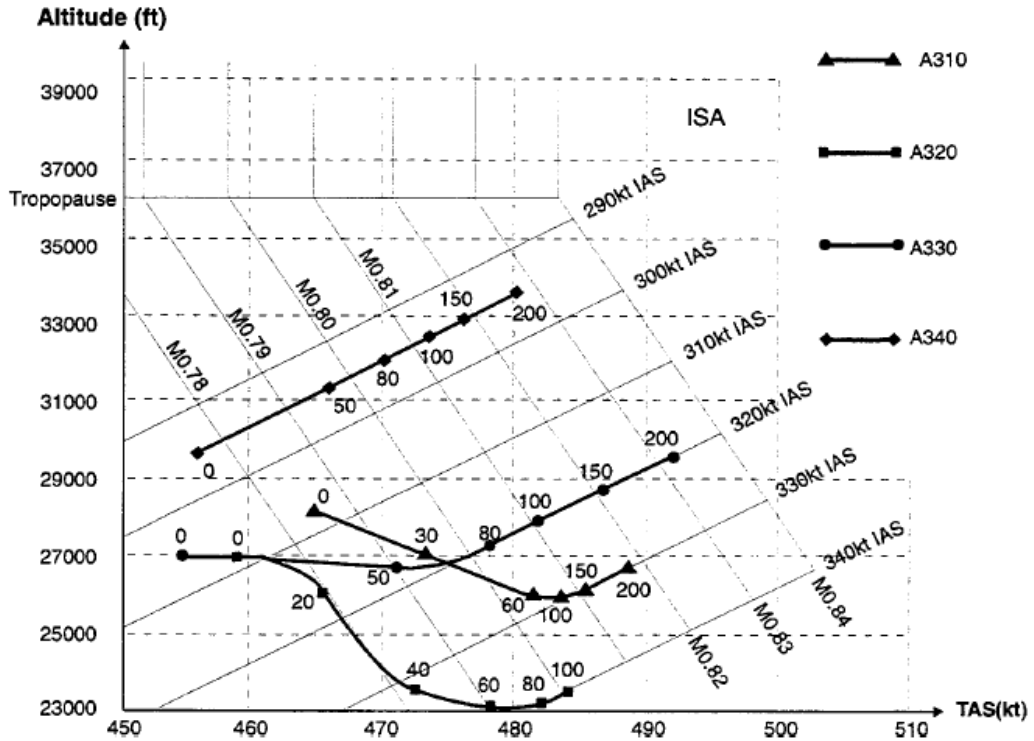


Figure 26: Dependence of the crossover altitude on the cost index for Airbus aircraft<sup>21</sup> [18]

We see that for the example we are using (aircraft of the size of an A320 and Boeing 737), the crossover altitude for a cost index equal to zero is 27,000ft. For the highest cost index (100), the crossover altitude is around 23,500ft.

Taking into account all these constraints and typical operating procedures, we can come up with an adapted, practical climb profile (see Figure 27) for the minimum climb time. In this profile, the reduced thrust setting is taken into account which will reduce the fuel burn and engine deterioration and increases the time between overhaul of the engine [30]. Because there are no limitations above 3,200ft, profiles similar to the ones retrieved before could be used above 3,200ft. This would mean a level part at 3,200ft would be flown until a speed of 250kts is reached, followed by a climb at constant speed to 10,000ft. At that level again a level acceleration part would take place until the point is reached where a line of constant energy height is tangent to a line of constant specific excess power.

---

<sup>21</sup> Airbus, "Getting to grips with the cost index," Blagnac, 1998.

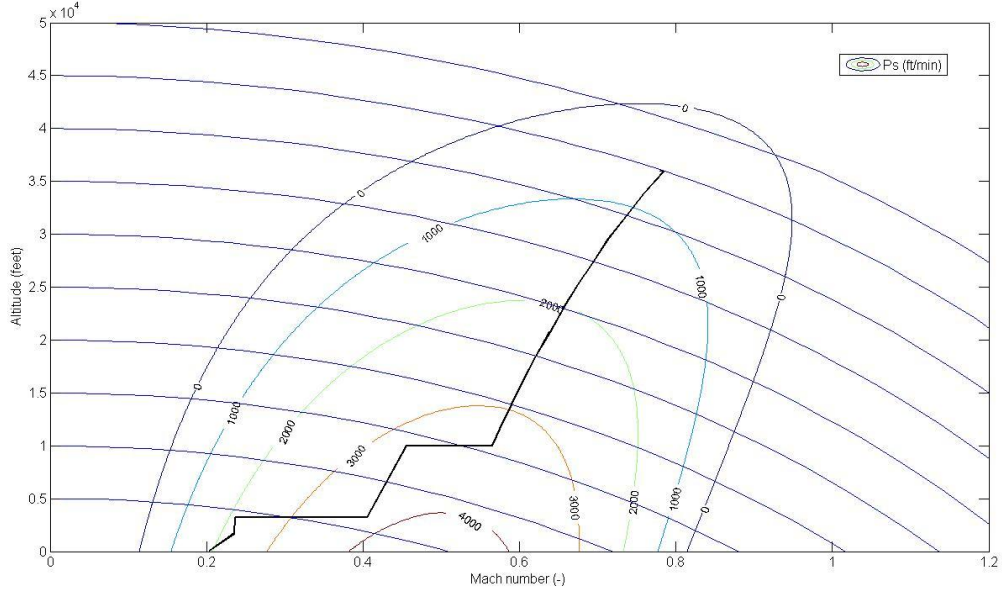


**Figure 27: Adapted profile for minimal climb time with respect to noise abatement procedures**

Similarly to the initial ideal profile, it is obvious that the first level part is again not so good for noise reasons. Additionally, it could be impossible to stay in level flight at 3,200ft because the aircraft has to be kept in the controlled airspace of Brussels Airport. Due to this, this part is replaced by a climb with a small rate of climb as it is generally done in current operations. To determine how much energy will be used for respectively acceleration and the increase of height, a factor is introduced. This is the "energy sharing factor" (a similar factor is the "kinetic energy factor") which reflects the sharing between the kinetic and potential energy as stated in [22], [31]. A common value for this factor is 0.3 which means that 30% of the energy is used for climbing and 70% for acceleration. The same factor is applied to replace the level part at FL100. This is done because the aircraft have to be able to reach a required altitude when leaving the Belgian airspace. In addition, a level part would not be beneficial for passenger comfort when levelling off and starting to climb again. This gives the profile which is taken as being the reference profile (see Figure 28).

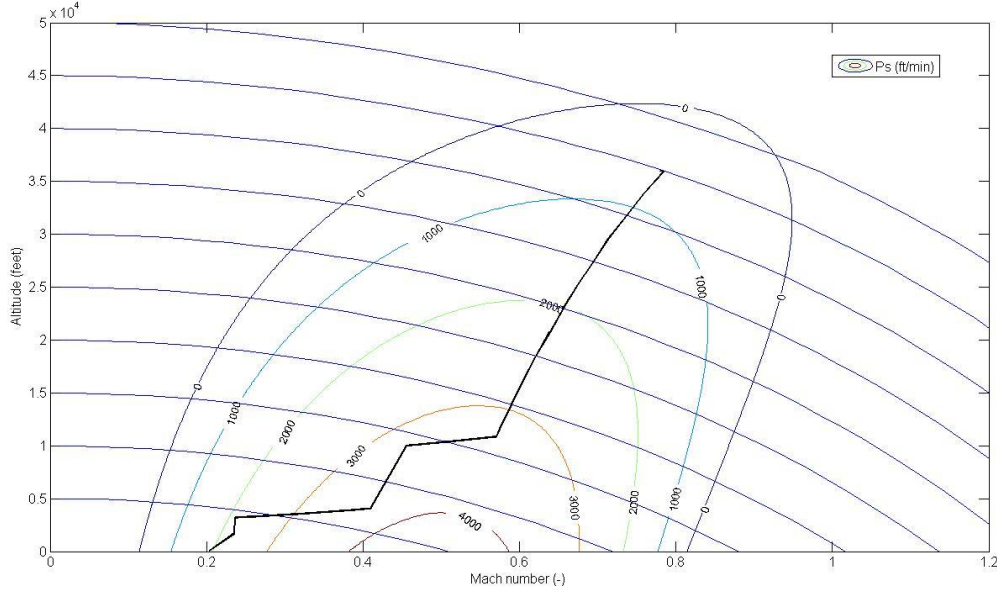


**Figure 28: Reference profile for minimal climb time**

The profile in Figure 28 results in a climb time of 23.1 minutes which is only 0.1 minutes more than the initially proposed profile. The calculated time to climb corresponds very well with the values in an Airbus brochure on getting to grips with the cost index [18]. Figure 29 shows the altitude of this profile as a function of the distance from the airport:

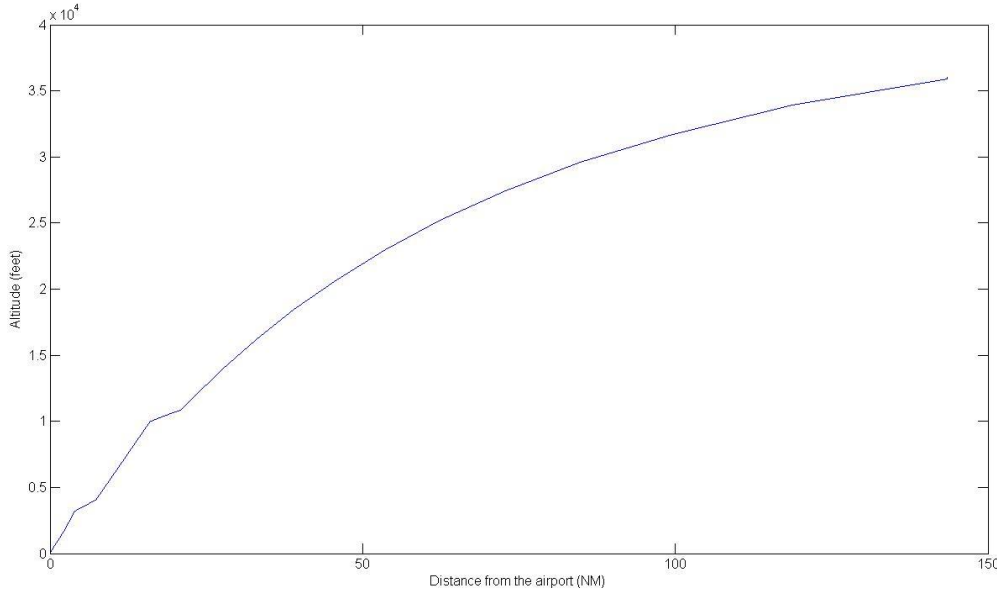


**Figure 29: Ideal climb profile for minimal time to climb as a function of the distance from the airport**

The same restrictions can be applied on the profile for minimum fuel used for the climb. Taking into account the noise abatement restrictions, the profile in Figure 30 is retrieved. In addition the last segment of the climb is replaced by a level part because it is hazardous to have an aircraft climbing higher than its cruise altitude and then descending again towards it. This is especially perilous when other aircraft are flying above the considered aircraft because certain separation minima have to be adhered to.

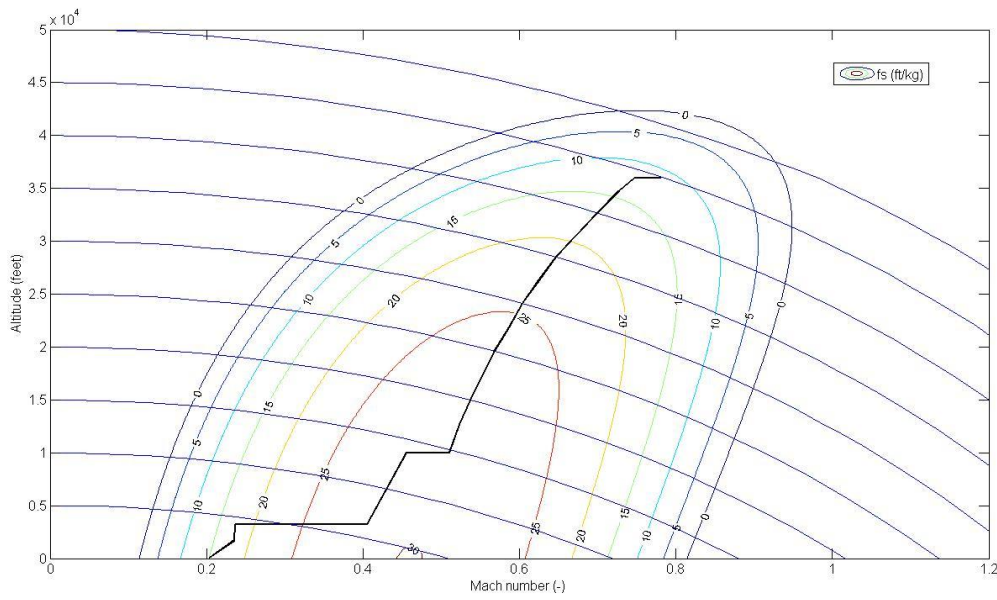


**Figure 30: Adapted profile for minimal climb fuel with respect to noise abatement procedures**

This climb profile would require 1967kg of fuel to get to the top of climb. Nevertheless the same remarks are valid for the level parts so the profile is adapted to the one in Figure 31.

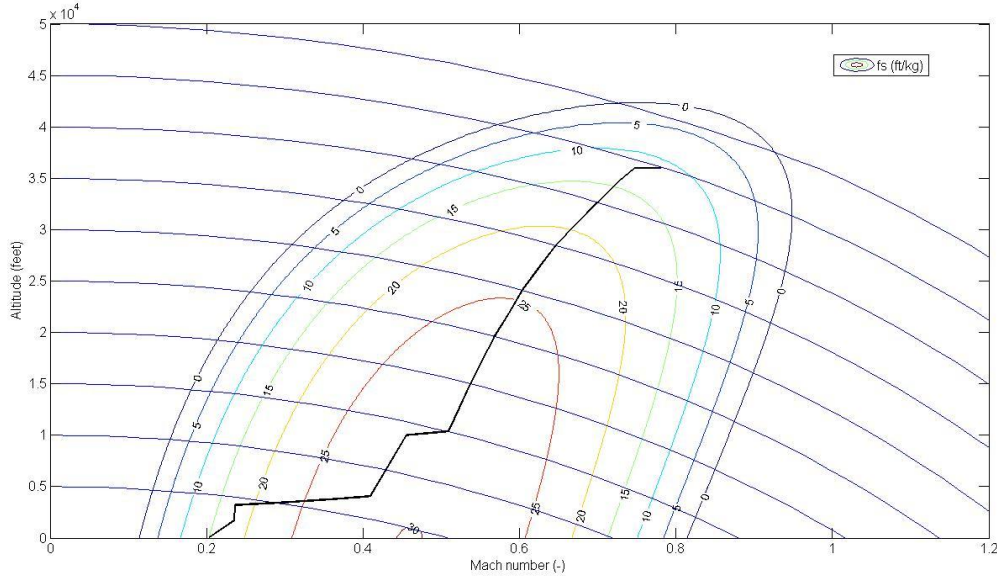


**Figure 31: Reference profile for minimal climb fuel**

Using this profile, the aircraft will use 1973kg of fuel which is 27kg more than the initial climb profile. It may seem unusual that the additional fuel consumption is rather limited because this profile is less convenient for fuel efficiency. However, the use of reduced thrust results in lower fuel consumption so the loss of efficiency is somewhat compensated. The profile in Figure 31 will be used as a reference for minimum fuel to climb. The altitude of the reference profile is plotted as a function of the distance from the airport in Figure 32:

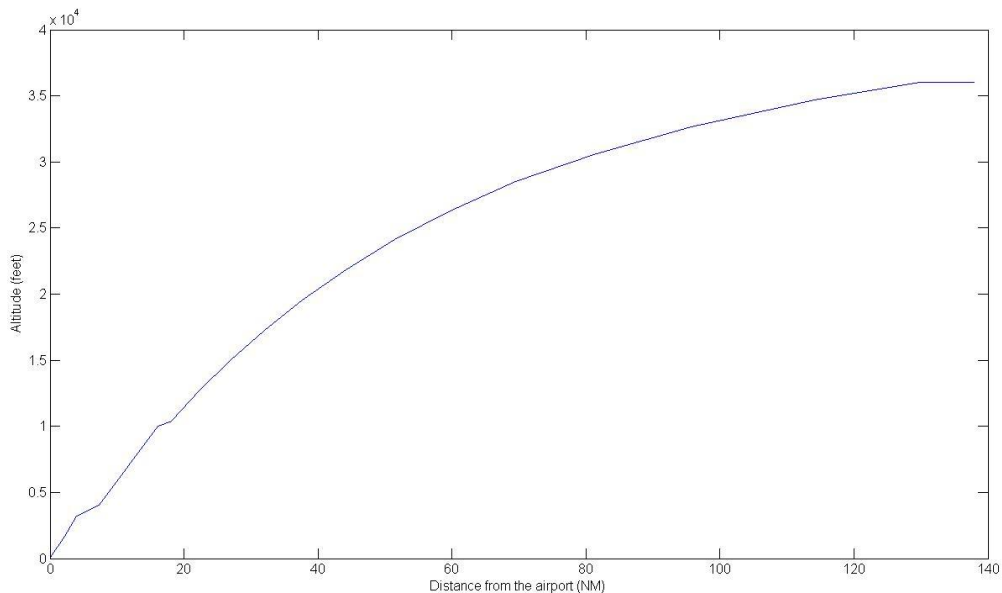


Figure 32: Ideal climb profile for minimal fuel to climb as a function of the distance from the airport

#### 4.3.5. Comparison of the optimal climb profiles

The two reference profiles are the profiles that should be flown to minimize either the fuel burn or the climb time which correspond to a cost index of respectively zero and the maximum value. The profile for minimum fuel will have a steeper climb profile and a lower climb speed, a shorter climb distance and a top of climb which is closer to the airport than the profile for minimum time.

As can be seen in Table 4, the climb profile for minimum fuel also remarkably features the least amount of time needed to fly the profile. This is because the two profiles are not ending at the same distance from the airport.

Table 4: Overview of the climb results

Cost index	Climb profile only			Climb profile with cruise segment		
	Fuel (kg)	Time (min)	Distance (NM)	Fuel (kg)	Time (min)	Distance (NM)
0	1910	22.4	129.7	2007	24.3	143.5
Maximum	2010	23.1	143.5	2010	23.1	143.5

So, in order to make an adequate comparison between these two profiles, a portion of the cruise phase has to be considered as well for the profile for minimum fuel. This is due to the fact that the top of climb of this profile is closer to the airport than for the other profile. So, in order to compare the profiles up to the same distance from the airport (up to the top of climb of the profile for minimum time), a cruise segment of 5.6NM is added to the profile for minimum fuel which brings the total level part at the end of the profile to 13.8NM. This segment takes 1.9 minutes and 97kg of fuel to fly it.

Figure 33 presents the two profiles with the extra cruise segment:

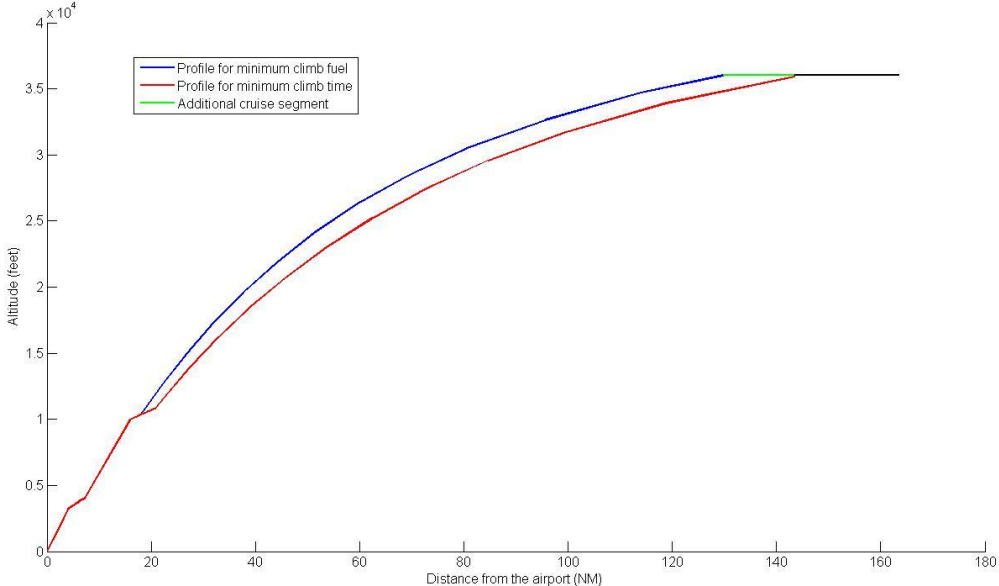


Figure 33: Overlay of the two climb profiles with the extra cruise segment

The values for the minimum fuel profile (climb profile only) in Table 4 do not take the level part at the end of the profile into account. This part is included in the extra cruise segment since the top of climb has been reached already at that stage.

Remarkably, the results of the fuel burn and the time needed for the climb are not very different for both profiles. There is only a difference of 3kg of fuel and 1.1 minute of climb time. Nevertheless, these results are similar to the results in [18] which confirms the validity of the results.

Figure 33 also clearly shows a shallower climb angle for the profile for minimum time, a longer climb distance and a top of climb further from the airport than for the minimum fuel profile which was expected.

All the calculated values were crosschecked with calculation methods from the BADA database, which gave almost exactly the same results as in Table 4. The difference between the results of the two methods is always less than 1%.

The two profiles which are proposed here are the two extreme cases that consider either fuel burn minimization or time minimization. In real life however, there will be an intermediate situation to trade off between fuel and time costs. This means that real life cost indices will lead to profiles being positioned between the two extreme situations. Hence the optimal profile will be located somewhere in between the two reference profiles.

#### 4.3.6. Comparison with flight data

Thanks to the good cooperation of Thomas Cook and Jetairfly, the proposed profiles can be compared to profiles which have been flown by their aircraft. It was very interesting to have their data because these two airlines fly Boeing 737s and Airbus 320s which are the aircraft taken for the calculation of the reference profiles. The data of the complete month of September 2012 was made available by these airlines which makes it possible to test the precise reference profiles. Because the received information is confidential, the detailed results of the comparisons can't be published in this work. Nevertheless, the results are as much as possible summarized hereafter.

Considering all the data of the departing flights, the average values of the relevant parameters were determined. Table 5 presents these values together with their standard deviation.

**Table 5: Average climb values of the flight data**

	Fuel (kg)		Time (min)		Distance (NM)	
	Average	Standard deviation	Average	Standard deviation	Average	Standard deviation
Flight data	1995	115	25.8	2.9	146.9	11

The available data only contain values for the climb profile until the top of climb so no additional cruise segment is considered as was done in the previous paragraph.

Before we can compare the values in Table 5 with the results from the reference profiles, we have to determine how well the data from the BADA database would lend themselves to qualitative calculations. To verify this, the parameters of the flight data are inserted in the programs made to determine the reference profiles. That way we can compare the real data with the calculated ones. A number of representative flights were taken for this test such that their takeoff weight was similar to the weight used for the reference profiles. The values of the flight data and the corresponding calculated values are summarized in Table 6:

**Table 6: Comparison of the flight data with the calculated values for the climb phase**

	Flight data		Calculated data		Fuel difference		Time difference	
	Fuel (kg)	Time (min)	Fuel (kg)	Time (min)	Kg	%	Min	%
Flight 1	2092	28.9	2524	28.8	432	22	0.1	0.3
Flight 2	2032	26.6	2388	26.5	356	18	0.1	0.6
Flight 3	2095	27.8	2519	27.6	424	21	0.2	0.6
Flight 4	2055	27.4	2438	27.3	383	18	0.1	0.2
Flight 5	2074	29.0	2580	28.8	506	25	0.2	0.7
Flight 6	1978	25.4	2300	25.3	322	16	0.1	0.4
Flight 7	2029	28.2	2471	28.1	442	22	0.1	0.6
Flight 8	2080	27.9	2451	27.8	371	19	0.1	0.2
Flight 9	1986	25.5	2266	25.5	280	13	0.0	0.1

The results from Table 6 show that the determination of the time from the calculations comes out very satisfactory. On the other hand, the fuel calculation for all the flights considered stands too high. On average, the fuel burn is 19% in excess to the flight data values. This means that the fuel consumption is overestimated by roughly some 20% when using the BADA method. Hence values calculated beforehand for the reference profiles should be adapted to have a better approximation. The new values for the optimal profiles are shown in Table 7:

**Table 7: Reference climb parameters after correction**

Cost index	Fuel (kg)	Climb profile only			Climb profile with cruise segment		
		Time (min)	Distance (NM)	Fuel (kg)	Time (min)	Distance (NM)	
0	1605	22.4	129.7	1687	24.3	143.5	
Maximum	1689	23.1	143.5	1689	23.1	143.5	

Comparing the values in Table 5 with the new ones of the reference profiles in Table 7, reveals that the amount of fuel used during the climb by the real flights is higher than the fuel for either of the two optimal profiles. The climb time is some minutes longer which could be the result of airline

policy when the cost index is rather low. This means that the fuel cost is more important so the flight time will be longer. The profiles of the flights in Table 6 are plotted next to each other and the reference profiles in Figure 34:

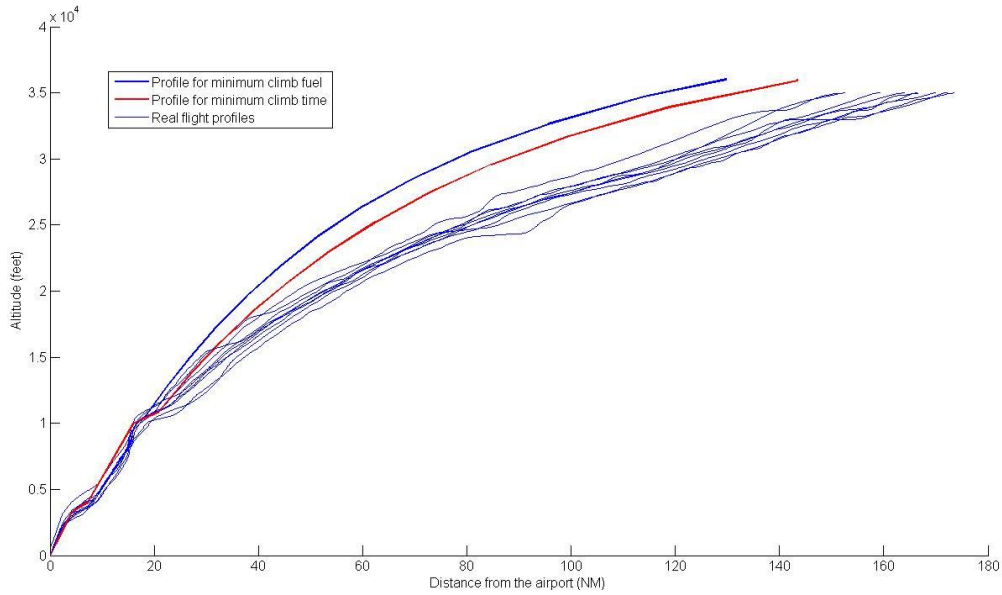


**Figure 34: Comparison between real flight profiles and the reference profiles**

Figure 34 reveals that the top of climb of the real flight profiles is further away from the airport than the top of climb of the reference profiles. The profiles are also less steep starting from around FL150 so the rate of climb is smaller than proposed in the reference profiles. To further investigate this, the altitude of the real profiles is plotted with respect to the Mach number as was done for the reference profiles (Figure 35):

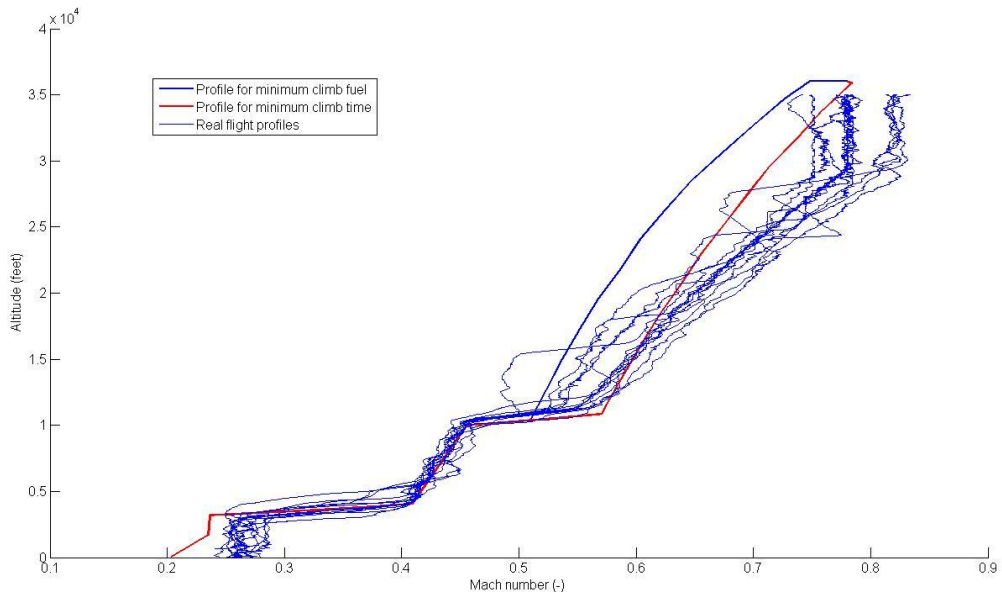


**Figure 35: Comparison between real flight profiles and the reference profiles**

From Figure 35 we clearly see that the flights are following the initial part of the reference profiles which is normal because this part of the profile is restricted by operational limitations. The profile above FL100 is thus the most interesting for optimization. In this part we see that initially almost all

the flights are flying a profile in between the two reference profiles which as we know can be attributed to an intermediate cost index. Unfortunately, the last parts of the climbs are not in between the two reference profiles. This is the result of the typical climb procedure used during the climb. As said before, the speed below FL100 is limited to 250 kIAS<sup>22</sup>. Above FL100, the aircraft speed is controlled using the indicated air speed until reaching the crossover altitude. The preferred indicated airspeed is determined by the cost index value. Above the crossover altitude the Autopilot Flight System under control of the FMS will switch to Mach number which again is determined from the cost index. During the climb the indicated airspeed and Mach number are continuously adapted to compensate for the wind. This method is of common use but this results in a higher fuel burn as can be seen when comparing the results of the real flights with the reference profiles from Table 5, Table 6 and Table 7. So due to the higher speeds in the last part of the real profiles and due to the lower rates of climb, the top of climb is further away from the airport, the fuel burn is higher and more time is needed to reach the top of climb. Specifically, around 306 to 390 kg of extra fuel is used, 2.7 to 3.4 minutes of extra time are needed and 3.4 to 17.2NM of extra track distance until the top of climb is flown.

The cost index of the airlines is a confidential value so we are not in a position to calculate an ideal profile for a specific airline. Nevertheless, the parts of the real flight paths just above FL100 in Figure 35 clearly show that the two reference profiles represent the extreme values of the cost index since the real paths are in between the references.

It might seem strange that the real flight profiles in Figure 34 are rather far away from the reference profiles. This is mainly because the wind is not taken into account in the reference profiles. Figure 36 shows the reference profiles corrected with the average winds of the real flights. This shows that the real flights are still not completely in between the two reference profiles but are more tending towards them.

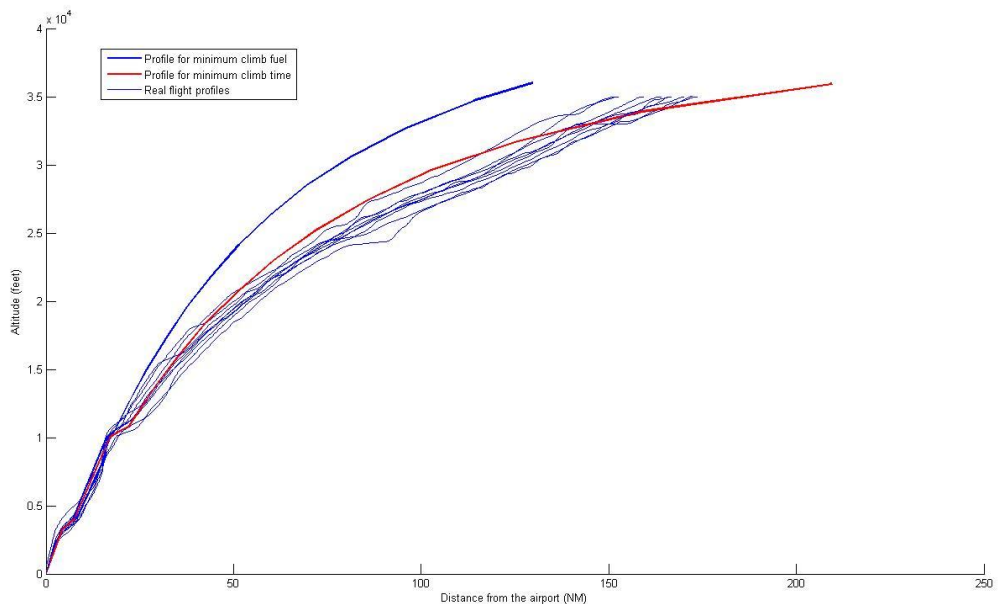


**Figure 36: Comparison between real flight profiles and the reference profiles corrected with the average winds**

According to a very experienced pilot, equivalent class aircraft (the Airbus 320 family and Boeing 737 family are considered equivalent aircraft) will climb more or less in the same way. This can be seen

---

<sup>22</sup> kIAS: knots Indicated Air Speed

for example in Figure 35 where flight data from both the Airbus 320 and the Boeing 737 are used. So if two or three categories of equivalent aircraft could be established, this could allow for two or three standard climb procedures to be optimized for the specific category. These standardized climb procedures would be sufficient to provide every aircraft with an optimized profile which would improve overall efficiency.

The reasoning here is specifically aimed at optimizing the climb profile so the rest of the flight is not taken into account. So, due to the many variables acting upon any flight, it might be possible that there are other preferred climb profiles that would be offering a better overall consideration of the complete flight. Since these variables are not all known, we limit ourselves to this study of the climb profiles.

#### 4.4. Performance during descent

During the descent, it would be ideal to turn off the engines and glide the aircraft down to the runway like for the Space Shuttle. This is of course impossible due to various safety constraints and operational reasons. However, the engines can be put in idle operation which lowers the engine power delivery to the strict minimum to supply all accessories. So in idle operation there is still some thrust delivered but this will be limited. Nevertheless, this is to be taken into account in the equations. To get the most out of this procedure, the aircraft's angle of descent should be such that the distance flown with engines in idle condition is maximum.

##### 4.4.1. Initial developments

Equations (4.14)-(4.16) remain valid and (4.14) can be rewritten to achieve the descent angle:

$$W \left( \frac{\dot{V}}{g} + \sin \gamma \right) = -\frac{1}{2} \rho V^2 S C_D + F_A \quad (4.39)$$

$$\dot{V} = \frac{dV}{dz} \frac{dz}{dt} = \frac{dV}{dz} V_z = \frac{dV}{dz} V \sin \gamma \quad (4.40)$$

$$W \sin \gamma \left( 1 + \frac{V}{g} \frac{dV}{dz} \right) = -\frac{1}{2} \rho V^2 S C_D + F_A \quad (4.41)$$

Using (4.16) we retrieve:

$$\tan \gamma = \left( -\frac{C_D}{C_L} + \frac{F_A}{\frac{1}{2} \rho V^2 S C_L} \right) \cdot \frac{1}{1 + \frac{V}{g} \frac{dV}{dz}} \quad (4.42)$$

This equation enables to calculate the optimum descent angle at every moment during the descent.

##### 4.4.2. Descent profile for minimal time to descent

When an airline considers the cost of time as being the most important, the descent should be done in the smallest amount of time possible. Equivalently, this means that the maximum cost index value is inserted in the FMC. The FMC will then calculate an optimum descent Mach number ( $MACH_{ECON}$ ) and descent speed ( $IAS_{ECON}$ ). The descent above the crossover altitude is flown at the optimum descent Mach number while the optimum descent indicated air speed is flown below this altitude until reaching FL100. Both optimum speeds are again corrected for the wind. Below FL100, the indicated airspeed is limited to 250kts due to air traffic control regulations. The descent profile is only considered up to the point where the aircraft intercepts the ILS glide slope (final approach fix) because the glide path towards the runway is then followed. In the ILS approach the necessary

engine power is depending on the relative position of the aircraft with respect to the glide path because the pilot may need to add power to stay on the glide slope. Before reaching the final approach fix, the aircraft has to decelerate to its approach speed. So, in the complete descent profile, there are two deceleration segments: one from the optimal descent speed to 250 kIAS before reaching FL100 and one before the final approach fix from 250 kIAS to the approach speed.

For the practical example, the same cruise parameters are taken as for the climb profiles: cruising at FL360 and M0.78 with an aircraft of the size of an Airbus 320 or Boeing 737 with a mass of 64000kg. A descent towards runway 25L is considered where the glide slope interception is done at 3000ft so the descent profile will only be calculated up to that point. More details on the precise ILS procedure can be found on the approach chart in ILS chart runway 25L.

Since we are trying to minimize the time needed for the descent, the aircraft will have to fly as fast as possible. Nevertheless, this speed is limited. In our example, the maximum Mach number  $M_{MO}$ <sup>23</sup> is M0.82 and the maximum speed  $V_{MO}$ <sup>24</sup> is 350 kIAS. As a safety measure, an extra 10 knots are deduced from the maximum speed so the maximum descent speed is 340 kIAS [18]. A similar safety margin for the maximum Mach number is taken: the Mach number is limited to  $M_{MO}-0.02$ , so M0.8 is the maximum Mach number [18]. The approach speed for the interception of the glide slope is taken to be 152 kIAS [32].

The crossover altitude is adapted to comply with the aircraft mass and the speed profile which brings the crossover altitude to 22,520ft.

Taking into account all these parameters and applying (4.42), we can come up with the trajectory depicted in Figure 37 which displays the altitude as a function of the true air speed:

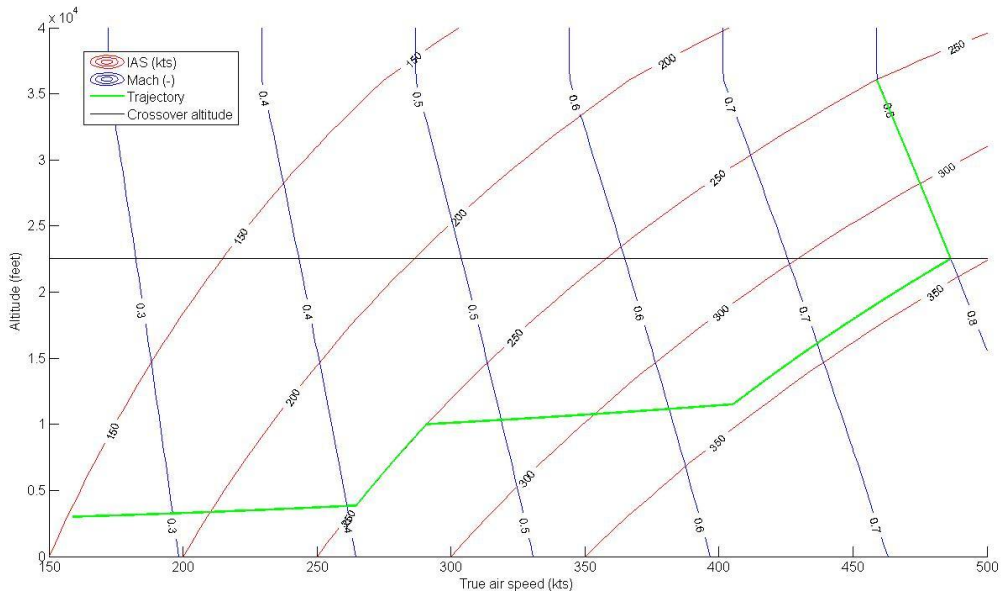


Figure 37: Ideal descent profile for minimal time to descent

The lines of constant Mach number and constant IAS are added to show the moment where a switch is made from flying on constant Mach number to constant IAS. Figure 38 represents the same trajectory as a function of the Mach number:

<sup>23</sup>  $M_{MO}$ : Maximum operating limit Mach number

<sup>24</sup>  $V_{MO}$ : Maximum operating limit speed (indicated airspeed)

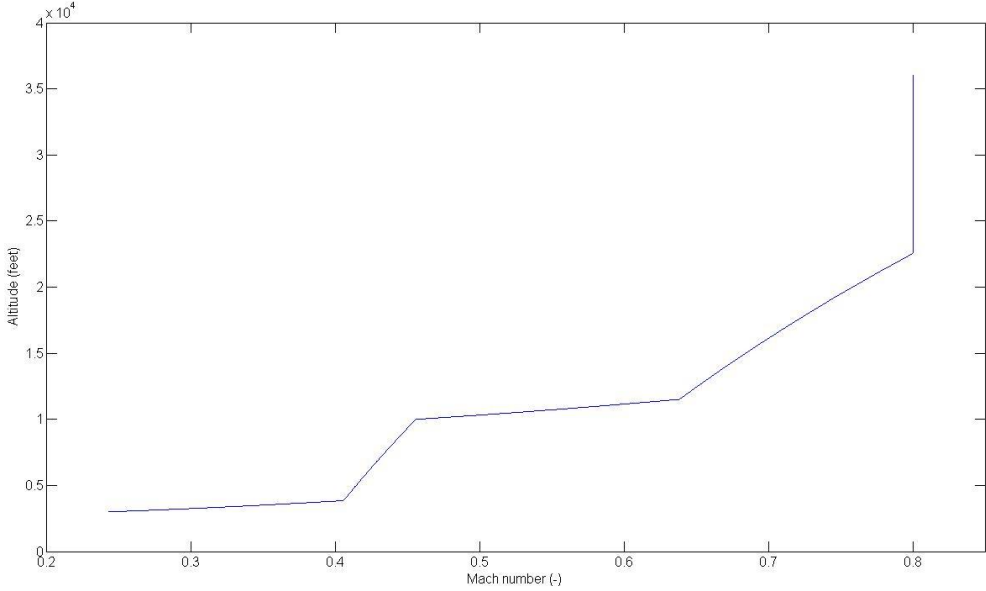


Figure 38: Ideal descent profile for minimal time to descent as a function of the Mach number

Figure 39 shows the trajectory as a function of the distance from the final approach fix:

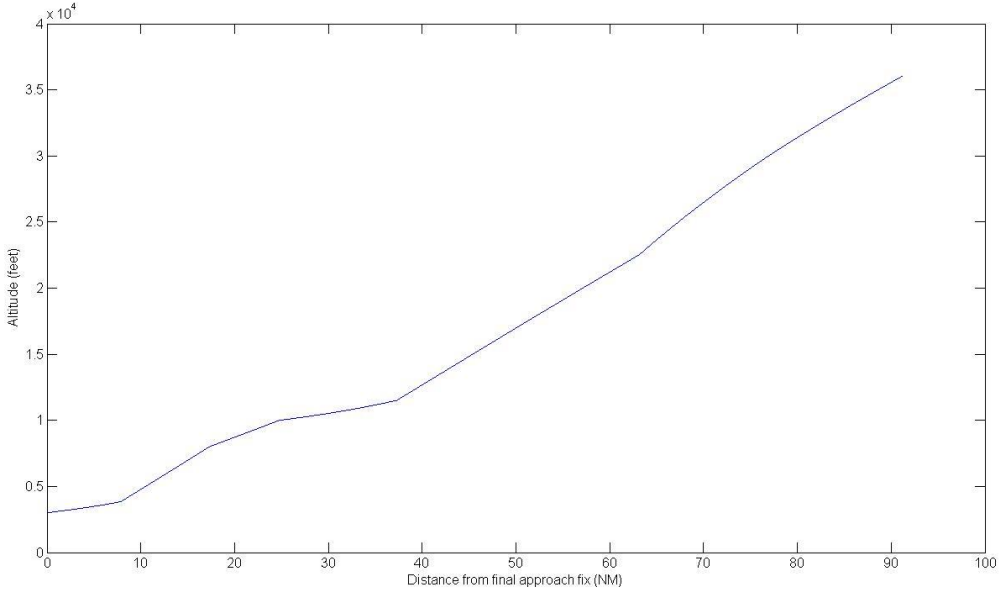


Figure 39: Ideal descent profile for minimal time to descent as a function of the distance from the final approach fix

This figure clearly shows that during the deceleration segments, the descent angle is reduced to allow the aircraft to decelerate sufficiently. To fly this profile, the top of descent is located at 91NM away from the final approach fix which corresponds to the values in [18]. This profile would require 15.2 minutes to reach the final approach fix and 169kg of fuel would be needed for this. The average descent angle is determined to be  $-3.1^\circ$ . The average rate of descent is 2170 ft/min which is well within the allowable limits.

#### 4.4.3. Descent profile for minimal fuel burn

When the cost of fuel is most important for an airline, this will result in a cost index of 0. Consequently, the descent speed is much lower. Indeed, because the descent is done at idle thrust

setting, the top of descent should be located as far away from the airport as possible. This allows to take advantage of the idle thrust setting and to reduce the overall fuel burn to the maximum extent possible. As a result, the FMC will determine  $IAS_{ECON}$  to be the minimum descent speed (250 kIAS in our example).  $MACH_{ECON}$  will be M0.764 as stated in [18]. Ideally, the speed below FL100 would have to be decreased as well to further reduce the fuel burn but 250 kIAS below FL100 is maintained because this enables ATC to provide the necessary separation more easily. This speed profile brings the crossover altitude to 34,160ft. Due to the lower speeds, the top of descent will be further away from the airport, the distance to descent will be longer and the descent path will be slightly shallower than for the profile for minimum descent time.

The results of the calculations are represented in following figures. Figure 40 presents the trajectory with respect to true air speed:

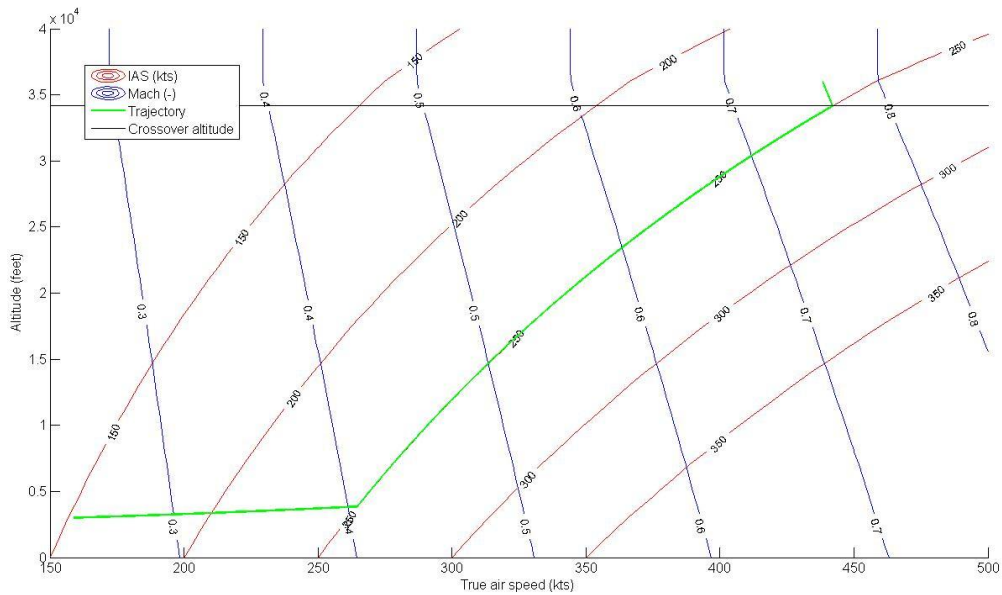


**Figure 40: Ideal descent profile for minimal fuel to descent**

Figure 41 and Figure 42 show the trajectory as a function of respectively the Mach number and the distance from the final approach fix.

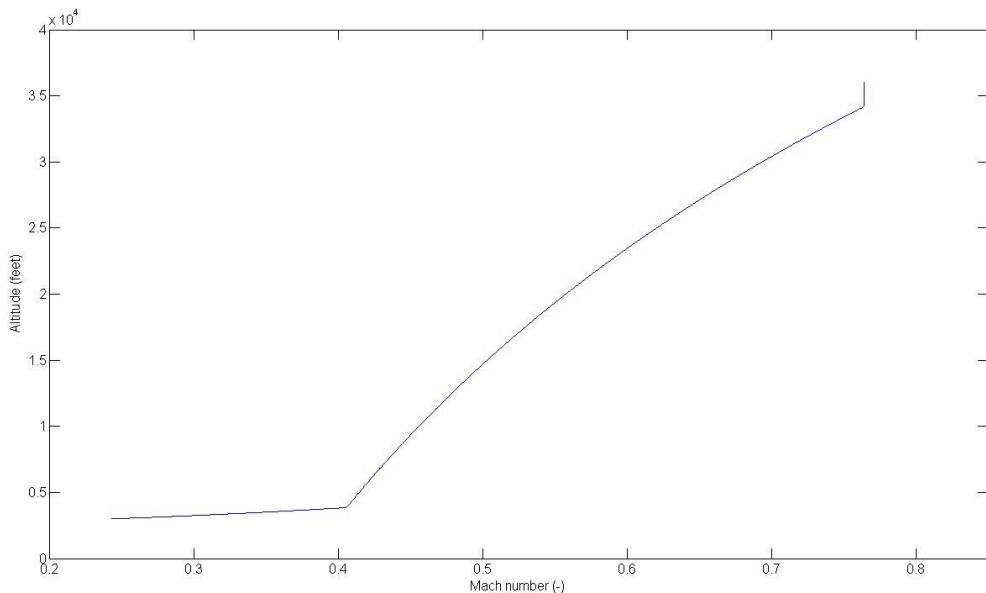


**Figure 41: Ideal descent profile for minimal fuel to descent as a function of the Mach number**

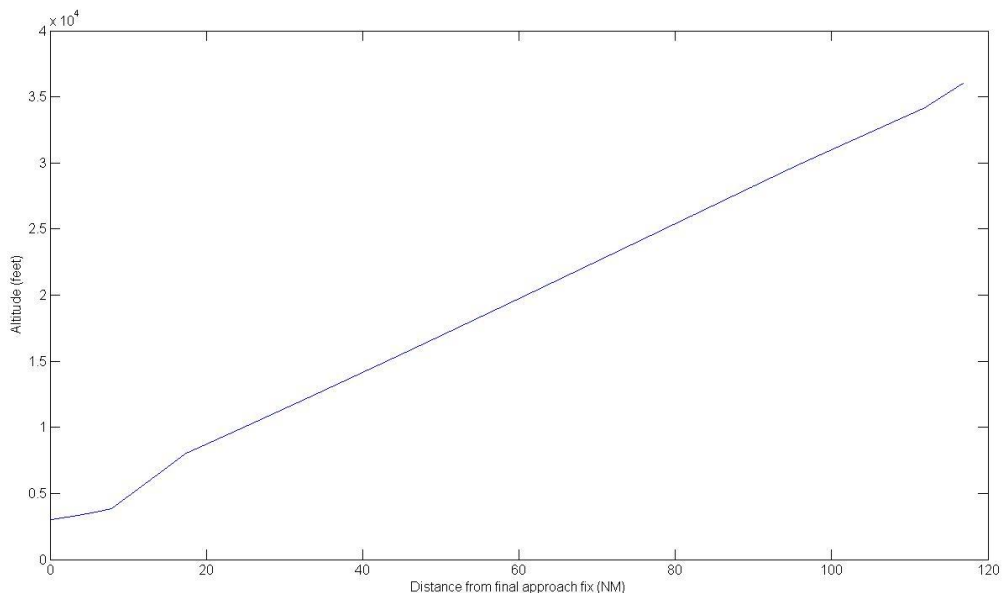


**Figure 42: Ideal descent profile for minimal fuel to descent as a function of the distance from the final approach fix**

Figure 41 shows clearly that there is only one deceleration segment now because the speed above and below FL100 is both 250 kIAS. This will be beneficial for passenger comfort since there is no transitional phase before FL100 with a change of descent angle as for the profile for minimum time. The top of descent is 117 NM away from the final approach fix, which is 26NM more than for the profile for minimum time to descent. This profile would require 226kg of fuel and 21.4 minutes to fly it. This is 6.2 minutes more and 57kg more than the profile for minimum time. The extra time was expected but the extra fuel not. This is due to the longer distance flown during the descent which will be further explained in the following paragraph. The average descent angle is  $-2.6^\circ$  which is less than the other profile as was expected. Also the rate of descent is lower: 1540 ft/min.

#### 4.4.4. Restrictions to the descent profiles

As can be seen in Figure 39 and Figure 42, the descent profiles should start at quite some distance away from the final approach fix. This would mean that the descent should be initiated outside the Belgian airspace. The aircraft is then still under the control of a neighbouring controlling agency. Unfortunately, the handover from the neighbouring controlling agency to the Belgian agency (Belgocontrol) can't happen at whatever altitude. This handover altitude is fixed and stated in the Letters of Agreement. These documents are not published but from a variety of different sources, we got some of these handover altitudes. Aircraft coming via Germany are handed over at FL220 to stay below the arriving traffic of Luxembourg Airport and aircraft arriving via France are handed over at FL240 to be below the departures from the airports of London and the arrivals of Amsterdam Airport. We now have to determine how far the aircraft are from the airport when they are handed over to Belgocontrol to assess what the magnitude of the impact stemming from these handover altitudes is. For this, the flight trajectories of a number of representative flights have been plotted on a map of Belgium (Figure 43):

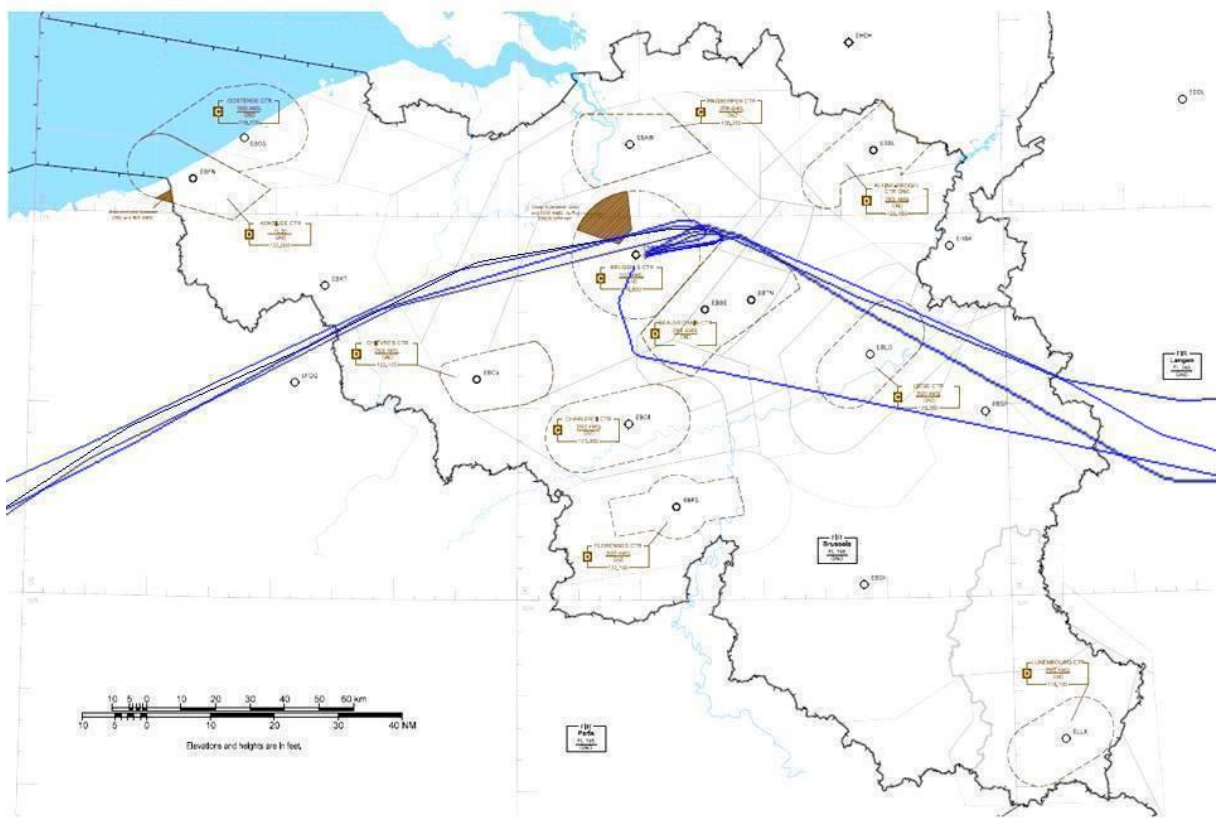
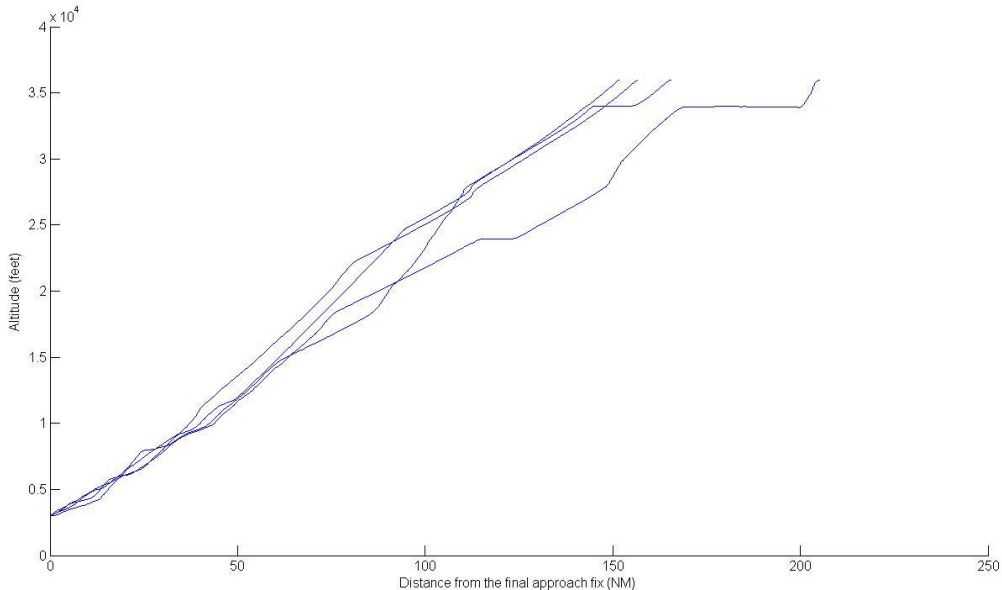


Figure 43: Flight trajectories of some representative flights towards Brussels Airport (chart<sup>25</sup> from [27])

The trajectories on Figure 43 show that all flights coming from a particular direction are crossing the border in the same region. Though, the trajectory flown within the Belgian airspace is not completely the same for all flights coming from a particular direction, which has an influence on the descent profile. This can be clearly seen for the flight coming from Germany and landing on runway 02 (the lower flight on Figure 43) instead of on runways 25 like the other flights. Next, the vertical profiles of the flights coming from France and Germany are shown in respectively Figure 44 and Figure 45.

<sup>25</sup> Belgocontrol AIM, “eAIS Package Belgium and G.-D. Luxembourg,” Belgocontrol, Steenokkerzeel, 2013.



**Figure 44: Vertical profiles of representative flights coming from France**

The vertical profiles of the flights coming from France show that the handover at FL240 happens 93 to 115NM away from the final approach fix. Remarkably these flights are doing more or less good continuous descents.

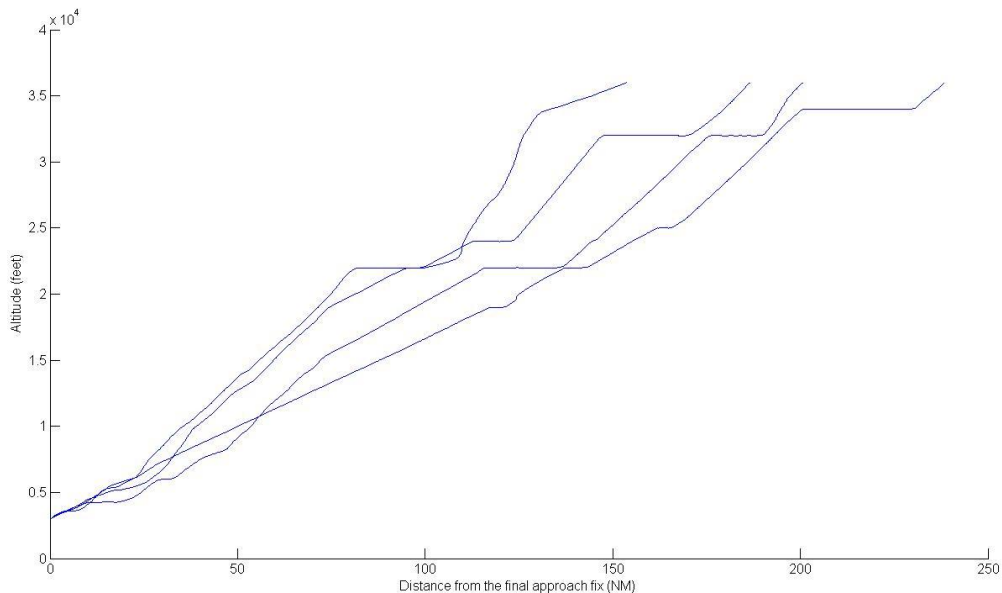


**Figure 45: Vertical profiles of representative flights coming from Germany**

The flights coming from Germany clearly have a level part at FL220 which is the altitude for the handover. This is probably due to the fact that the handover happens in a region where a lot of traffic streams are crossing each other. The most right hand profile is the one from the flight landing on runway 02. Figure 45 confirms that this flight has a longer flight distance between the handover and the final approach fix. The handover is done between 81 to 137NM from the final approach fix. To come up with reference profiles, we will consider only the situation for the flights coming from Germany because most of the flights are arriving in this way. A reference profile will be made for a handover at FL220 with a level part of 10NM between 104 and 114 NM from the final approach fix.

The handover altitude is a constraint which significantly hinders the execution of an optimized continuous descent. Nevertheless, the profile above the handover altitude can be optimized so this part will be exactly the same as the part of the ideal profile above FL220. Figure 46 and Figure 47 show the overlay of the ideal profile and the profile adapted to the handover constraint for respectively minimum fuel burn and minimum descent time:

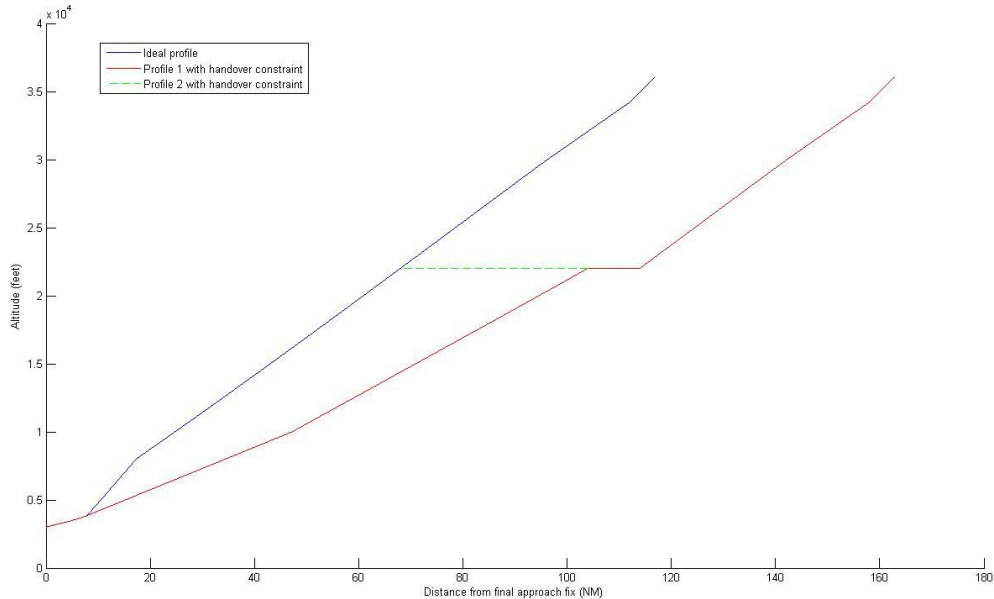


**Figure 46: Overlay of the ideal profile for minimum fuel burn with and without the handover constraint**

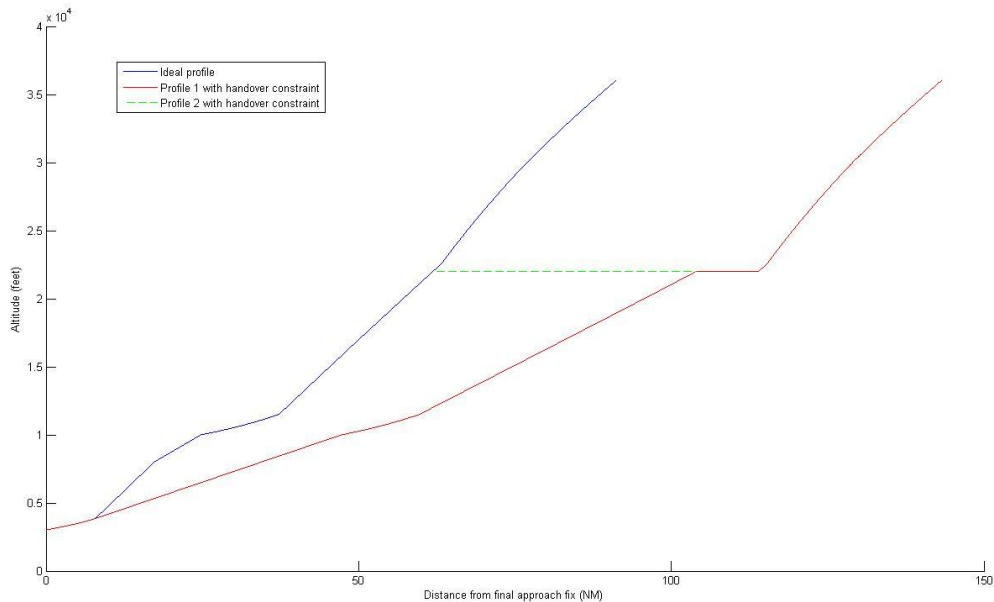


**Figure 47: Overlay of the ideal profile for minimum descent time with and without the handover constraint**

In Figure 46 and Figure 47, two possible efficient trajectories after the handover are depicted. The red trajectory considers that the parts of the trajectory of constant indicated air speed below the handover altitude are flown at a constant descent angle (profile 1). The other possibility would be to stay at the handover altitude until the ideal profile (profile 2: the green dashed profile in Figure 46

and Figure 47) is intercepted. This idea is based on the fact that flying at higher altitudes is more fuel efficient. The fuel burn and descent times of these two possibilities are summarized in Table 8:

**Table 8: Fuel burn and descent time for the possible trajectories**

	Profile 1		Profile 2	
	Fuel burn (kg)	Descent time (min)	Fuel burn (kg)	Descent time (min)
Profile for minimum fuel	448	30.5	542	26.2
Profile for minimum time	365	24.0	453	19.2

#### 4.4.5. Comparison of the optimal descent profiles

The calculated necessary fuel for the profile with minimal fuel burn can seem rather strange in Table 8 because it's more than the fuel needed for the profile for minimum time to descent. But to compare these two profiles in a representative way, we will consider the descents starting from the same distance from the final approach fix and assume that the same cruise and climb is performed before this point. After all, it's the overall fuel burn and descent time that is important and not only the parameters from the descent phase. For this we will add an extra cruise segment to the profile for minimal time. This will end at the top of descent of the profile for minimum fuel. Figure 48 clarifies this method. For clarity, only profiles number 1 are shown in Figure 48.

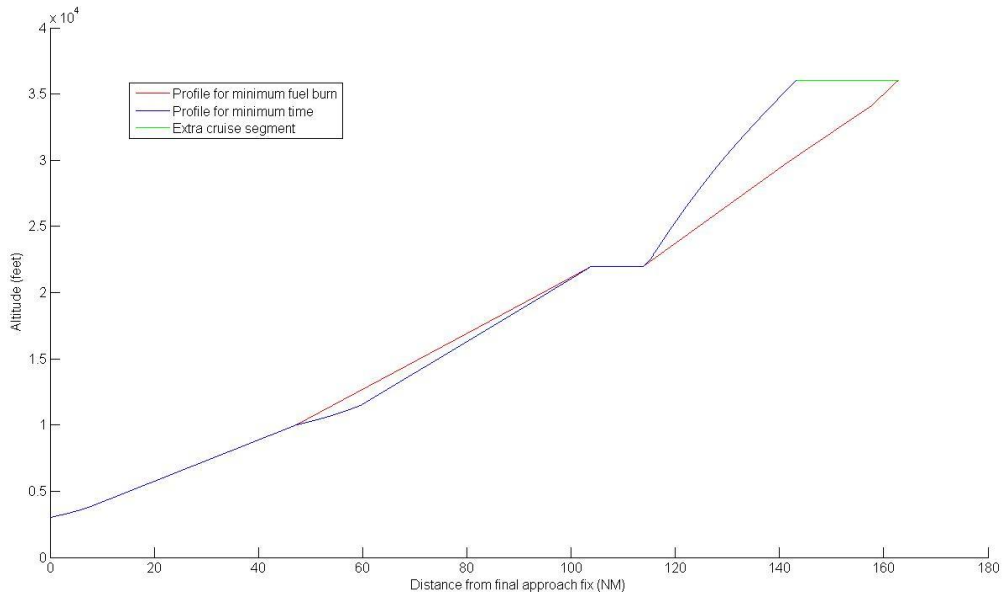


**Figure 48: Overlay of the two profiles with the extra cruise segment**

For the calculation of the fuel consumption during the cruise segment, we need to know the cruise Mach number which is also depending on the cost index. [18] gives us the optimal cruise Mach number as a function of the cost index and the flight level: 0.797 for the maximum cost index. The tops of descent of the two profiles are 19.6NM apart from each other so the extra cruise segment will have that length. Using the BADA database, the fuel used in the cruise segment is calculated to be 133kg and 2.6 minutes are needed to fly it. The results of the fuel burn and the descent time with the cruise segment are summarized in Table 9:

**Table 9: Fuel burn and descent time for the possible trajectories (extra cruise segment considered)**

	Profile 1		Profile 2	
	Fuel burn (kg)	Descent time (min)	Fuel burn (kg)	Descent time (min)
Profile for minimum fuel	448	30.5	542	26.2
Profile for minimum time	498	26.6	591	21.8

The results in Table 9 show that profile 1 in Figure 46 is the best for airlines flying with a cost index of 0. To the contrary, profile 2 in Figure 47 is ideal when the maximum cost index is used. These two profiles will be used as reference profiles as from now on.

From the data in Table 9, it is clear that profile 2 for minimum time has indeed the lowest time needed, even with the extra cruise segment. This confirms that flying at the maximum cost index minimizes the time to fly but this has a drawback on the fuel burn. Indeed, the profile for minimum time consumes 143kg more fuel during the complete procedure (descent and extra cruise segment). Inversely, the profile for minimum fuel burn takes 8.7 minutes more than the profile for minimum time.

Remarkably, the profile for minimum time is going below the profile for minimum fuel burn just above FL100 as can be seen on Figure 48. We would rather expect that the minimum time profile would stay above but this is due to the necessary deceleration segment for the profile for minimum descent time, which is not present for the other profile. Obviously, the two profiles coincide below FL100 because the same speeds are used in that part of the descent.

The two profiles considered here are the two extreme cases which can happen. When an airline is flying at an intermediate cost index, the ideal profile will be somewhere in between the two presented profiles. As said before, all of this is to minimize the overall costs of the flight.

As was expected, Figure 48 shows that the top of descent of the profile for minimum time is much closer to the final approach fix, consequently the descent distance is shorter and the descent path is slightly steeper. This is all a direct result of the higher speeds involved during this descent procedure.

#### 4.4.6. Comparison with flight data

As was done for the climb profiles in 4.3.6, the optimal descent profiles are compared to real flight data from Thomas Cook and Jetairfly. The comparison is done analogously to the comparison of the climb profiles. Again the flight data from September 2012 was used for this. First, the average values of the relevant parameters were determined and these are shown in Table 10:

**Table 10: Average descent values of the flight data**

	Fuel (kg)		Time (min)		Distance (NM)	
	Average	Standard deviation	Average	Standard deviation	Average	Standard deviation
Flight data	539	115	27.7	5.8	141.5	20.2

The values in Table 10 are considering the descent from top of descent until touchdown on the runway so no additional cruise segment is considered as was done for the optimal profile for minimum time.

Calculations for the descent phase are done using other coefficients from the BADA database so we once more have to put the flight data in the programs which are used to calculate the different

parameters. This way, we will determine how good the estimations with the BADA database are. A number of relevant flights with approximately the same weight at their top of descent are taken for the verification of the calculations. Table 11 gives an overview of the real flight data and the corresponding calculated data:

**Table 11: Comparison of the flight data with the calculated values for the descent phase**

	Flight data		Calculated data		Fuel difference		Time difference	
	Fuel (kg)	Time (min)	Fuel (kg)	Time (min)	Kg	%	Min	%
Flight 1	448	22,6	237,9	22,1	-210,1	-47%	0,5	2%
Flight 2	463	28,7	511,1	28,4	48,1	10%	0,3	1%
Flight 3	509	29,7	632,4	29,4	123,4	24%	0,3	1%
Flight 4	498	29,6	300,8	29,3	-197,2	-40%	0,3	1%
Flight 5	501	21,7	240,9	21,7	-260,1	-52%	0,0	0%
Flight 6	504	32,4	409,8	32,4	-94,2	-19%	0,0	0%
Flight 7	550	30,2	316,7	30,2	-233,3	-42%	0,0	0%
Flight 8	577	28,6	652,6	28,4	75,6	13%	0,2	1%
Flight 9	714	34,5	738,6	34,3	24,6	3%	0,2	1%
Flight 10	680	37,5	723,2	37,5	43,2	6%	0,0	0%

The results from Table 11 show that the calculation of the descent time is rather good: the calculated values differ on average 0.7% from the flight data. The results of the fuel calculations however differ a lot. This is due to the fact that there are separate coefficients in BADA for the calculation of the fuel flow in idle setting and in level flight when thrust is needed. Unfortunately, the flight data do not allow for separating the fuel burn of the level parts and the one of the idle parts. Since we are considering flights coming via Germany, we will take into account only the values of those flights in Table 11 (flights 2, 3, 9 and 10). Remarkably, the other flights almost all have fuel estimations that are lower than the real flight data values. This is probably because these flights are coming via France without a level part during the handover. This could be an indication that the fuel burn estimation of BADA for the idle operation is less accurate. On average, we see that the fuel burn is overestimated by 11% for flights 2, 3, 9 and 10. So the values from Table 9 are adapted with this correction to improve the fuel estimation. Table 12 provides the corrected values for the descent parameters:

**Table 12: Reference descent parameters after correction**

	Reference profiles	
	Fuel burn (kg)	Descent time (min)
Profile for minimum fuel	407	30.5
Profile for minimum time	537	21.8

Since the values of flights coming from different directions can have quite different values for fuel burn, descent time and flying distance, the average values of the considered flights from Germany are calculated (Table 13):

**Table 13: Average descent values of the considered flights coming from Germany**

Flight data	Average fuel (kg)	Average time (min)	Average distance (NM)
	592	32.6	148.4

The values of the proposed profiles are calculated up to the point where the ILS path is followed, starting at 3000ft in this case. The flight data are calculated up to the landing so the fuel used during the ILS approach should be deduced. On average, this part takes 3.4 minutes and 84 kg of fuel is used so the average descent time is 29.2 minutes and the average fuel used is 508kg during the descent until the final approach fix. Comparing these values with the values in Table 12, it is very remarkable that the average fuel burn value of the flight data is in the range of the reference profiles but rather on the high side. The same is seen for the descent time of the flight data. This asks for further research to find possible causes. For this, the profiles of the considered flights are plotted together with the reference profiles in Figure 49:

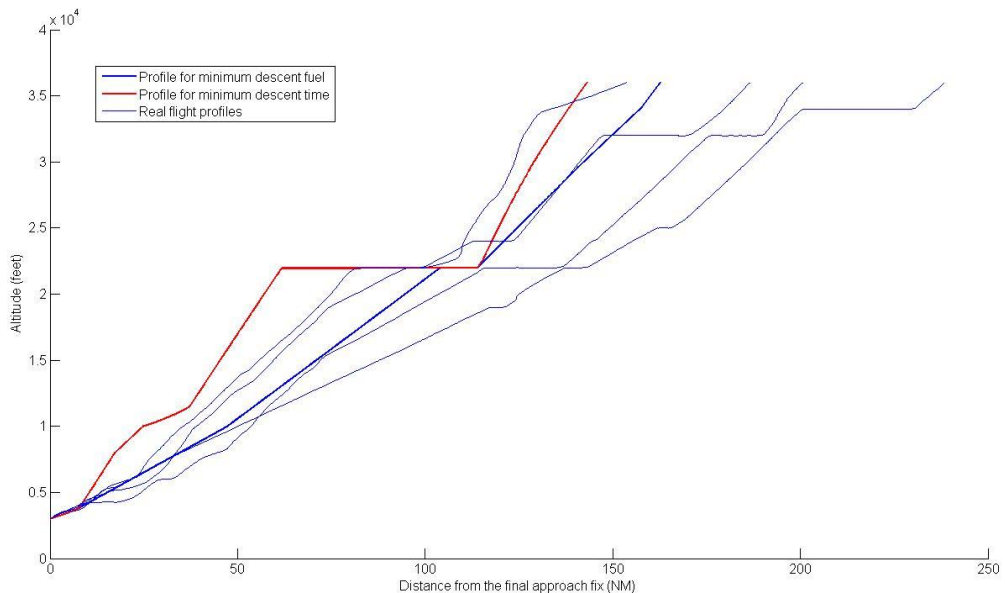


**Figure 49: Comparison between real flight profiles and the reference profiles**

Almost all the flight profiles in Figure 49 feature some parts with level flight during their descent apart from the level handover part at FL220. This shows how difficult it is to fly a purely continuous descent. As said before, this can be attributed to airspace restrictions, ATC procedures, letters of agreement, ATC controllers' coordination and workload...

Figure 49 confirms the values from Table 13: the top of descent is in general further away from the final approach fix for the real flights which could result in rather high values for the fuel consumption and the time needed for the descent. Nevertheless, the speed profiles should be looked at as well to have a complete idea of the situation. So, the altitude of the real profiles is also plotted with respect to the true air speed together with the optimal profiles in Figure 50 enabling to further look into this:

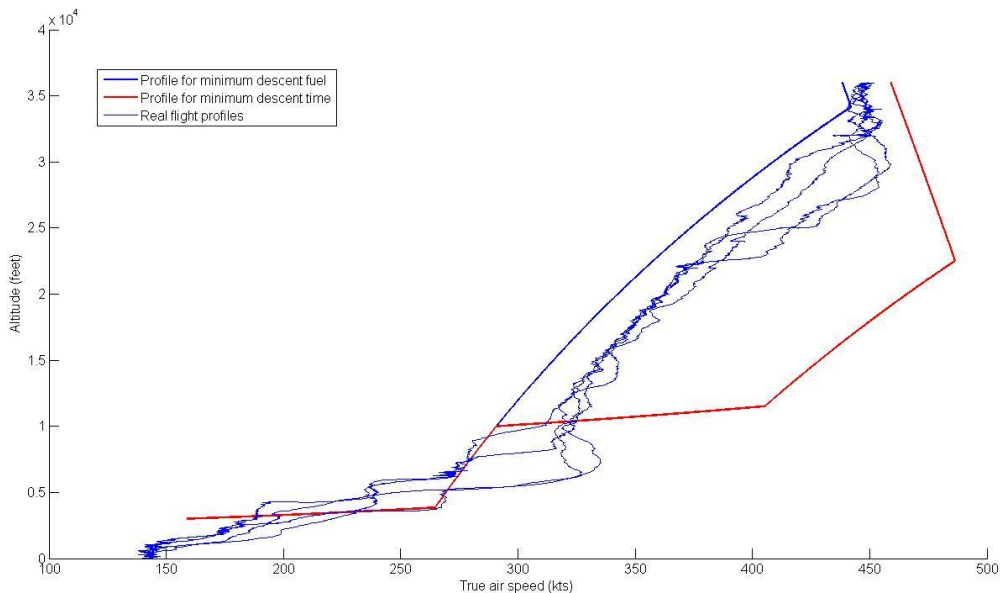


**Figure 50: Comparison between real flight profiles and the reference profiles**

Figure 50 nicely displays the commonly used method for descending: first descending at a constant Mach number until the crossover altitude, then at constant indicated air speed and finally at 250 kIAS below FL100. Apparently, the last restriction is not adhered to by some flights. It is clear that the flights have descended at a rather low cost index since the flights are more tending towards the profile for minimum descent fuel. Airlines could apparently tend to use these low cost indices because of the high fuel prices.

Coming back to the discussion of the different values of the descent fuel and time, we see however that the speeds used during the real flights are in between speeds for the two optimal profiles. So this is not the reason for the lower values of fuel burn and descent time for the reference profiles. In fact, since the top of descent is earlier for the real flights, the descent will take more time. Due to this and due to the intermediate level parts during the descent, more fuel is used in the real flights. As explained earlier in 2.7, because the flights are not following the reference profiles, there will be a time and/or fuel penalty which explains the high values for fuel burn and descent time for the flight data.

#### 4.4.7. Influence of the crossover altitude

The crossover altitude is a function of the cost index (Figure 26) so since aircraft are flying at different cost indices, their crossover altitudes are all different. This has an impact on the variation of the true air speed during the descent. This can be seen when looking at Figure 50: aircraft flying the profile for minimum time will achieve a much higher true air speed before reaching the crossover altitude than aircraft flying the profile for minimum fuel.

Additionally, there are many different types of aircraft flying around which all have different speeds during their descents. To have an idea about the variation of the crossover altitudes, the typical mix of aircraft types in Belgium is used.

Table 14 gives an overview of the mix of aircraft types that arrived to and departed from Brussels Airport in September 2012:

**Table 14: Percentages of flights per aircraft category**

Aircraft category	Percentage
Light	23.7%
Medium	58.1%
Heavy	11.6%

Light aircraft in Table 14 are aircraft from the Avro, Fokker and small Embraer family. Medium aircraft are aircraft such as the Airbus 320, Boeing 737 and Embraer 170 and 190 while heavy aircraft are aircraft like the Airbus 330, 340, Boeing 747, 757, 767 and 777. A detailed overview of the distribution of the aircraft types at Brussels airport is given in Distribution of aircraft types at Brussels airport.

The values in Table 14 show that most aircraft flying to and from Brussels Airport are of the medium category, which corresponds to the type of aircraft used for the determination of the optimal profiles. So, the distribution of the crossover altitudes will be dominated by the crossover altitudes of these types. As can be seen on Figure 26, these types will have their crossover altitude between FL230 and FL270, but this can be higher when low speeds are used such as the speeds used for the profile for minimum fuel consumption. Light aircraft generally fly at slower speeds which results in slightly lower crossover altitudes around FL220. Heavy aircraft to the contrary fly at the same speeds as the medium aircraft so their crossover altitudes are in the same range.

In short, the crossover altitude depends of the cost index of the flight and of the flight type so there is quite some variation in these crossover altitudes.

#### **4.5. Optimal climb versus optimal descent**

After all these considerations about continuous climb and continuous descent operations, one could ask whether it is possible to facilitate both at the same time and if not, which of the two should get the priority.

The first question depends on the traffic situation which is changing all the time. It's pretty hard for air traffic controllers to estimate where an arriving and a departing aircraft could get too close to each other when both aircraft are respectively doing a continuous descent and continuous climb. Some kind of predictability would be very useful in that case. Figure 51 shows some very simplified CDO and CCO profiles with respect to the distance from the airport:

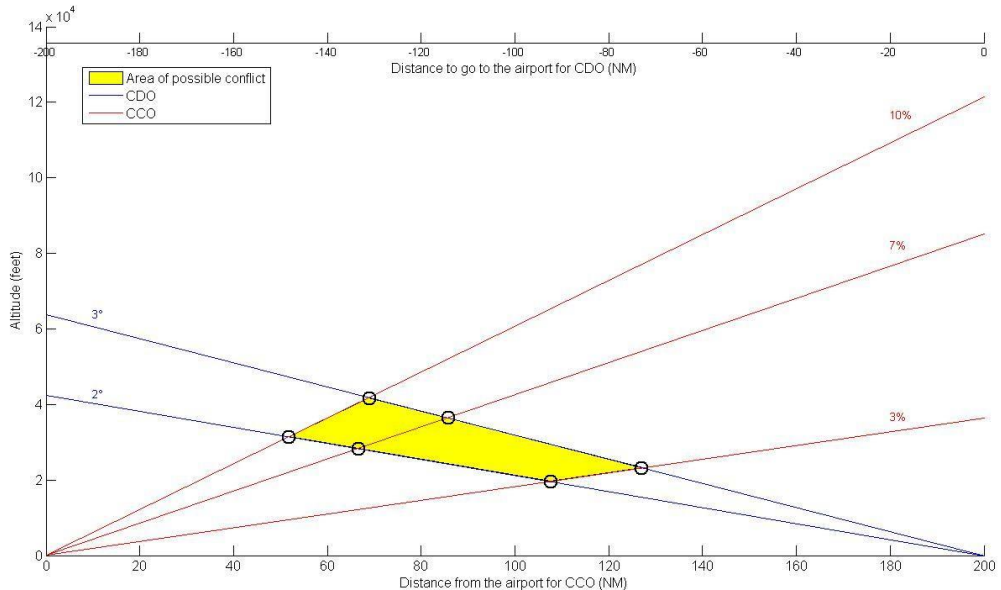


Figure 51: Overlay of simple CDO and CCO profiles

Knowing the descent angle and the climb and descent gradient or having a good estimate of these values, allows the air traffic controller to approximately determine where the two aircraft could get too close to each other. This would allow the air traffic controller to intervene for example by telling the departing aircraft to climb at a higher rate of climb to have sufficient separation between the two aircraft. The predictability of the descent and climb profiles is one of the major issues when trying to implement continuous descent and continuous climb procedures. So this could improve it!

When continuous climb and continuous descent operations cannot be allowed at the same time, the question remains which of the two should get the priority to have the best overall fuel efficiency and cost efficiency.

SAS has conducted a small analysis of this problem because there were no facts and figures available [33]. They concluded that whenever a constraint is necessary, it will have a similar influence on departing and arriving traffic when the constraint is known well in advance. However, when the constraint comes all of a sudden during the approach or climb, it would be more fuel efficient to give a constraint to a departing aircraft rather than to an arriving aircraft. Nevertheless, it is highly depending on the type and amount of restriction and the traffic situation which aircraft should ideally be left undisturbed.

According to Airbus [34], descent techniques have more effect on fuel and time than climb techniques. Comparing the values of fuel burn and time for the reference profiles, we see that there is indeed a much larger variation in the values for the descent profiles than for the climb profiles. This shows that there are much more opportunities in the descent phase to minimize the total operating costs than during the climb phase.

Considering all these facts, it is clearly not possible to say whether continuous climb or continuous descent should be prioritized. This is very dependent on the traffic situation and local regulations so it should be rather decided every time a conflict arises.

## 5. Dynamic CDO

The previous part on the climb and descent profiles always considered the profile of a particular type of aircraft. Nevertheless, aircraft are not alone in the air and they are influencing each other's flight paths. To go further into this, a simulation was made to determine the optimal profiles to be flown by arriving aircraft taking into account several constraints such as airspace restrictions, other aircraft, separation minima,... Only the descent profiles are considered in the simulation because this part of the flight can be more optimized than the climb part as discussed before.

### 5.1. Concept

Dynamic CDO is a simulation method to determine the best possible trajectory to descent to the airport taking into account the actual traffic situation and the aircraft performance. For this, different objectives can be set such as low noise, low emission, low fuel burn, least descent time or a combination of all these. This would enable air traffic controllers to dynamically determine the routes of arriving traffic and choose the best one for them and the pilots.

The objective of the simulation is to apply dynamic CDO in the Brussels FIR/UIR. The methodology of [35] will be used as a basis and extended to be applied in the Brussels FIR/UIR. The simulation enables to consider all possible variations of available airspace so a real life airspace configuration can be used. For the testing, real life data from Belgocontrol will be used to have a realistic amount of traffic in the simulations. Using these simulations, the possible advantages and disadvantages of CDO implementation will be examined. Initially, only arriving traffic will be considered.

The big advantage of dynamic CDO is that predictability is increased which is good for both air traffic control and pilots. In the future, this system can be implemented to have a real time decision making tool for CDO.

### 5.2. Implementation

The simulation will be performed assuming ISA conditions (see 4.1) and no wind. We will consider the airspace up to 75 NM from Brussels Airport and up to an altitude of 24,000ft. The following paragraphs illustrate the steps taken in these simulation runs.

#### 5.2.1. Discretization of the airspace

The considered airspace is discretized into 15 concentric cylinders, with the airport as centre, spaced 5NM apart. These cylinders are further discretized into 22 levels, with a separation of 1000ft. Each level of a cylinder has artificial waypoints so that all waypoints are 1.5NM apart for safe separation. The lower limit of the airspace is 3000ft because we consider an ILS approach to runway 25L which has its final approach fix at 3000ft altitude. The final approach fix is assumed to be at 5NM distance from the airport for simplification. The inner cylinder has only one level at 3000ft because the final approach fix is located on that cylinder. The discretization of the airspace is visualized in Figure 52:

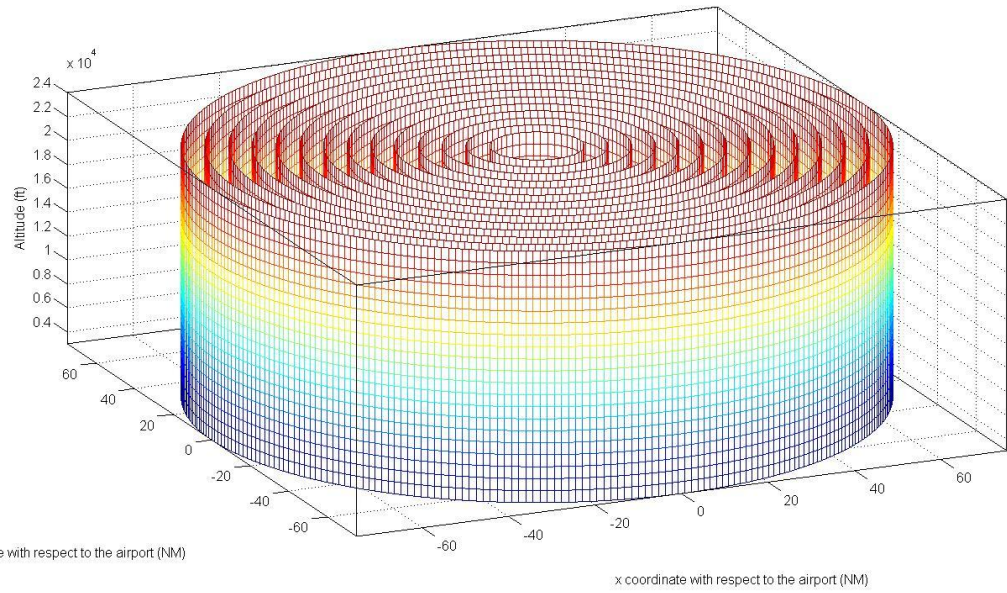


**Figure 52: Discretized airspace around Brussels Airport**

The Belgian airspace cannot be completely used by civil aviation, due to airspaces that are dedicated to the military, amongst others. To deal with various situations of available airspace, the waypoints in airspaces that are not available can be blocked. For example, the waypoints inside the military training area TSA26A at the top level (24,000ft) are depicted in yellow in Figure 53:

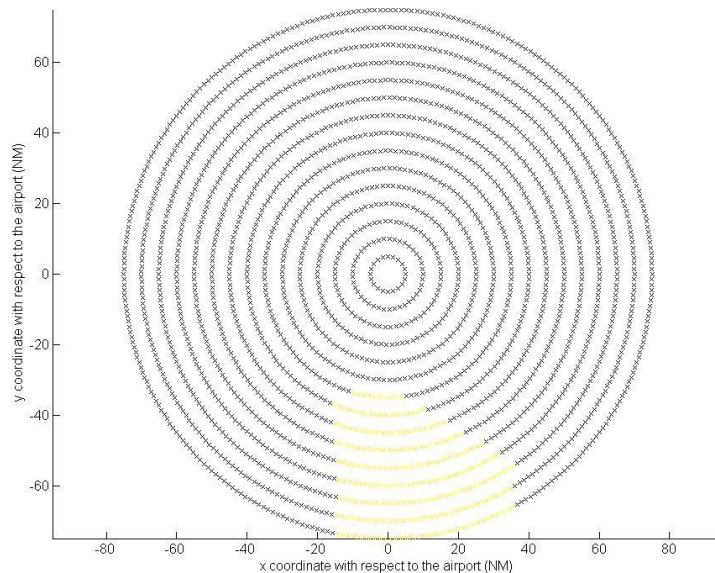


**Figure 53: Waypoints in TSA26A at 24,000ft highlighted in yellow**

### 5.2.2. Determination of the optimal trajectory

To determine whether or not an aircraft can go from one waypoint to another, the required rate of heading change and required rate of descent between these waypoints is calculated. These values are compared to the maximum rate of heading change and rate of descent within the aircraft performance envelope. The maximum rates are taken from the BADA database [22]. For each waypoint, a list of waypoints that can be reached is saved together with the time and fuel needed for

each of these transitions. Figure 54 shows the possible transitions for the 5 innermost rings for the Airbus 320:

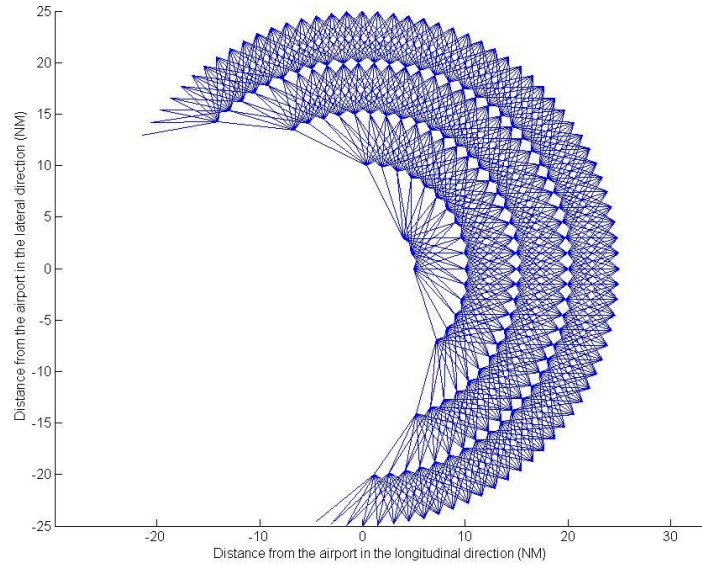


**Figure 54: Possible transitions for the Airbus 320 between the 5 most inner rings**

Now that all possible transitions are known, the optimal trajectory is to be searched for. Once again, this is performed by taking into account the cost index. Unfortunately, we don't know the cost indices which are used by the airlines so representative values are taken. Due to calculation capability limitations, we only consider a number of aircraft types which give a good representation of the traffic distribution at Brussels Airport. These types and the related cost indices according to [36] that are used in the simulation are given in Table 15:

**Table 15: Aircraft types with their respective cost indices for the simulation**

Aircraft type	Cost index
A319	12
A320	15
A321	20
A330-200	30
B737-400	15
B737-800	15
B767-300	30
DH8D	10
Embraer 145	10
Embraer 190	12
RJ1H	10

### 5.2.3. Multiple aircraft scenario

The most interesting part of the simulation is the use of multiple aircraft. The big difficulty comes from the different performance characteristics of different aircraft types. Since all aircraft need to be separated, this could have a drawback on the throughput of the airspace and of the runways. So the goal is to search for the best, conflict-free route with due respect for the time and fuel costs since we

are using the cost index parameter. The separation in the simulation is done by blocking waypoints behind an aircraft for a certain time period. This time period is depending on the wake turbulence category (WTC) of the concerned aircraft and the following aircraft [37]. Table 16 shows the applicable horizontal separation minima for aircraft flying at the same altitude:

**Table 16: Standard separation minima for aircraft flying at the same altitude**

WTC preceding aircraft	WTC following aircraft	Minimum separation
Heavy	Heavy	4.0 NM
Heavy	Medium	5.0 NM
Heavy	Light	6.0 NM
Medium	Light	5.0 NM

When aircraft aren't flying at the same altitude, a minimum vertical separation of 1000ft is required. For the simulation, a representative traffic situation from September 2012 is taken so that the considered traffic is as realistic as possible. The "First come, first serve" method is used so that aircraft are handled in the same order as they arrive at the boundary of the considered airspace. A sequence of aircraft with a mix of light, medium and heavy aircraft has been chosen and is shown in Table 17:

**Table 17: Simulation sequence (aircraft type and initiation time)**

Aircraft number	Aircraft type	Initiation time (s)
1	RJ1H	0
2	A320	560
3	E145	712
4	A319	896
5	B738	1028
6	A321	1080
7	E190	1208
8	A320	1328
9	A332	1513
10	RJ1H	1796
11	B763	2009

The sequence in Table 17 shows a typical mix of aircraft landing at Brussels Airport and coming from different directions.

### 5.3. Results

Since we are mainly interested in minimizing the cost of each flight, only the fuel and time flown are optimized taking into account the cost indices in Table 15. Table 18 shows the descent times, fuel consumptions and the estimated total costs of the flights. The total cost is estimated using a fuel price of 0.93 €/kg [38]. The cost of time was calculated using the cost index for every aircraft type (equation (2.2)).

**Table 18: Results of the simulation**

Aircraft number	Aircraft type	Descent time (min)	Descent fuel (kg)	Total cost (€)
1	RJ1H	18.4	219	375
2	A320	16.9	187	410
3	E145	18.1	121	280
4	A319	16.6	163	337
5	B738	17.4	190	419
6	A321	16.9	187	489
7	E190	18.4	172	365
8	A320	17.4	190	419
9	A332	16.6	348	788
10	RJ1H	18.4	219	375
11	B763	16.6	238	685

We clearly see that the light aircraft have a longer descent time because they are flying slower. However, this is not a problem since the simulation takes into account the separation standards. Nowadays, this is resolved by air traffic control giving speed and heading instructions to the aircraft. The simulation does something similar: it looks for a trajectory which will probably not be the best one but the second best one, third best one,... Figure 55 shows this for the first two aircraft of the sequence:

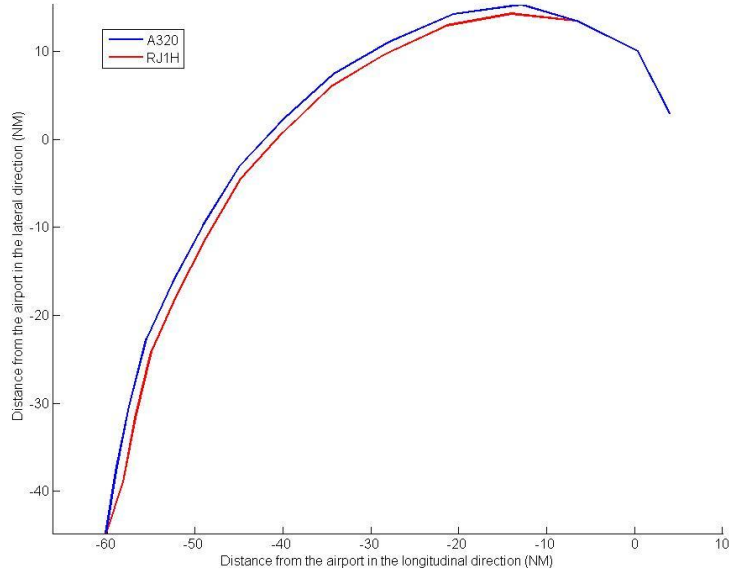


**Figure 55: Horizontal trajectories of the two first aircraft in the simulation sequence**

Ideally, we would like to keep the same sequence of arriving aircraft which all follow more or less the same flight pattern. A solution for this is that the separation could be done some time before the aircraft start their descents. This separation could be done using tools which are being developed [39], but this topic falls outside the scope of this work.

Another conclusion that can be made is that the separation conflicts can lead to a reduced throughput. However, since Brussels Airport is not congested, there is no problem, which is clear from the simulation results because we see that the aircraft arrive at approximately the same time as they did in real life.

A big advantage of dynamic CDO is that it also optimizes the horizontal profile. The horizontal profiles of simulated flights coming from France and Germany are presented over a chart of Belgium in Figure 56:

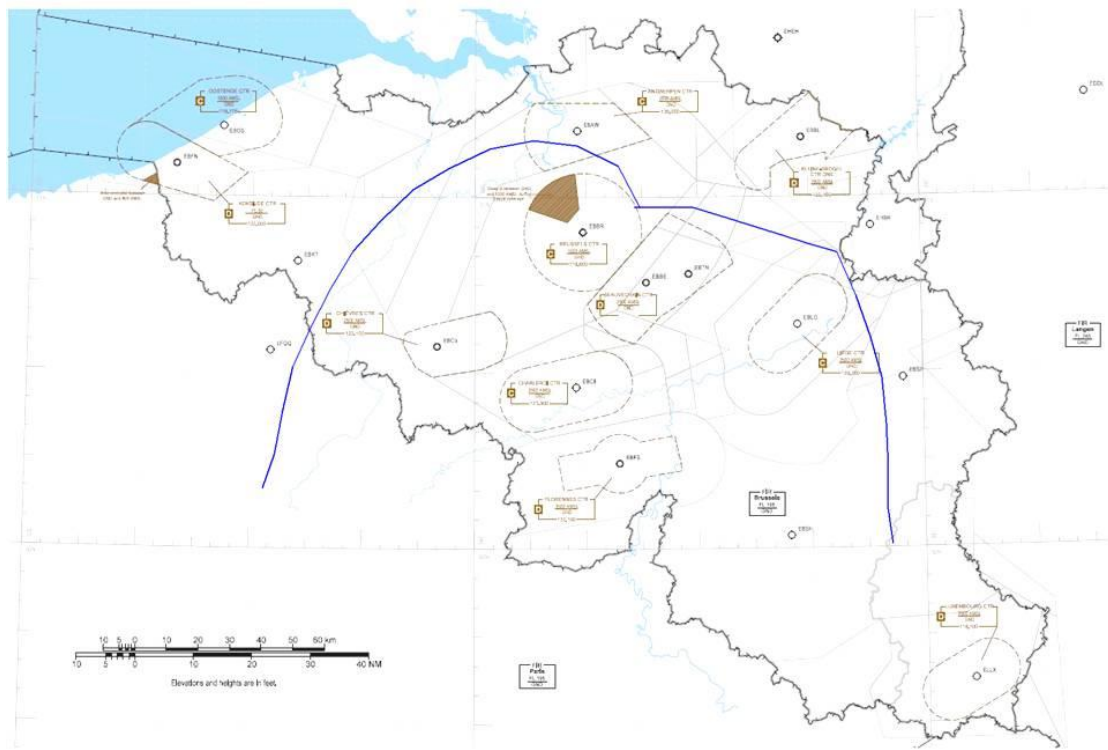


Figure 56: Optimal trajectories of flights coming from France and Germany (chart<sup>26</sup> from [27])

When comparing these flight paths with the real flight paths which are flown nowadays, we see that they are corresponding quite well (Figure 57). Though, the aircraft are staying at higher altitudes for a longer time.

---

<sup>26</sup> Belgocontrol AIM, “eAIS Package Belgium and G.-D. Luxembourg,” Belgocontrol, Steenokkerzeel, 2013.

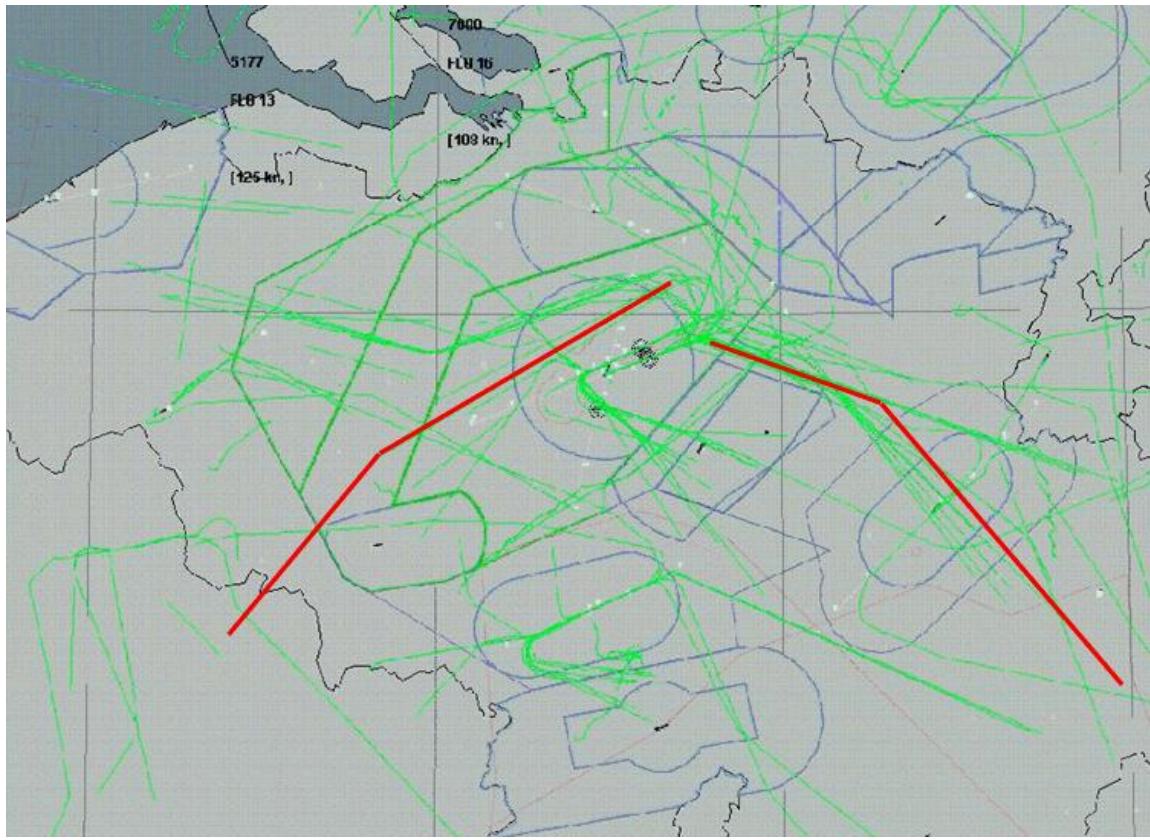


Figure 57: Radar image from Belgocontrol highlighting the main traffic flows from France and Germany

In general, we can say that the dynamic CDO simulation is quite nice to calculate and present optimal profiles for every arriving aircraft. So, the planning of flights by means of dynamic CDO increases predictability but some additional tools might be necessary to really get a step closer to 4D flights.

## 6. Future perspectives

The research in trajectory optimization in the SESAR context is far from being finished. What was done in this work is just a part of the bigger picture. Ideally, the complete flight should be optimized, from the moment the engines are started to the moment when they are shut down.

### 6.1. Cost reduction tool

The contents of this work could be used in a cost reduction tool which incorporates the optimization of all phases of the flight. Essentially, this would come down to building a tool which calculates the most cost efficient cost index as in [40]. To be able to build this tool, the intense cooperation of an airline will be necessary, bearing in mind confidentiality of cost items and figures.

The tool should be a combination of several smaller building blocks, each of them considering a specific part of the flight (taxi in/out, take off, climb, cruise and descent).

#### 6.1.1. Taxi in/out

The taxi phase can consume quite some fuel when a lot of aircraft are scheduled to take off at almost the same time. This means that the aircraft has to wait for its turn while the engines are running and consuming fuel. The Wheeltug system could be a solution for this problem [41].

#### 6.1.2. Takeoff

The takeoff phase is highly controlled due to safety restrictions so that room for optimization is limited. Nevertheless, nowadays most airlines use reduced takeoff power to reduce engine deterioration, and hence maintenance costs and fuel burn, which helps optimizing the take off in the process.

#### 6.1.3. Climb and descent

The main ideas of the climb and descent profiles have been examined in this work. However, a number of additional aspects could be implemented to get even closer to reality. For example, the average winds during the descent and climb could be taken into account because they can have a large effect. A study of EUMETNET [42] showed that up to 165 kg per flight could be saved when the actual wind is known more accurately and is taken into account.

On the aerodynamic side, the PERF and IDLE factors [43] could be taken into account for every individual aircraft. The PERF factor is a corrective factor that adjusts the performance model of the FMS to the real aircraft performance. It reflects the combined effect of engine and aerodynamic deterioration which is inevitable over time. This factor is used in calculations to correct the fuel flow and it has an impact on the specific range of the aircraft (the amount of mileage obtained per input of fuel). With time this specific range could be reduced by up to 4-5%. The IDLE factor tunes the idle rate of the FMS predictions to the real idle thrust. This is very important for the calculation of the descent profile because it influences the optimal position of the top of descent.

The ideal profiles can be determined depending on the cost index by balancing the methods of the specific excess power and the fuel specific energy.

#### 6.1.4. Cruise

The cruise phase is the longest part of the flight and therefore it is very important to optimize it. Especially the wind is a critical parameter because with wind, the air distance is different from the

ground distance flown. The Breguet equation for the specific range (SR) with the wind component (W/V) can be used to optimize the fuel needed for the cruise phase [44], [45]. This equation integrates the segments of the cruise part between point 0 (the top of climb) and point n (the top of descent).

$$SR = \int_0^{n-1} \frac{(Ground\ distance)_i + W/V_{mean,i} * \Delta t}{(Fuel\ used)_i} \quad (6.1)$$

With:

$$W/V_{mean,i} = \frac{1}{\Delta t} \int_{t_i}^{t_{i+1}} W/V_{longitudinal} dt \quad (6.2)$$

$$\Delta t = t_{i+1} - t_i \quad (6.3)$$

Using (2.1), we can define a cost function  $\tau$  which has to be minimized:

$$\tau = \frac{C}{C_F} = \Delta F + CI * \Delta T \quad (6.4)$$

This cost function can be determined for 1NM:

$$\tau (1NM) = \frac{1}{SR} + CI * \frac{1}{V} \quad (6.5)$$

This cost function can then be optimized to be minimal and the outcome will be the optimal cruise speed.

## 6.2. Point merge

The point merge method could be examined using the CDO profiles described in this work. Since this method is being considered in the SESAR programme, it might be interesting to look into the advantages and/or disadvantages of its implementation at Brussels Airport.

## 6.3. Dynamic CDO

The dynamic CDO simulation can further be extended by adding traffic departing from Brussels Airport and adding overflying traffic. Here also, the average winds in the Brussels airspace could be added to be more realistic.

## 7. Conclusions

From the introductory texts it can be concluded that the air traffic management industry is very eager to improve air traffic management. Nevertheless, a lot of issues remain unsolved. This is mainly due to the fact that when changing one thing, a lot of other problems arise. This should not hinder us however to try to improve current working methods. In this work, the focus was put on the cost reduction of the climb and descent profiles. These were optimized considering an aircraft of the size of the Airbus 320.

The optimization of the climb profile was done using the specific excess power and fuel specific energy of the aircraft. Initially, the ideal profile without any constraints was calculated. Then, noise abatement and other operational restrictions were added. The optimal profiles depend upon the cost index, which balances between the cost of time and the cost of fuel. Optimal profiles were calculated for two cost indices: a cost index equal to zero and a maximum value. The resulting optimal profiles were compared to flight profiles that have been flown in real life. This revealed that, depending on the cost index, 306 to 390kg of fuel and 2.7 to 3.4 minutes could be saved when the optimal profiles would be flown.

The descent profiles are optimized by calculating the optimal descent angle at every moment during the descent such that the distance flown in idle condition is maximal. Again, the ideal profiles without constraints are calculated, after which the several restrictions were added. The most severe restriction is the fixed handover altitude when aircraft are handed over from foreign air traffic control to the Belgian air traffic control. This restriction is especially hindering an optimal CDO for aircraft coming from Germany. The handover happens then over the Belgian-German border at FL220 which means that they have to fly level for quite some time. Comparing the optimal profiles with the flight profiles of the real flights, we see that they more or less correspond. However, the real flights generally have to descend earlier than they would like and some intermediate level parts are present in the descent. This is of course to be avoided because level parts ask for an increase in thrust and consequently command more fuel burn.

Next, a closer look was taken to an air traffic control problem: should a departing aircraft be given priority over an arriving aircraft or vice versa? The answer is highly depending on the actual traffic situation so there is no clear-cut answer to this question. However, a simple tool to determine the position where the two aircraft will meet and come into conflict is proposed.

The last part of this work, the dynamic CDO simulation, is tending more towards a real traffic situation by considering multiple aircraft, different airspace constraints and separation minima for the descending aircraft. So here not only the vertical profile is being optimized but also the horizontal one. The Belgian airspace is considered and was discretized into a number of waypoints. All possible trajectories, taking into account the different aircraft performance characteristics, are determined and the most cost efficient one is selected. This is done using an estimated value for the cost index of every aircraft. The traffic scenario was made from a mix of the typical aircraft types that are seen at Brussels Airport. In order to have a realistic situation, the sequence and timing between aircraft initiations was taken from real flights. Results show that optimal trajectories are almost following the trajectories of real flights nowadays. The big advantage is that the simulation allows having better predictability, which is one of the main hurdles for the implementation and facilitation of CDOs.

Although required research into continuous descents and continuous climbs commands a lot more extensive work than what was performed here, most of the essential aspects of the issues at stake were effectively addressed and examined. There is however still ample room for further research and development around this fascinating theme.



## 8. References

- [1] J.-J. Speyer, "Driving Flight Operations Excellence," in *3rd Annual Flight Operations Excellence, Marcus Evans Conference, Barcelona*, 2011.
- [2] B3 SESAR JU Project, "Phase two report," 2012.
- [3] Eurocontrol, "Continuous descent: A guide to implementing continuous descent," 2011.
- [4] CAA, NATS, BAA, Virgin Atlantic, British Airways, Easyjet, DfT, Mytravel, "Noise from arriving aircraft," 2006.
- [5] ICAO, "Continuous climb operations (CCO)," 2012.
- [6] SESAR Joint Undertaking, "Performance of flight trials and demonstrations validating solutions for the reduction of CO2 emissions," 2010.
- [7] SESAR Joint Undertaking AIRE, "Reduction of emissions on the North Atlantic by the implementation of ADS-B," 2010.
- [8] SESAR JU, "MINT project: Continuous descent approach procedure using RNP-AR," 2009.
- [9] RETA-CDA Consortium, "Reduction of emissions in terminal areas using continuous descent approaches," 2010.
- [10] Eurocontrol, "FABs," 2011. [Online]. Available: [www.eurocontrol.int](http://www.eurocontrol.int). [Accessed 21 April 2013].
- [11] Eurocontrol, "Point merge: a more efficient way of sequencing arrivals," 2011.
- [12] Eurocontrol, "Point Merge successfully implemented in Dublin," 25 January 2013. [Online]. Available: <http://www.eurocontrol.int/news/point-merge-successfully-implemented-dublin>. [Accessed 25 April 2013].
- [13] Eurocontrol, "CDA Map Tool," 2010. [Online]. Available: <http://extranet.eurocontrol.int>. [Accessed 10 April 2013].
- [14] R. De Muynck, S. Raynaud and B. Korn, "Optimal User Forum: Session 1 - Continuous descent approach," 2008.
- [15] J.-J. Speyer, "Getting to Grips with the Cost Index," in *2nd Annual Flight Operations Excellence, Marcus Evans Conference, Amsterdam*, 2010.
- [16] Flugwerkzeuge aviation software gmbh, "Airsavings: Cost Index Administrator Application User Documentation," Vienna, 2005.
- [17] J.-J. Speyer, Airbus, "Are we finally Getting to Grips with the Cost Index?," in *Airline economics seminar*, Blagnac, France, 2008.

- [18] Airbus, "Getting to grips with the cost index," Blagnac, 1998.
- [19] J.-J. Speyer, "The Cost Index as a Concept in Flight Operations," in *3rd Annual Flight Operations Excellence*, Marcus Evans Conference, Barcelona, 2011.
- [20] J.-J. Speyer, Airbus, "Airbus views on fuel economy," in *15th Performance & Operations conference*, Puerto Vallarta, 2007.
- [21] European Union, "Commission implementing regulation (EU) No 391/2013 of 3 May 2013 laying down a common charging scheme for air navigation services," 2013.
- [22] Eurocontrol, "User manual for the base of aircraft data (BADA) revision 3.9," Brussels, 2011.
- [23] Eurocontrol, "Eurocontrol standard document for surveillance data exchange: Part 9: Category 062: SDPS Track messages," 2009.
- [24] Airbus, "Getting to grips with aircraft performance," Airbus Industries, Blagnac, France, 2002.
- [25] W. Bosschaerts, Aircraft performance, 2011.
- [26] A. Mair, Aircraft performance, Cambridge: Cambridge University Press, 1992.
- [27] Belgocontrol AIM, "eAIS Package Belgium and G.-D. Luxembourg," Belgocontrol, Steenokkerzeel, 2013.
- [28] P. Hopff, "Noise abatement procedures - Departures," 2013.
- [29] ICAO, "Aeroplane operating procedures," in *PANS-OPS 8168 Volume I*, 2007.
- [30] IATA, "IATA Fuel Book 3rd edition," 2008.
- [31] Schaufele, The elements of aircraft preliminary design, 2000.
- [32] Airbus, "Flight crew operating manual," Blagnac, 2012.
- [33] Scandinavian Airlines System, Stockholm, 2011.
- [34] J.-J. Speyer, Airbus, "Getting to grips with fuel economy," Blagnac, 2004.
- [35] S. Alam, M. H. Nguyen, H. A. Abbass, C. Lokan, M. Ellejmi and S. Kirby, "A Dynamic Continuous Descent Approach Methodology for Low Noise and Emission," 2010.
- [36] J.-J. Speyer, "AirS@vings: Getting to grips with the cost index," in *16th Performance & Operations conference*, Paris, 2009.
- [37] SKYbrary, "Mitigation of Wake Turbulence Hazard," 29 October 2012. [Online]. Available: [http://www.skybrary.aero/index.php/Mitigation\\_of\\_Wake\\_Turbulence\\_Hazard](http://www.skybrary.aero/index.php/Mitigation_of_Wake_Turbulence_Hazard). [Accessed 7

May 2013].

- [38] IATA, "Jet fuel price monitor," 2013. [Online]. Available: <http://www.iata.org/publications/economics/fuel-monitor/Pages/index.aspx>. [Accessed 2 June 2013].
- [39] d. L. A.M.P., A. van der Eijk, M. Tielrooij and M. Mulder, "A time-space diagram based controller support tool for continuous descent operations," 2011.
- [40] J.-J. Speyer, Airbus, "Best practices for fuel economy," in *Tunisair Fuel Economy Workshop*, Tunis, 2008.
- [41] G. Dumoulin, Feasibility of electrical taxi systems / WheelTug™ to civil aircraft and to airport types., Brussels, 2013.
- [42] R. Lapsley, "Meteorology in Continuous Descent Operations," in *CDO Workshop, Eurocontrol Headquarters Brussels*, 2013.
- [43] J. Ple, "Use of PERF and IDLE factors," Airbus, 2006.
- [44] J.-J. Speyer, Specificatie en Certificatie van vliegtuigen, BruFace Lecture Delivery Presentations, Vrije Universiteit Brussel, 2013, p. 84.
- [45] J.-J. Speyer, Airbus, "Fuel used method (specific range)," in *7th Performance and Operations conference*, Cancun, 1992.

## 9. Appendix

#### A. Airspace structure in the Brussels FIR

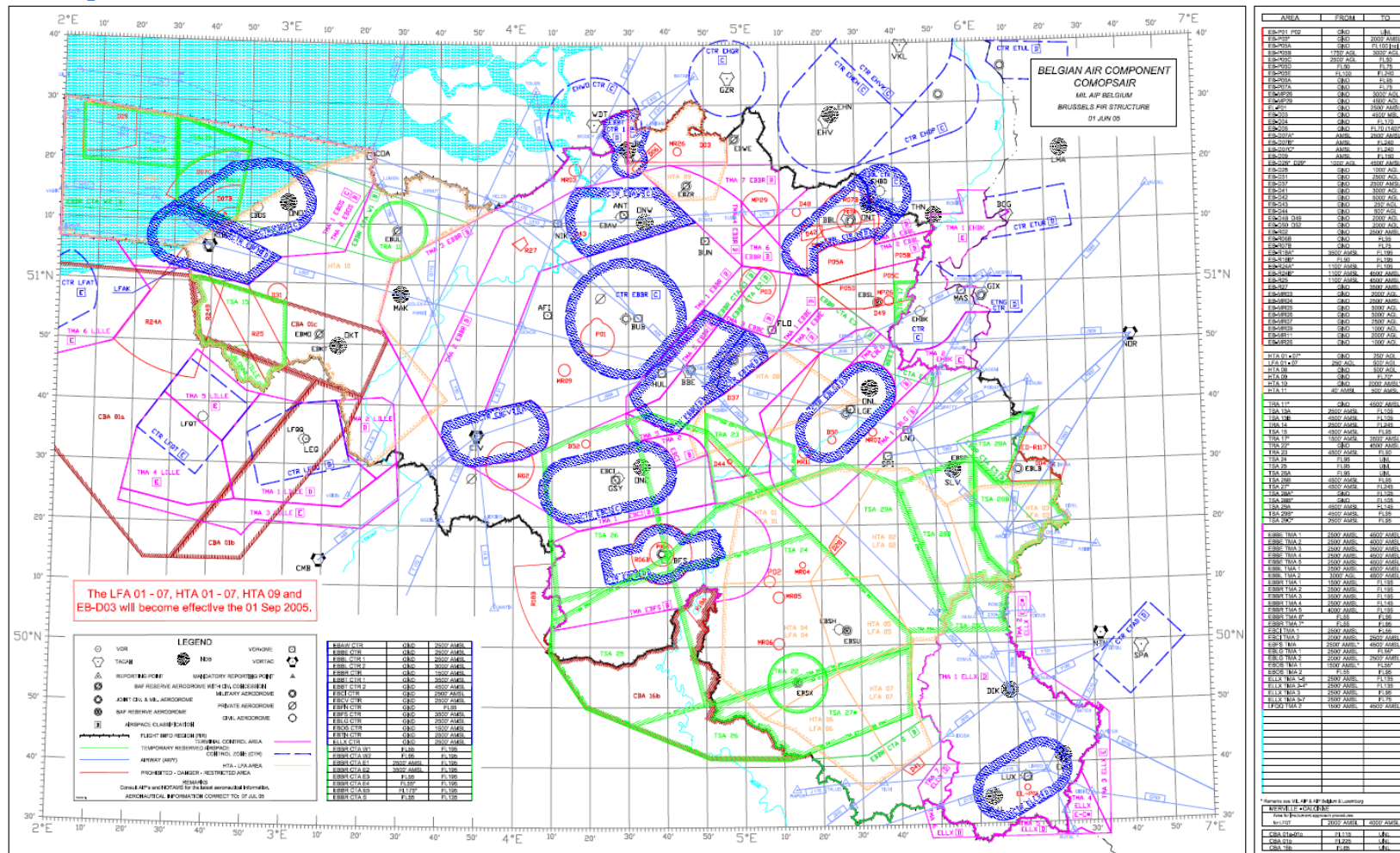


**Figure 58: Chart of the airspaces in the Belgian Flight Information Region**

## B. Results of the climb analyses

	RWY	Directions	# Flights	% flights with level segment	Average total distance (NM)		Average level distance (NM) <sup>27</sup>	Average % level distance (NM) <sup>27</sup>	Average fuel burn (kg)		Average CO <sub>2</sub> (kg)	Average total time	Average level time <sup>27</sup>	Average climb angle (°)
					STD	Avg			Avg	CO <sub>2</sub>				
All flights	07	N	123	4,9%		61,0	18,4	3,7	6,0%	818,0	2576,8	0:12:10	0:00:40	3,9
		E-SE	497	10,5%		65,3	12,0	7,2	11,1%	1092,6	3441,8	0:12:07	0:01:07	3,6
		SW	187	9,6%		65,4	13,7	5,5	8,4%	1223,4	3853,7	0:12:35	0:00:54	3,6
		WNW	125	19,2%		61,9	16,1	7,8	12,7%	1177,3	3708,6	0:12:42	0:01:22	3,6
		Total	932	10,7% Overall		64,3	14,1	6,9	10,7%	1116,8	3517,8	0:12:18	0:01:06	3,6
20	N		3	0,0%		70,0	6,2	0,0	0,0%	1049,8	3306,8	0:12:16	0:00:00	3,3
	E-SE		369	4,3%		62,6	11,7	3,9	6,2%	1115,2	3512,8	0:11:36	0:00:41	3,7
	SW		6	0,0%		55,3	12,5	0,0	0,0%	1101,0	3468,0	0:10:39	0:00:00	4,4
	WNW		0											
	Total		378	4,2% Overall		62,6	11,7	3,9	6,2%	1123,3	3538,5	0:11:35	0:00:41	3,7
25	N		1039	8,6%		62,4	15,5	4,3	6,8%	809,4	2549,7	0:12:18	0:00:52	3,7
	E-SE		4379	9,8%		65,8	12,3	8,4	12,8%	1082,0	3408,2	0:12:06	0:01:19	3,5
	SW		1679	4,7%		61,0	13,0	7,4	12,2%	1135,6	3577,2	0:11:54	0:01:28	3,9
	WNW		1234	14,5%		57,3	16,0	5,8	10,1%	1164,8	3669,1	0:11:56	0:01:07	3,9
	Total		8331	9,3% Overall		63,2	13,8	7,3	11,5%	1098,2	3459,4	0:12:03	0:01:14	3,7

<sup>27</sup> Only the flights that have a level part in their climb profile were taken into account.

Day	07	N	122	4,9%	60,9	18,5	3,7	6,0%	816,3	2571,4	0:12:10	0:00:40	3,9
		E-SE	494	10,5%	65,4	11,9	7,2	11,1%	1091,3	3437,7	0:12:08	0:01:07	3,6
		SW	185	9,7%	65,5	13,8	5,5	8,4%	1217,4	3834,9	0:12:35	0:00:54	3,6
		WNW	124	18,5%	61,9	16,1	8,0	12,9%	1177,3	3708,5	0:12:43	0:01:24	3,6
		Total	925	10,7% Overall	64,4	14,0	6,9	10,7%	1114,7	3511,3	0:12:18	0:01:07	3,6
20		N	0										
		E-SE	217	5,5%	63,5	10,5	3,9	6,2%	960,7	3026,3	0:11:57	0:00:41	3,7
		SW	1	0,0%	39,0	0,0	0,0	0,0%	137,1	432,0	0:09:24	0:00:00	6,0
		WNW	0										
		Total	218	5,5% Overall	63,3	10,6	3,9	6,2%	956,9	3014,3	0:11:57	0:00:41	3,7
25		N	997	8,8%	62,5	15,6	4,3	6,9%	802,6	2528,2	0:12:21	0:00:53	3,7
		E-SE	4350	9,9%	65,8	12,2	8,5	12,8%	1079,6	3400,9	0:12:06	0:01:19	3,5
		SW	1622	4,8%	61,2	13,1	7,4	12,1%	1132,5	3567,3	0:11:55	0:01:27	3,9
		WNW	1186	14,8%	57,5	16,1	5,8	10,0%	1174,3	3699,0	0:11:53	0:01:07	3,9
		Total	8155	9,5% Overall	63,3	13,8	7,3	11,5%	1094,7	3448,5	0:12:04	0:01:14	3,7

Night	07	N	1	0,0%	70,0	0,0	0,0	0,0%	1027,7	3237,3	0:12:17	0:00:00	3,3
		E-SE	3	0,0%	47,0	15,1	0,0	0,0%	1310,1	4126,7	0:09:27	0:00:00	4,6
		SW	2	0,0%	57,5	0,5	0,0	0,0%	1774,5	5589,8	0:12:01	0:00:00	4,0
		WNW	1	100,0%	65,0	0,0	4,0	6,2%	1181,1	3720,6	0:12:12	0:00:32	3,5
		Total	7	14,3% Overall	55,9	13,2	4,0	7,2%	1384,0	4359,7	0:10:59	0:00:32	4,1
20	20	N	3	0,0%	70,0	6,2	0,0	0,0%	1049,8	3306,8	0:12:16	0:00:00	3,3
		E-SE	152	2,6%	61,5	13,0	3,8	6,1%	1342,0	4227,2	0:11:05	0:00:39	3,8
		SW	5	0,0%	58,6	11,1	0,0	0,0%	1293,7	4075,2	0:10:54	0:00:00	4,1
		WNW	0										
	Total		160	2,5% Overall	61,6	12,9	3,8	6,1%	1351,9	4258,5	0:11:06	0:00:39	3,8
25	25	N	42	2,4%	59,2	11,8	1,0	1,7%	971,4	3059,9	0:10:49	0:00:20	4,0
		E-SE	29	3,4%	63,2	13,1	4,0	6,3%	1430,5	4505,9	0:11:23	0:00:28	3,8
		SW	57	1,8%	57,2	10,3	12,0	21,0%	1225,1	3859,1	0:11:09	0:02:08	4,1
		WNW	48	6,3%	50,4	10,8	7,7	15,2%	930,0	2929,4	0:13:08	0:01:44	3,8
	Total		176	3,4% Overall	56,8	12,1	6,7	11,7%	1277,6	4024,5	0:11:39	0:01:21	4,0

## C. Profiles of departing traffic

a. Friday 14/09/2012



Figure 59: Horizontal profiles of the flights leaving to the North

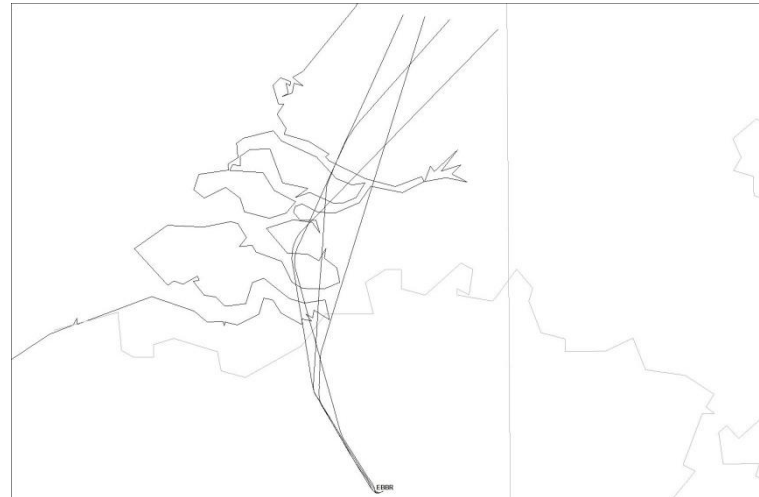


Figure 60: Horizontal profiles of the flights with a level part leaving to the North

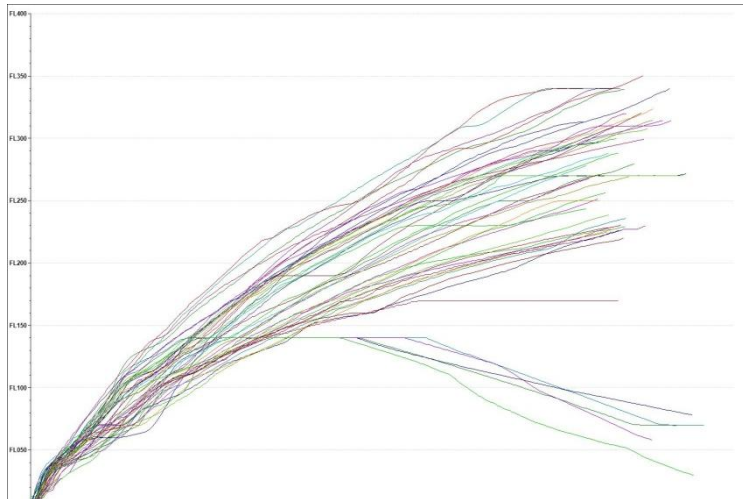


Figure 61: Vertical profiles of the flights leaving to the North

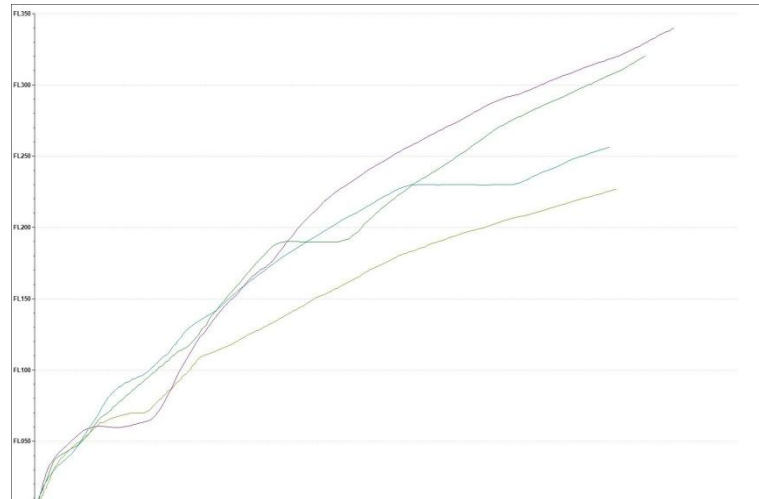


Figure 62: Vertical profiles of the flights with a level part leaving to the North

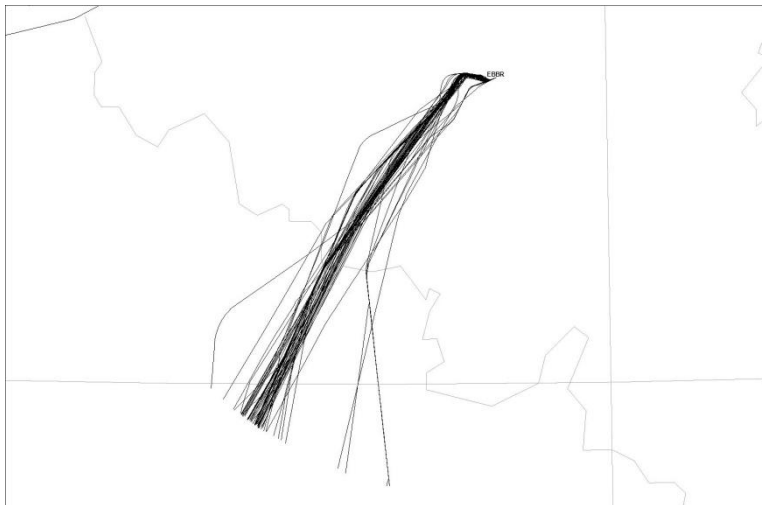


Figure 63: Horizontal profiles of the flights leaving to the Southwest



Figure 64: Horizontal profiles of the flights with a level part leaving to the Southwest

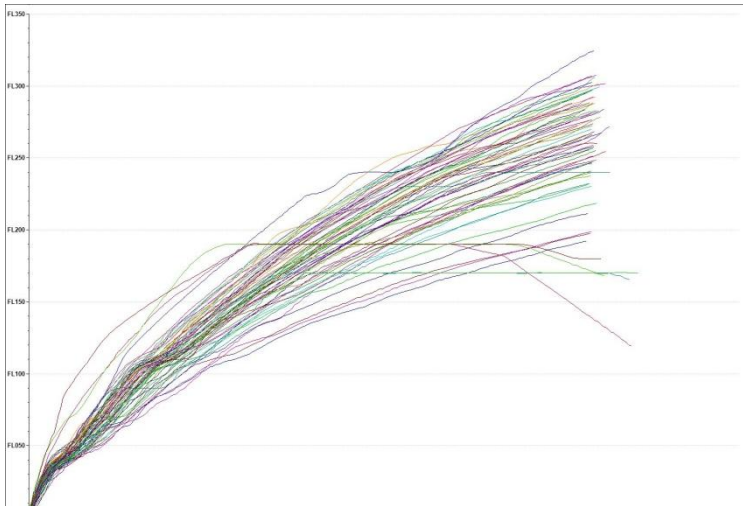


Figure 65: Vertical profiles of the flights leaving to the Southwest

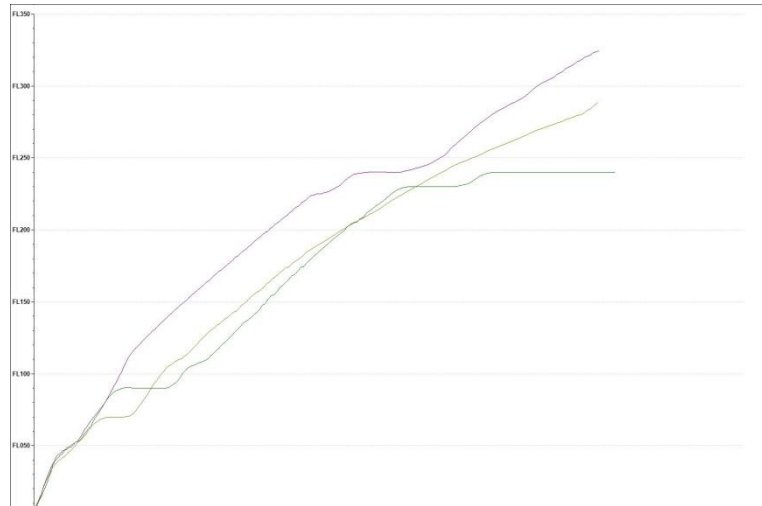


Figure 66: Vertical profiles of the flights with a level part leaving to the Southwest



Figure 67: Horizontal profiles of the flights leaving to the West Northwest



Figure 68: Horizontal profiles of the flights with a level part leaving to the West Northwest

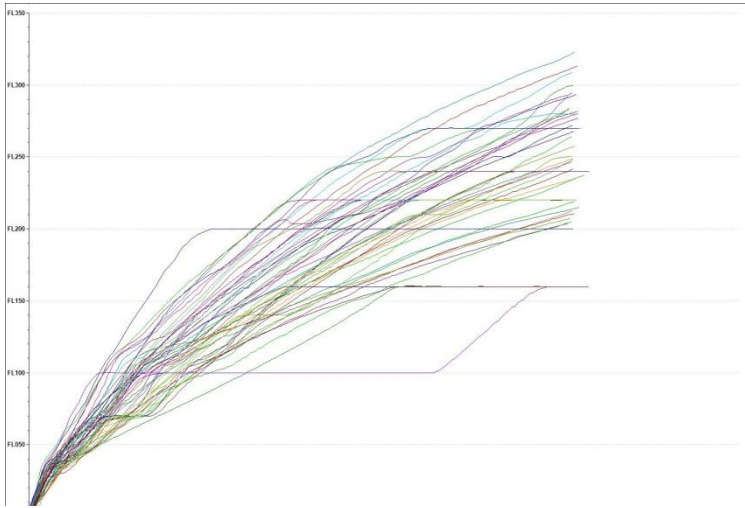


Figure 69: Vertical profiles of the flights leaving to the West Northwest

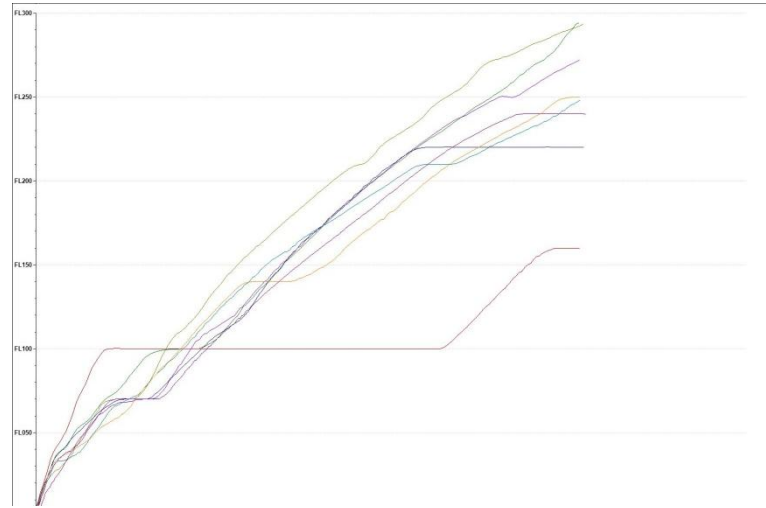


Figure 70: Vertical profiles of the flights with a level part leaving to the West Northwest

b. Sunday 23/09/2012



Figure 71: Horizontal profiles of the flights leaving to the North



Figure 72: Horizontal profiles of the flights with a level part leaving to the North

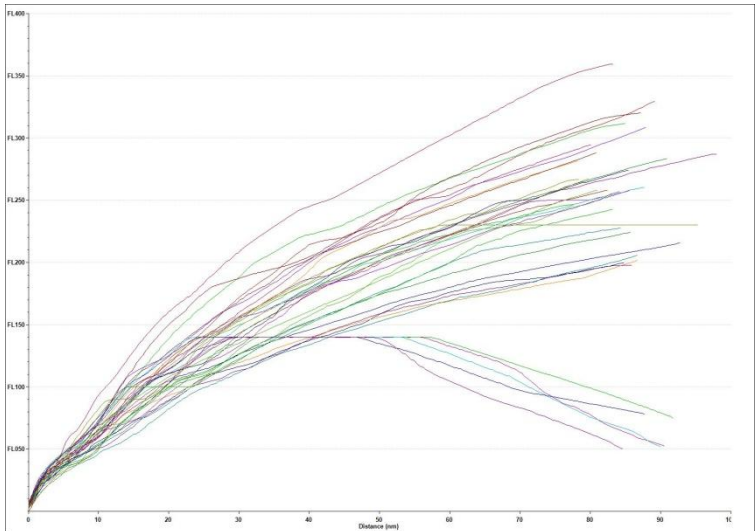


Figure 73: Vertical profiles of the flights leaving to the North

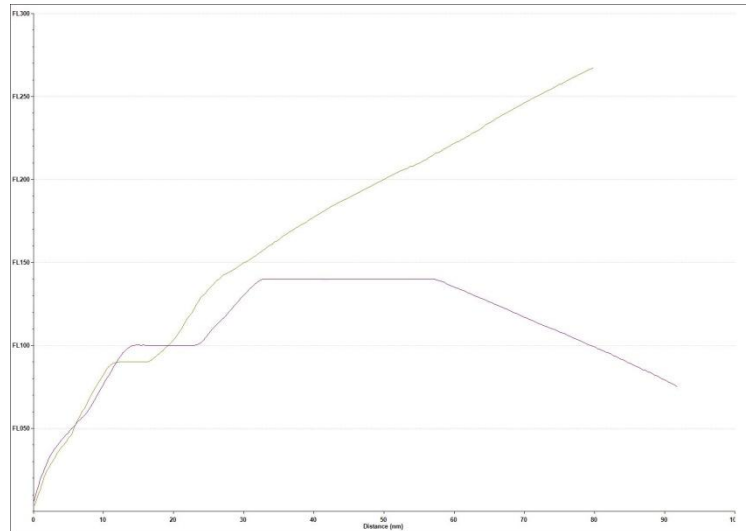


Figure 74: Vertical profiles of the flights with a level part leaving to the North



Figure 75: Horizontal profiles of the flights leaving to the East and Southeast

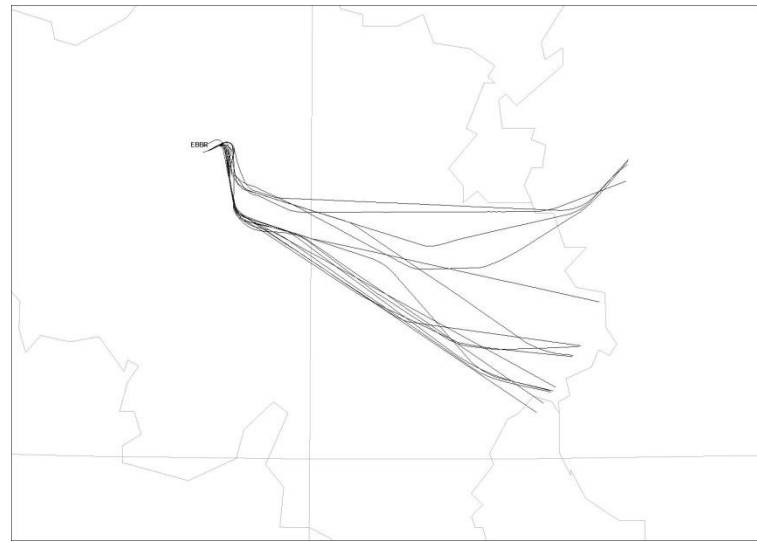


Figure 76: Horizontal profiles of the flights with a level part leaving to the East and Southeast

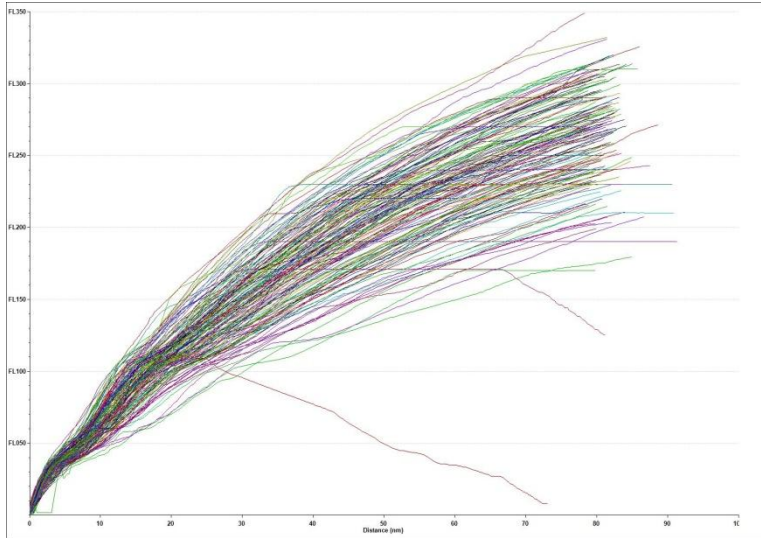


Figure 77: Vertical profiles of the flights leaving to the East and Southeast

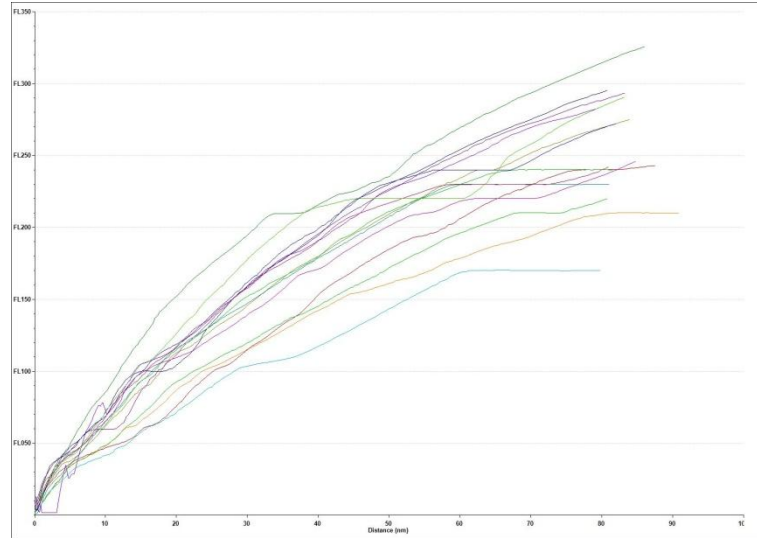


Figure 78: Vertical profiles of the flights with a level part leaving to the East and Southeast



Figure 79: Horizontal profiles of the flights leaving to the Southwest

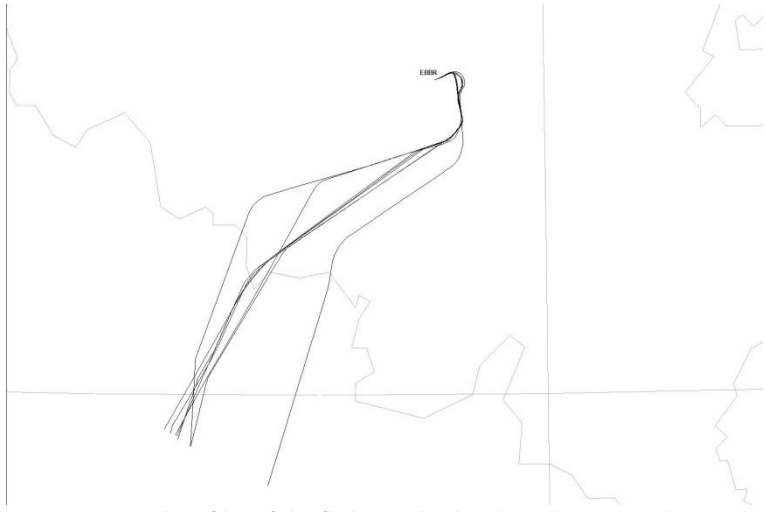


Figure 80: Horizontal profiles of the flights with a level part leaving to the Southwest

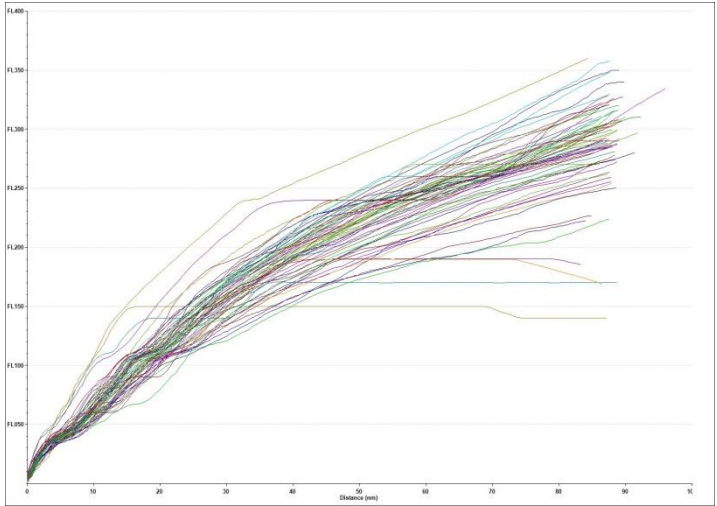


Figure 81: Vertical profiles of the flights leaving to the Southwest

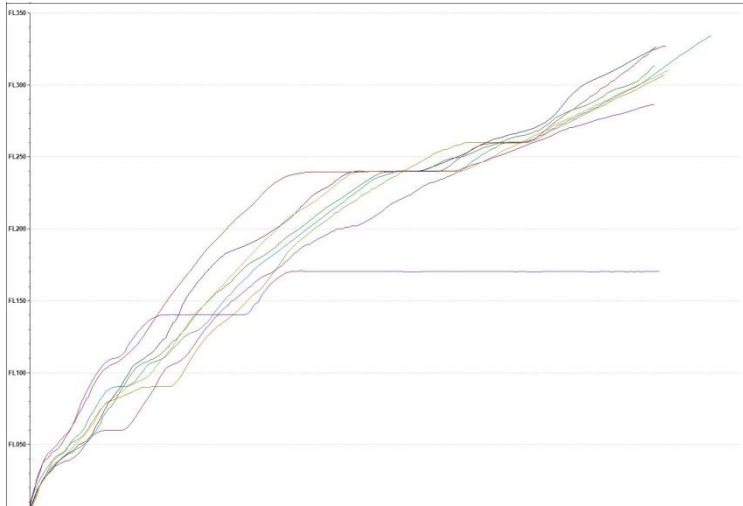


Figure 82: Vertical profiles of the flights with a level part leaving to the Southwest

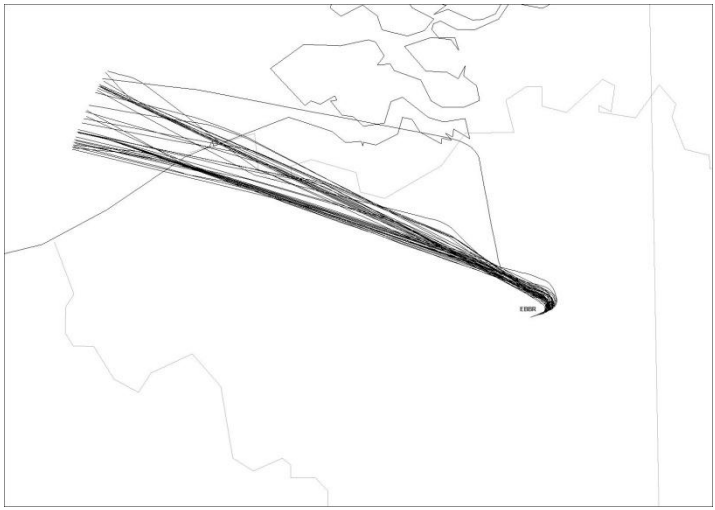


Figure 83: Horizontal profiles of the flights leaving to the West Northwest



Figure 84: Horizontal profiles of the flights with a level part leaving to the West Northwest

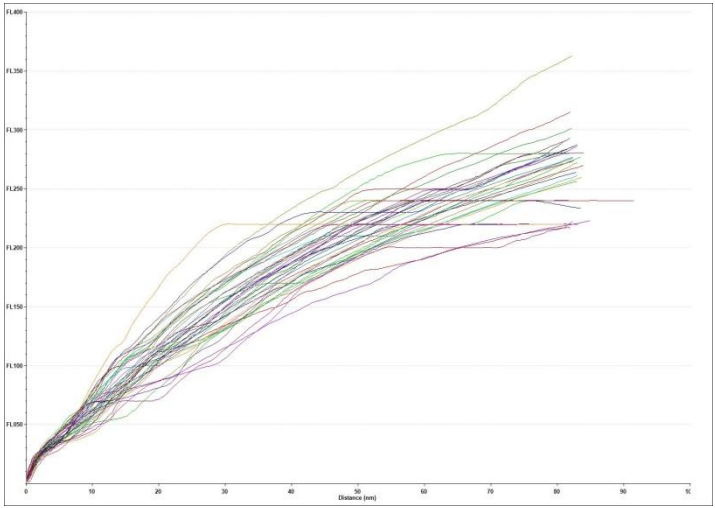


Figure 85: Vertical profiles of the flights leaving to the West Northwest

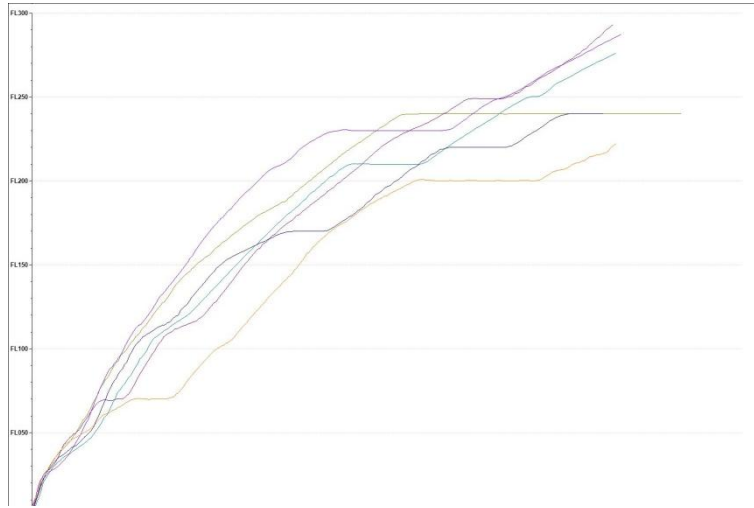


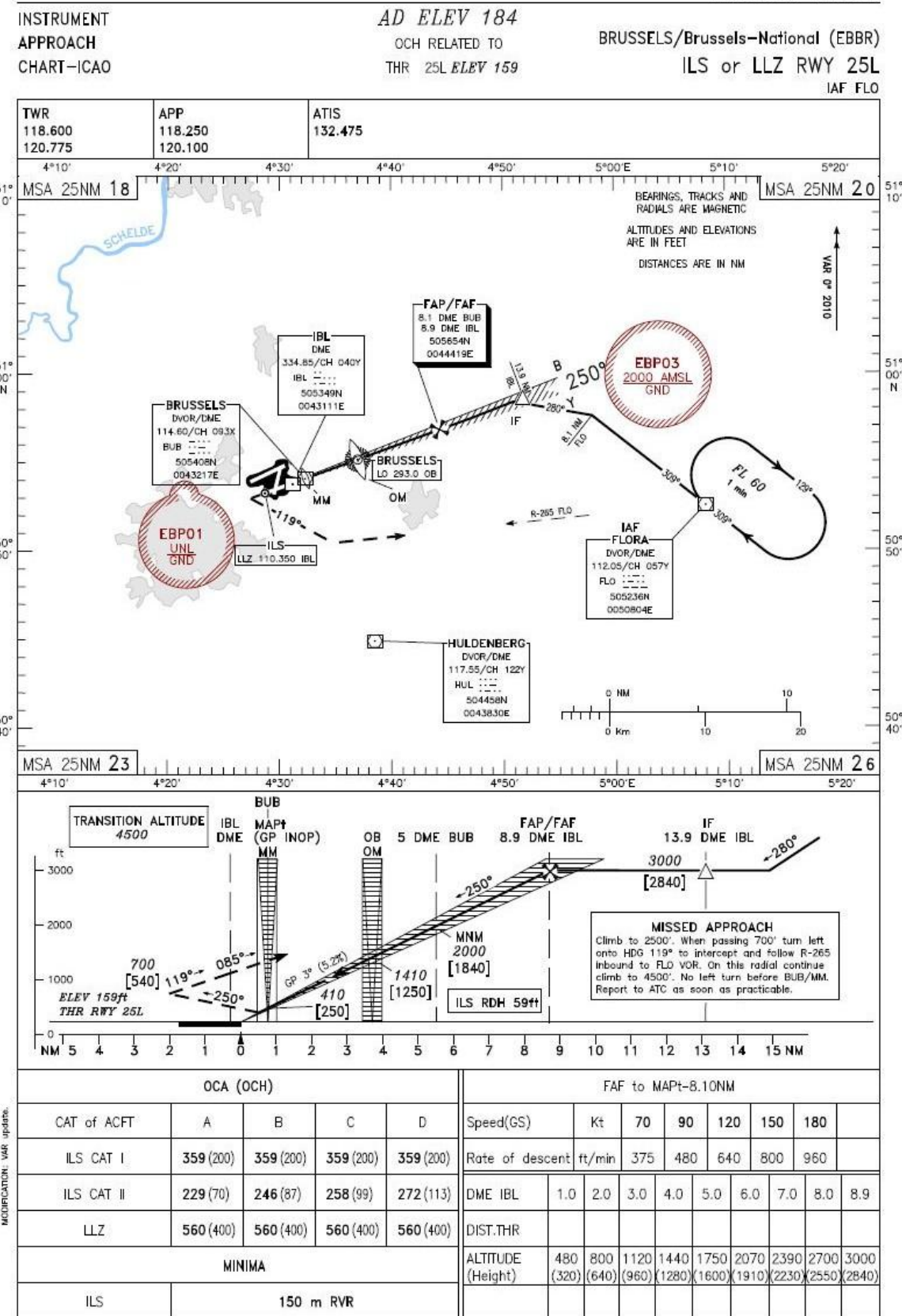
Figure 86: Vertical profiles of the flights with a level part leaving to the West Northwest

## D. ILS chart runway 25L

AIP BELGIUM AND G.D. OF LUXEMBOURG

AD2 EBBR IAC.03

Effective: 05 APR 2012



© BELGOCONTROL AIM, 2012

Figure 87: ILS approach chart for runway 25L at Brussels Airport [27]

### E. Distribution of aircraft types at Brussels airport

%	Departure	Arrival	All	%	Departure	Arrival	All	%	Departure	Arrival	All
A306	0,2%	0,2%	0,2%	C510	0,1%	0,1%	0,1%	LJ45	0,1%	0,1%	0,1%
A30B	0,2%	0,2%	0,2%	C525	0,1%	0,1%	0,1%	LJ60	0,1%	0,1%	0,1%
A310	0,3%	0,3%	0,3%	C550	0,2%	0,2%	0,2%	MD11	0,2%	0,2%	0,2%
A318	0,0%	0,0%	0,0%	C560	0,1%	0,1%	0,1%	MD82	0,7%	0,7%	0,7%
A319	18,4%	18,6%	18,5%	C56X	0,5%	0,5%	0,5%	MD87	0,0%	0,0%	0,0%
A320	15,4%	15,4%	15,4%	C650	0,0%	0,0%	0,0%	MU30	0,0%	0,0%	0,0%
A321	3,6%	3,6%	3,6%	C680	0,0%	0,0%	0,0%	P180	0,1%	0,1%	0,1%
A332	2,8%	2,9%	2,9%	CL30	0,0%	0,0%	0,0%	P46T	0,0%	0,0%	0,0%
A333	1,6%	1,6%	1,6%	CL60	0,2%	0,2%	0,2%	PAY3	0,0%	0,0%	0,0%
A342	0,0%	0,0%	0,0%	CRJ2	0,3%	0,3%	0,3%	PC12	0,1%	0,0%	0,0%
A343	0,1%	0,1%	0,1%	CRJ7	0,5%	0,6%	0,6%	PRM1	0,0%	0,0%	0,0%
AN28	0,0%	0,0%	0,0%	CRJ9	0,9%	0,9%	0,9%	RJ1H	10,3%	10,4%	10,3%
ATP	0,2%	0,2%	0,2%	D328	0,4%	0,4%	0,4%	RJ85	2,6%	2,6%	2,6%
B350	0,1%	0,1%	0,1%	DA42	0,0%	0,0%	0,0%	SB20	0,1%	0,1%	0,1%
B462	0,0%	0,0%	0,0%	DH8D	4,1%	4,1%	4,1%	SW4	0,1%	0,1%	0,1%
B463	0,2%	0,2%	0,2%	E120	0,0%	0,0%	0,0%	TBM7	0,0%	0,0%	0,0%
B733	2,1%	2,1%	2,1%	E135	0,9%	0,9%	0,9%	YK40	0,0%	0,0%	0,0%
B734	2,6%	2,5%	2,6%	E145	3,5%	3,6%	3,6%				
B735	1,6%	1,6%	1,6%	E170	0,5%	0,5%	0,5%				
B736	0,6%	0,6%	0,6%	E190	4,0%	4,0%	4,0%				
B737	2,2%	2,2%	2,2%	E50P	0,1%	0,0%	0,1%				
B738	6,2%	6,1%	6,2%	E55P	0,0%	0,0%	0,0%				
B739	0,1%	0,1%	0,1%	F100	0,7%	0,7%	0,7%				
B742	0,1%	0,1%	0,1%	F2TH	0,2%	0,2%	0,2%				
B744	0,9%	0,9%	0,9%	F50	0,0%	0,0%	0,0%				
B752	1,6%	1,6%	1,6%	F70	1,5%	1,5%	1,5%				
B762	0,2%	0,2%	0,2%	F900	0,1%	0,1%	0,1%				
B763	2,4%	2,5%	2,4%	FA10	0,0%	0,0%	0,0%				
B772	0,7%	0,8%	0,7%	FA50	0,1%	0,1%	0,1%				
B77L	0,2%	0,2%	0,2%	FA7X	0,1%	0,1%	0,1%				
B77W	0,1%	0,1%	0,1%	G150	0,0%	0,0%	0,0%				
B788	0,0%	0,0%	0,0%	GALX	0,0%	0,0%	0,0%				
BE20	0,1%	0,1%	0,1%	GL5T	0,0%	0,0%	0,0%				
BE30	0,0%	0,0%	0,0%	GLEX	0,1%	0,1%	0,1%				
BE40	0,0%	0,0%	0,0%	GLF4	0,1%	0,1%	0,1%				
BE9L	0,0%	0,0%	0,0%	GLF5	0,1%	0,1%	0,1%				
C130	0,0%	0,0%	0,0%	H25B	0,2%	0,2%	0,2%				
C25A	0,2%	0,2%	0,2%	J328	0,1%	0,1%	0,1%				
C25B	0,2%	0,1%	0,1%	JS32	0,1%	0,1%	0,1%				
C30J	0,0%	0,0%	0,0%	JS41	0,2%	0,2%	0,2%				
C441	0,0%	0,0%	0,0%	LJ35	0,1%	0,1%	0,1%				

## F. Matlab code

### a. Temperature model

```
function result=T(h) %K
T0=15+273.15;
alpha=1.98;
if h>36089 %ft
    result=216.69;
else
    result=T0-alpha*h/1000;
end
end
```

### b. Pressure model

```
function result=P(h) %Pa
P0=101325;
Pt=22615;
alpha=0.0065;
T0=288.15;
Tt=216.69;
g=9.81;
R=287.053;

h=h*0.3048; %m
ht=11000;

if h>11000
    result=Pt*exp(-g/R/Tt*(h-ht));
else
    result=P0*(1-alpha*h/T0)^(g/alpha/R);
end
end
```

### c. Density model

```
function result=rho(h) %kg/m^3
R=287.053;
result=P(h)/R/T(h);
end
```

### d. Profile for minimum climb time

```
b=34.1; %m
S=122.6; %m^2
AR=b^2/S;
mact=72000; %kg
W=mact*9.81; %N
CD0=0.026984;
k=0.035074; %CD2
Ctc1=158520;
Ctc2=45206;
Ctc3=0.11771*10^(-9);
h=0:100:50000; %feet
Fa=Ctc1*(1.-h/Ctc2+Ctc3.*h.^2); %N
M=0:0.01:1.5;
hmax=35396; %feet
mmax=83000; %kg
mmin=47800; %kg
ES=0.3; %Energy sharing factor
g=9.81;
```

```

Cf1=0.72987;
Cf2=1236.9;

Ps=zeros(length(h),length(M));
for i=1:length(h)
    for j=1:length(M)
        V=M(j)*a(h(i));
        Ps(i,j)=V*(Fa(i)/W-CD0*rho(h(i))*(V)^2*S/2/W-
W^2/S/rho(h(i))/(V)^2*k);
    end
end
Ps=Ps./0.3048.*60; %ft/min

[C,h]=contour(M,h,Ps,[0 1000 2000 3000 4000]);
clabel(C,h)
legend('Ps (ft/min)');

V=0:10:600; %m/s
V2=V./0.3048; %feet/s
he=5000:5000:50000; %feet
h=zeros(length(he),length(V));
for i=1:length(he)
    for j=1:length(V)
        h(i,j,1)=he(i)-V2(j)^2/2/(9.81/0.3048);
        h(i,j,2)=V(j)/a(h(i,j,1));
    end
end
hold on
for i=1:length(he)
    plot(h(i,:,2),h(i,:,1),'b')
end
axis([0 1.2 0 50000])
xlabel('Mach number (-)')
ylabel('Altitude (feet)')

Clmax=2.5;
Vs=sqrt(2*W/rho(0)/S/Clmax);

V2=1.13*Vs; %m/s
V2=V2*3.6/1.852; %kts
TX=[V2 V2+20 V2+20];
TY=[35 1700 3200];
n=length(TX);
Cred=0.15;
Cpred=1-Cred*(mmax-mact)/(mmax-mmin);
dt=1; %s

while TX(n)<250/sqrt(rho(TY(n))/1.225)
    h=TY(n); %ft
    V=TX(n)*1.852/3.6; %m/s
    Fa=Ctc1*(1-h/Ctc2+Ctc3*h^2);
    Ps=V*(Fa/W-CD0*rho(h)*(V)^2*S/2/W-W^2/S/rho(h)/(V)^2*k); %m/s
    dh=Ps/0.3048*ES*dt*Cpred; %ft
    h=h+dh;
    TY=[TY h];
    dV=Ps*(1-ES)*9.81*dt/V;
    V=(V+dV)/1.852*3.6;
    TX=[TX V];
    n=length(TX);
end

```

```

TX=[TX 250/sqrt(rho(10000)/1.225)];
TY=[TY 10000];
n=length(TX);

while TX(n)<362
    h=TY(n); %ft
    V=TX(n)*1.852/3.6; %m/s
    Fa=Ctc1*(1-h/Ctc2+Ctc3*h^2);
    Ps=V*(Fa/W-CD0*rho(h)*(V)^2*S/2/W-W*2/S/rho(h)/(V)^2*k); %m/s
    dh=Ps/0.3048*ES*dt*Cpred; %ft
    h=h+dh;
    TY=[TY h];
    dV=Ps*(1-ES)*9.81*dt/V;
    V=(V+dV)/1.852*3.6;
    TX=[TX V];
    n=length(TX);
end

for i=1:length(TX)
    TX(i)=(TX(i)*1.852/3.6)/a(TY(i));
end
TX=[TX 0.575 0.59 0.605 0.621 0.639 0.656 0.675 0.695 0.714 0.7375
0.76 0.784 0.78];
TY=[TY 11600 13900 16200 18470 20730 23000 25200 27450 29600 31720
33900 35900 36000];
plot(TX,TY,'k','LineWidth',2)

Wf=0;
x=0; %NM
t=0; %s
xplot=x;
Gamma=[];
Fuel=0;
for i=1:length(TX)-1
    h1=TY(i);
    h2=TY(i+1);
    dh=h2-h1; %ft
    h=(h1+h2)/2;
    V1=TX(i)*a(h1);
    V2=TX(i+1)*a(h2);
    dV=V2-V1; %m/s
    V=(V1+V2)/2;
    Cl=2*W/(rho(h)*(V)^2*S);
    Cd=CD0+k*Cl^2;
    Fa1=Ctc1*(1-h1/Ctc2+Ctc3*h1^2);
    Fa2=Ctc1*(1-h2/Ctc2+Ctc3*h2^2);
    Fa=(Fa1+Fa2)/2;
    gamma=atan((-Cd/Cl+Fa/(0.5*rho(h)*V^2*S*Cl))*1/(1+V/g*dV/dh));
    Gamma=[Gamma gamma];
    TSFC=Cf1*(1+V*3.6/1.852/Cf2); %kg/min/kN
    TSFC=TSFC/60000; %kg/s/N
    Ps1=V1*(Fa1/W-CD0*rho(h1)*V1^2*S/2/W-W*2/S/rho(h1)/V1^2*k); %m/s
    Ps2=V2*(Fa2/W-CD0*rho(h2)*V2^2*S/2/W-W*2/S/rho(h2)/V2^2*k); %m/s
    Psavg=0.5*(1/Ps1+1/Ps2)*0.3048; %s/ft
    TSFC1=Cf1*(1+V1*3.6/1.852/Cf2)/60/1000; %kg/s/N
    TSFC2=Cf1*(1+V2*3.6/1.852/Cf2)/60/1000; %kg/s/N
    fs1=Ps1/TSFC1/Fa1; %m/kg
    fs2=Ps2/TSFC2/Fa2; %m/kg
    fsavg=0.5*(1/fs1+1/fs2)*0.3048; %kg/ft
    he1=h1+(V1/0.3048)^2/2/9.81*0.3048; %ft

```

```

he2=h2+(V2/0.3048)^2/2/9.81*0.3048; %ft
Wf=Wf+fsavg*(he2-he1); %kg
dt=Psavg*(he2-he1); %s
t=t+dt;
dx=V*dt*cos(gamma); %m
x=x+dx; %m
xplot=[xplot x];
FF=TSFC*Fa; %kg/s
Fuel=Fuel+FF*dt; %kg
end
t
Wf
Fuel

figure
xplot=xplot/1852; %NM
plot(xplot,TY)
xlabel('Distance from the airport (NM)')
ylabel('Altitude (feet)')

```

### e. Profile for minimum climb fuel

```

b=34.1; %m
S=122.6; %m^2
AR=b^2/S;
mact=72000; %kg
W=mact*9.81; %N
CD0=0.026984;
k=0.035074; %CD2
Ctc1=158520;
Ctc2=45206;
Ctc3=0.11771*10^(-9);
Cf1=0.72987;
Cf2=1236.9;
h=0:100:50000; %feet
M=0:0.01:1.5;
hmax=35396; %feet
mmax=83000; %kg
mmin=47800; %kg
ES=0.3; %Energy sharing factor
g=9.81;

Ps=zeros(length(h),length(M));
Fa=zeros(length(h),length(M));
for i=1:length(h)
    for j=1:length(M)
        Fa(i,j)=Ctc1*(1.-h(i)/Ctc2+Ctc3.*h(i).^2); %N
        V=M(j)*a(h(i));
        Ps(i,j)=V*(Fa(i)/W-CD0*rho(h(i))*(V)^2*S/2/W-
W*2/S/rho(h(i))/(V)^2*k); %m/s
    end
end

TSFC=zeros(length(h),length(M));
for i=1:length(h)
    for j=1:length(M)
        V=M(j)*a(h(i))*3.6/1.852;
        TSFC(i,j)=Cf1*(1+V/Cf2); %kg/min/kN
    end
end

```

```

TSFC=TSFC/60/1000; %kg/s/N

fs=Ps./TSFC./Fa; %m/kg
fs=fs./0.3048; %ft/kg

[C,h]=contour(M,h,fs,[0 5 10 15 20 25 30]);
clabel(C,h)
legend('fs (ft/kg)');

V=0:10:600; %m/s
V2=V./0.3048; %feet/s
he=5000:5000:50000; %feet
h=zeros(length(he),length(V));
for i=1:length(he)
    for j=1:length(V)
        h(i,j,1)=he(i)-V2(j)^2/2/(9.81/0.3048);
        h(i,j,2)=V(j)/a(h(i,j,1));
    end
end
hold on
for i=1:length(he)
    plot(h(i,:,:2),h(i,:,:1),'b')
end
axis([0 1.2 0 50000])
xlabel('Mach number (-)')
ylabel('Altitude (feet)')

Clmax=2.5;
Vs=sqrt(2*W/rho(0)/S/Clmax);

V2=1.13*Vs; %m/s
V2=V2*3.6/1.852; %kts
TX=[V2 V2+20 V2+20];
TY=[35 1700 3200];

n=length(TX);
Cred=0.15;
Cpred=1-Cred*(mmax-mact)/(mmax-mmin);
dt=1; %s

while TX(n)<250/sqrt(rho(TY(n))/1.225)
    h=TY(n); %ft
    V=TX(n)*1.852/3.6; %m/s
    Fa=Ctc1*(1-h/Ctc2+Ctc3*h^2);
    Ps=V*(Fa/W-CD0*rho(h)*(V)^2*S/2/W-W*2/S/rho(h)/(V)^2*k); %m/s
    dh=Ps/0.3048*ES*dt*Cpred; %ft
    h=h+dh;
    TY=[TY h];
    dV=Ps*(1-ES)*9.81*dt/V;
    V=(V+dV)/1.852*3.6;
    TX=[TX V];
    n=length(TX);
end

TX=[TX 250/sqrt(rho(10000)/1.225)];
TY=[TY 10000];
n=length(TX);

while TX(n)<324
    h=TY(n); %ft

```

```

V=TX(n)*1.852/3.6; %m/s
Fa=Ctc1*(1-h/Ctc2+Ctc3*h^2);
Ps=V*(Fa/W-CD0*rho(h)*(V)^2*S/2/W-W*2/S/rho(h)/(V)^2*k); %m/s
dh=Ps/0.3048*ES*dt*Cpred; %ft
h=h+dh;
TY=[TY h];
dV=Ps*(1-ES)*9.81*dt/V;
V=(V+dV)/1.852*3.6;
TX=[TX V];
n=length(TX);
end

for i=1:length(TX)
    TX(i)=(TX(i)*1.852/3.6)/a(TY(i));
end
TrajectoryX=[TX 0.523 0.537 0.552 0.568 0.587 0.604 0.625 0.647 0.673
0.7 0.727 0.7475 0.78];
TrajectoryY=[TY 12670 14980 17280 19580 21850 24120 26300 28500 30560
32650 34700 36000 36000];
plot(TrajectoryX,TrajectoryY,'k','LineWidth',2)

Wf=0;
x=0; %NM
t=0; %s
xplot=x;
Gamma=[];
Fuel=0;
for i=1:length(TrajectoryX)-1
    h1=TrajectoryY(i);
    h2=TrajectoryY(i+1);
    dh=h2-h1; %ft
    h=(h1+h2)/2;
    M1=TrajectoryX(i);
    M2=TrajectoryX(i+1);
    V1=M1*a(h1);
    V2=M2*a(h2);
    dV=V2-V1; %m/s
    V=(V1+V2)/2;
    C1=2*W/(rho(h)*(V)^2*S);
    Cd=CD0+k*C1^2;
    Fa1=Ctc1*(1-h1/Ctc2+Ctc3*h1^2);
    Fa2=Ctc1*(1-h2/Ctc2+Ctc3*h2^2);
    Fa=(Fa1+Fa2)/2;
    gamma=atan((-Cd/C1+Fa/(0.5*rho(h)*V^2*S*C1))*1/(1+V/g*dV/dh));
    Gamma=[Gamma gamma];
    TSFC=Cf1*(1+V*3.6/1.852/Cf2); %kg/min/kN
    TSFC=TSFC/60000; %kg/s/N
    k1=round(TrajectoryY(i)/100)+1;
    k2=round(TrajectoryY(i+1)/100)+1;
    j1=round(TrajectoryX(i)*100)+1;
    j2=round(TrajectoryX(i+1)*100)+1;
    j1=int64(j1);
    j2=int64(j2);
    fs1=fs(k1,j1); %ft/kg
    fs2=fs(k2,j2);
    fsavg=0.5*(1/fs1+1/fs2);
    he1=h1+(V1/0.3048)^2/2/9.81*0.3048; %ft
    he2=h2+(V2/0.3048)^2/2/9.81*0.3048;
    Wf=Wf+fsavg*(he2-he1); %kg
    Ps1=V1*(Fa1/W-CD0*rho(h1)*V1^2*S/2/W-W*2/S/rho(h1)/V1^2*k); %m/s
    Ps2=V2*(Fa2/W-CD0*rho(h2)*V2^2*S/2/W-W*2/S/rho(h2)/V2^2*k);

```

```

Psavg=0.5*(1/Ps1+1/Ps2)*0.3048; %s/ft
dt=Psavg*(he2-he1); %s
t=t+dt;
dx=V*dt*cos(gamma); %m
x=x+dx; %m
xplot=[xplot x];
FF=TSFC*Fa; %kg/s
Fuel=Fuel+FF*dt; %kg
end
Wftotal=Wf
t
Fuel

figure
xplot=xplot/1852; %NM
plot(xplot,TrajectoryY)
xlabel('Distance from the airport (NM)')
ylabel('Altitude (feet)')

```

### f. Profile for minimum descent time

```

MinI=0.8; %MMO=0.82 --> MMO-0.02 max
hini=36000; %ft
Vini=340; %kIAS
Vini=Vini*1.852/3.6; % m/s IAS
hfinal=3000; %ft
Vapp=152*sqrt(1.225/rho(hfinal)); %kIAS
Vapp=Vapp*1.852/3.6; %m/s
g=9.81; %m/s^2
Ctc1=158520;
Ctc2=45206;
Ctc3=0.11771*10^(-9);
hpdes=29831; %ft
Ctdeshigh=0.13603;
Ctdeslow=0.10847;
Ctdesapp=0.15749;
m=64000; %kg
W=m*g; %N
dt=0.1; %s
S=122.6; %m^2
Cf3=14.159;
Cf4=68867;
Crossoveralt=22520; %ft
Crossx=[150 500];
Crossy=[Crossoveralt Crossoveralt];
Handoveralt=22000; %ft
Handoverdist=104; %NM
Cfcrr=0.96358;
Cf1=0.72987;
Cf2=1236.9;
CTcr=0.95;

h=hfinal;
V=Vapp;
M=Vapp/a(h);
x=0; %NM
t=0;
Wf=0;
Mplot=M;
hplot=h;
xplot=x;

```

```

Vplot=V;
Gamma=[];
ias=0;

while h<hini
    if (V*sqrt(rho(h)/1.225)<(250*1.852/3.6))&&(h<10000)
        ES=0.3;
    elseif (V*sqrt(rho(h)/1.225)<Vini)&&(h>10000)&&(h<Crossoveralt)
        ES=0.3;
    elseif (h>Crossoveralt)
        M=Mini;
        V=M*a(h);
        ES=(1+1.4*287*(-0.0065)/2/9.81*M^2)^(-1);
    else ES=(1+1.4*287*(-0.0065)/2/9.81*M^2+(1+0.2*M^2)^(-1/0.4)*((1+0.2*M^2)^(1.4/0.4)-1))^(-1);
        ias=1;
    end
    if (x>104*1852)&&(x<114*1852)
        ES=0;
    end
    if h>8000
        CD0=0.026984;
        k=0.035074; %CD2
    else CD0=0.047354;
        k=0.040818; %CD2
    end
    if h>hpdes
        K=Ctdeshigh;
    elseif h>8000
        K=Ctdeslow;
    else K=Ctdesapp;
    end
    Fa=Ctc1*(1-h/Ctc2+Ctc3*h^2)*K; %N
    Ps=V*(Fa/W-CD0*rho(h)*(V)^2*S/2/W-W^2/S/rho(h)/(V)^2*k); %m/s
    if ES==0
        dV=0;
    else dV=(1-ES)*Ps*g*dt/V;
    end
    Cl=2*W/(rho(h)*V^2*S);
    Cd=CD0+k*Cl^2;
    dz=ES*Ps*dt; %m
    if (h<Handoveralt)&&(ias==1)
        if h<10000
            gamma=-atan((10000-
h)/((10000/Handoveralt*Handoverdist*1852-x)/0.3048));
            else gamma=-atan((Handoveralt-h)/((Handoverdist*1852-
x)/0.3048));
        end
        dz=V*dt*sin(gamma);
        dV=(1-ES)*dz/dt/ES*g*dt/V;
    elseif ES==0
        gamma=0;
    else gamma=atan((-Cd/Cl+Fa/(0.5*rho(h)*V^2*S*Cl))*1/(1+V/g*dV/dz));
    end
    ias=0;
    dx=V*dt*cos(gamma); %m
    x=x+dx; %m
    xplot=[xplot x];
    V=V-dV;
    h=h-dz/0.3048; %ft
end

```

```

M=V/a(h);
t=t+dt
if (x>104*1852) && (x<114*1852)
    TSFC=Cf1*(1+V*3.6/1.852/Cf2); %kg/min/kN
    TSFC=TSFC/60/1000; %kg/s/N
    Fa=Ctc1*(1-h/Ctc2+Ctc3*h^2)*CTcr; %N
    FF=TSFC*Fa*Cfcr; %kg/s
    dWf=FF*dt;
else dWf=Cf3*(1-h/Cf4)/60*dt; %kg
end
Wf=Wf+dWf;
Mplot=[Mplot M];
hplot=[hplot h];
Vplot=[Vplot V];
Gamma=[Gamma gamma];
end

plot(Mplot,hplot)
xlabel('Mach number (-)')
ylabel('Altitude (feet)')
axis([0.2 0.85 0 40000])

figure
hold on
h=0:1000:40000;
TAS=150:25:500;
IAS=zeros(length(h),length(TAS));

for i=1:length(h)
    for j=1:length(TAS)
        IAS(i,j)=TAS(j)*sqrt(rho(h(i))/1.225);
    end
end

[C,h]=contour(TAS,h,IAS,150:50:350,'r');
clabel(C,h)

h=0:1000:40000;
TAS=150:25:500;
M=zeros(length(h),length(TAS));

for i=1:length(h)
    for j=1:length(TAS)
        M(i,j)=TAS(j)*1.852/3.6/a(h(i));
    end
end

[C,h]=contour(TAS,h,M,0.1:0.1:0.9,'b');
clabel(C,h)

Vplot=Vplot*3.6/1.852;
plot(Vplot,hplot,'g','LineWidth',2)
xlabel('True air speed (kts)')
ylabel('Altitude (feet)')
plot(Crossx,Crossy,'k')
legend('IAS (kts)', 'Mach (-)', 'Trajectory', 'Crossover altitude');

xplot=xplot/1852;
figure
plot(xplot,hplot)

```

```

xlabel('Distance from final approach fix (NM)')
ylabel('Altitude (feet)')

figure
Gamma=[Gamma 0];
plot(xplot, Gamma*180/pi)

t
Wf

sum=0;
for i=1:length(Gamma)
sum=sum+Gamma(i);
end
avgGamma=sum/length(Gamma)*180/pi

```

### **g. Profile for minimum descent fuel**

```

MinI=0.764; %MMO=0.82 --> MMO-0.02 max
hini=36000; %ft
Vini=250; %kIAS
Vini=Vini*1.852/3.6; % m/s IAS
hfinal=3000; %ft
Vapp=152*sqrt(1.225/rho(hfinal)); %kIAS
Vapp=Vapp*1.852/3.6; %m/s
g=9.81; %m/s^2
Ctc1=158520;
Ctc2=45206;
Ctc3=0.11771*10^(-9);
hpdes=29831; %ft
Ctdeshigh=0.13603;
Ctdeslow=0.10847;
Ctdesapp=0.15749;
m=64000; %kg
W=m*g; %N
dt=0.1; %s
S=122.6; %m^2
Cf3=14.159;
Cf4=68867;
Crossoveralt=34160; %ft
Crossx=[150 500];
Crossy=[Crossoveralt Crossoveralt];
Handoveralt=22000; %ft
Handoverdist=104; %NM
Cfcr=0.96358;
Cf1=0.72987;
Cf2=1236.9;
CTcr=0.95;

h=hfinal;
V=Vapp;
M=Vapp/a(h);
x=0; %NM
t=0;
Wf=0;
Mplot=M;
hplot=h;
xplot=x;
Vplot=V;
Gamma=[];

```

```

ias=0;

while h<hini
    if (V*sqrt(rho(h)/1.225)<(250*1.852/3.6)) && (h<10000)
        ES=0.3;
    elseif (V*sqrt(rho(h)/1.225)<Vini) && (h>10000) && (h<Crossoveralt)
        ES=0.3;
    elseif (h>Crossoveralt)
        M=Mini;
        V=M*a(h);
        ES=(1+1.4*287*(-0.0065)/2/9.81*M^2)^(-1);
    else ES=(1+1.4*287*(-0.0065)/2/9.81*M^2+(1+0.2*M^2)^(-1/0.4)*((1+0.2*M^2)^(1.4/0.4)-1))^(-1);
        ias=1;
    end
    if (x>104*1852) && (x<114*1852)
        ES=0;
    end
    if h>8000
        CD0=0.026984;
        k=0.035074; %CD2
    else CD0=0.047354;
        k=0.040818; %CD2
    end
    if h>hpdes
        K=Ctdeshigh;
    elseif h>8000
        K=Ctdeslow;
    else K=Ctdesapp;
    end
Fa=Ctc1*(1-h/Ctc2+Ctc3*h^2)*K; %N
Ps=V*(Fa/W-CD0*rho(h)*(V)^2*S/2/W-W^2/S/rho(h)/(V)^2*k); %m/s
if ES==0
    dV=0;
else dV=(1-ES)*Ps*g*dt/V;
end
Cl=2*W/(rho(h)*V^2*S);
Cd=CD0+k*Cl^2;
dz=ES*Ps*dt; %m
if (h<Handoveralt) && (ias==1)
    if h<10000
        gamma=-atan((10000-h)/((10000/Handoveralt*Handoverdist*1852-x)/0.3048));
    else gamma=-atan((Handoveralt-h)/((Handoverdist*1852-x)/0.3048));
    end
    dz=V*dt*sin(gamma);
    dV=(1-ES)*dz/dt/ES*g*dt/V;
elseif ES==0
    gamma=0;
else gamma=atan(-
Cd/Cl+Fa/(0.5*rho(h)*V^2*S*Cl))*1/(1+V/g*dV/dz));
    end
ias=0;
dx=V*dt*cos(gamma); %m
x=x+dx; %m
xplot=[xplot x];
V=V-dV;
h=h-dz/0.3048; %ft
M=V/a(h);
t=t+dt

```

```

if (x>104*1852) && (x<114*1852)
    TSFC=Cf1*(1+V*3.6/1.852/Cf2); %kg/min/kN
    TSFC=TSFC/60/1000; %kg/s/N
    Fa=Ctc1*(1-h/Ctc2+Ctc3*h^2)*CTcr; %N
    FF=TSFC*Fa*Cfcr; %kg/s
    dWf=FF*dt;
else dWf=Cf3*(1-h/Cf4)/60*dt; %kg
end
Wf=Wf+dWf;
Mplot=[Mplot M];
hplot=[hplot h];
Vplot=[Vplot V];
Gamma=[Gamma gamma];
end

plot(Mplot,hplot)
xlabel('Mach number (-)')
ylabel('Altitude (feet)')
axis([0.2 0.85 0 40000])

figure
hold on
h=0:1000:40000;
TAS=150:25:500;
IAS=zeros(length(h),length(TAS));

for i=1:length(h)
    for j=1:length(TAS)
        IAS(i,j)=TAS(j)*sqrt(rho(h(i))/1.225);
    end
end

[C,h]=contour(TAS,h,IAS,150:50:350,'r');
clabel(C,h)

h=0:1000:40000;
TAS=150:25:500;
M=zeros(length(h),length(TAS));

for i=1:length(h)
    for j=1:length(TAS)
        M(i,j)=TAS(j)*1.852/3.6/a(h(i));
    end
end

[C,h]=contour(TAS,h,M,0.1:0.1:0.9,'b');
clabel(C,h)

Vplot=Vplot*3.6/1.852;
plot(Vplot,hplot,'g','LineWidth',2)
xlabel('True air speed (kts)')
ylabel('Altitude (feet)')
plot(Crossx,Crossy,'k')
legend('IAS (kts)', 'Mach (-)', 'Trajectory', 'Crossover altitude');

xplot=xplot/1852;
figure
plot(xplot,hplot)
xlabel('Distance from final approach fix (NM)')
ylabel('Altitude (feet)')

```

```

figure
Gamma=[Gamma 0];
plot(xplot, Gamma*180/pi)

t
Wf

sum=0;
for i=1:length(Gamma)
sum=sum+Gamma(i);
end
avgGamma=sum/length(Gamma)*180/pi

h. Dynamic CDO simulation
%% Dynamic CDA for EBBU
%% Initialization of parameters

HorSep=5; %NM
VertSep=1000; %feet
WedgeSep=1.5; %NM
Radius=75; %NM
numRings=Radius/HorSep;
TopLevel=24000; %feet
numLevels=(TopLevel-3000)/1000+1; % FAF at 3000ft, 5NM
numWedge=zeros(numRings,1);
for i=1:numRings
    numWedge(i)=floor(2*pi*i*HorSep/WedgeSep);
end
numWedgemax=floor(2*pi*Radius/WedgeSep);

%% Grid in cartesian coordinates

Gridcart=zeros(numRings,numLevels,numWedgemax,3);
for i=1:numRings
    for j=1:numLevels
        for k=1:numWedge(i)
            theta=2*pi/numWedge(i);
            Gridcart(i,j,k,1)=i*HorSep*cos((k-1)*theta); %NM
            Gridcart(i,j,k,2)=i*HorSep*sin((k-1)*theta); %NM
            if i==1
                Gridcart(i,1,k,3)=3000; %ft
            else
                Gridcart(i,j,k,3)=(j-1)*VertSep+3000; %ft
            end
        end
    end
end

%% Availability Matrix
Av=Availability(numRings,numLevels,numWedgemax,Gridcart);

%% Determining the possible transitions
Path='C:\Users\Sam\Dropbox\Thesis\Matlab\Links\' ;
[num, txt]=xlsread('Aircraftlist.xlsx');
nbracft=max(num(:,1)); % Number of aircraft
for j=1:nbracft
    Type(j,:)=sprintf('%s',char(txt(j+1,3))); % Types of aircraft
end
Starttime=num(1:nbracft,4);

```

```

Origin=[4.4844444 50.9013889 184*0.3048]; % Aerodrome Reference Point
[degN degE m]
Pos=[num(1:nbracft,5) num(1:nbracft,6) num(1:nbracft,7)]; % Initial
position [degE degN ft]
Pos(:,1)=(Pos(:,1)-Origin(1))*38; % NM
Pos(:,2)=(Pos(:,2)-Origin(2))*60; % NM
CI=num(:,8);
Landed=0; % Number of aircraft that have reached the FAF
t=2;
Arracft=1; % Number of the first aircraft outside the 75 NM radius
Trajectories=zeros(3,numRings,nbracft); % Trajectories of the
aircraft
Trialtraj=zeros(3,numRings);
Landingtime=zeros(nbracft);
Timematrix=zeros(nbracft,15);
Fuelmatrix=zeros(nbracft,15);

while Landed<nbracft
    % Calculation of the best trajectory when an aircraft arrives
    if Starttime(Arracft)==t
        Cost=1*10^30;
        Acft=Type(Arracft,:);
        Costindex=CI(Arracft);
        % Determination of the closest waypoint to the aircraft on
        the edge of the airspace
        dist1=1000; %NM
        for i=1:numWedgemax
            x1=Gridcart(numRings,numLevels,i,1);
            y1=Gridcart(numRings,numLevels,i,2);
            h1=Gridcart(numRings,numLevels,i,3);
            if Av(numRings,numLevels,i)<t
                dist2=sqrt((x1-Pos(Arracft,1))^2+(y1-
                Pos(Arracft,2))^2+((h1-Pos(Arracft,3))*0.3048/1852)^2); %NM
                if dist2<dist1
                    IP=[numRings numLevels i 0 0]; %Initial Point
                    dist1=dist2;
                end
            end
        end
    end

    Links=load(sprintf('%s%s%s%s',Path,Acft,'\', 'Links'));

```

```

links1=Links.links{IP(1),IP(2),IP(3)};
for a=1:size(links1,1)
Time=links1(a,4)/60;
if Av(links1(a,1),links1(a,2),links1(a,3))<t
Fuel=links1(a,5);
Trialcost=Time*CI(Arracft)+Fuel; %kg
if Trialcost<Cost
links2=Links.links{links1(a,1),links1(a,2),links1(a,3)};
for b=1:size(links2,1)
Time=(links1(a,4)+links2(b,4))/60;
if Av(links2(b,1),links2(b,2),links2(b,3))<t+60*Time
Fuel=links1(a,5)+links2(b,5);
Trialcost=Time*CI(Arracft)+Fuel; %kg
if Trialcost<Cost
links3=Links.links{links2(b,1),links2(b,2),links2(b,3)};
for c=1:size(links3,1)
Index=[a b c]
Time=(links1(a,4)+links2(b,4)+links3(c,4))/60;
if Av(links3(c,1),links3(c,2),links3(c,3))<t+60*Time
Fuel=links1(a,5)+links2(b,5)+links3(c,5);
Trialcost=Time*CI(Arracft)+Fuel; %kg
if Trialcost<Cost
links4=Links.links{links3(c,1),links3(c,2),links3(c,3)};
for d=1:size(links4,1)
Time=(links1(a,4)+links2(b,4)+links3(c,4)+links4(d,4))/60;
if Av(links4(d,1),links4(d,2),links4(d,3))<t+60*Time
Fuel=links1(a,5)+links2(b,5)+links3(c,5)+links4(d,5);
Trialcost=Time*CI(Arracft)+Fuel; %kg
if Trialcost<Cost
links5=Links.links{links4(d,1),links4(d,2),links4(d,3)};
for e=1:size(links5,1)
Time=(links1(a,4)+links2(b,4)+links3(c,4)+links4(d,4)+links5(e,4))/60;
if Av(links5(e,1),links5(e,2),links5(e,3))<t+60*Time
Fuel=links1(a,5)+links2(b,5)+links3(c,5)+links4(d,5)+links5(e,5);
Trialcost=Time*CI(Arracft)+Fuel; %kg
if Trialcost<Cost
links6=Links.links{links5(e,1),links5(e,2),links5(e,3)};
for f=1:size(links6,1)

```

```

Time=(links1(a,4)+links2(b,4)+links3(c,4)+links4(d,4)+links5(e,4)+links6(f,4))/60;
if Av(links6(f,1),links6(f,2),links6(f,3))<t+60*Time
Fuel=links1(a,5)+links2(b,5)+links3(c,5)+links4(d,5)+links5(e,5)+links6(f,5);
Trialcost=Time*CI(Arracft)+Fuel; %kg
if Trialcost<Cost
links7=Links.links{links6(f,1),links6(f,2),links6(f,3)};
for g=1:size(links7,1)
Time=(links1(a,4)+links2(b,4)+links3(c,4)+links4(d,4)+links5(e,4)+links6(f,4)+links7(g,4))/60;
if Av(links7(g,1),links7(g,2),links7(g,3))<t+60*Time
Fuel=links1(a,5)+links2(b,5)+links3(c,5)+links4(d,5)+links5(e,5)+links6(f,5)+links7(g,5);
Trialcost=Time*CI(Arracft)+Fuel; %kg
if Trialcost<Cost
links8=Links.links{links7(g,1),links7(g,2),links7(g,3)};
for h=1:size(links8,1)
Time=(links1(a,4)+links2(b,4)+links3(c,4)+links4(d,4)+links5(e,4)+links6(f,4)+links7(g,4)+links8(h,4))/60;
if Av(links8(h,1),links8(h,2),links8(h,3))<t+60*Time
Fuel=links1(a,5)+links2(b,5)+links3(c,5)+links4(d,5)+links5(e,5)+links6(f,5)+links7(g,5)+links8(h,5);
Trialcost=Time*CI(Arracft)+Fuel; %kg
if Trialcost<Cost
links9=Links.links{links8(h,1),links8(h,2),links8(h,3)};
for i=1:size(links9,1)
Time=(links1(a,4)+links2(b,4)+links3(c,4)+links4(d,4)+links5(e,4)+links6(f,4)+links7(g,4)+links8(h,4)+links9(i,4))/60;
if Av(links9(i,1),links9(i,2),links9(i,3))<t+60*Time
Fuel=links1(a,5)+links2(b,5)+links3(c,5)+links4(d,5)+links5(e,5)+links6(f,5)+links7(g,5)+links8(h,5)+links9(i,5);
Trialcost=Time*CI(Arracft)+Fuel; %kg
if Trialcost<Cost
links10=Links.links{links9(i,1),links9(i,2),links9(i,3)};
for j=1:size(links10,1)
Time=(links1(a,4)+links2(b,4)+links3(c,4)+links4(d,4)+links5(e,4)+links6(f,4)+links7(g,4)+links8(h,4)+links9(i,4)+links10(j,4))/60;
if Av(links10(j,1),links10(j,2),links10(j,3))<t+60*Time
Fuel=links1(a,5)+links2(b,5)+links3(c,5)+links4(d,5)+links5(e,5)+links6(f,5)+links7(g,5)+links8(h,5)+links9(i,5)+links10(j,5);
Trialcost=Time*CI(Arracft)+Fuel; %kg
if Trialcost<Cost
links11=Links.links{links10(j,1),links10(j,2),links10(j,3)};

```

```

for k=1:size(links11,1)
Time=(links1(a,4)+links2(b,4)+links3(c,4)+links4(d,4)+links5(e,4)+links6(f,4) +
links7(g,4)+links8(h,4)+links9(i,4)+links10(j,4)+links11(k,4))/60;
if Av(links11(k,1),links11(k,2),links11(k,3))<t+60*Time
Fuel=links1(a,5)+links2(b,5)+links3(c,5)+links4(d,5)+links5(e,5)+links6(f,5) +
links7(g,5)+links8(h,5)+links9(i,5)+links10(j,5)+links11(k,5);
Trialcost=Time*CI(Arracft)+Fuel; %kg
if Trialcost<Cost
links12=Links.links{links11(k,1),links11(k,2),links11(k,3)};
for l=1:size(links12,1)
Time=(links1(a,4)+links2(b,4)+links3(c,4)+links4(d,4)+links5(e,4)+links6(f,4) +
links7(g,4)+links8(h,4)+links9(i,4)+links10(j,4)+links11(k,4)+links12(l,4))/60;
if Av(links12(l,1),links12(l,2),links12(l,3))<t+60*Time
Fuel=links1(a,5)+links2(b,5)+links3(c,5)+links4(d,5)+links5(e,5)+links6(f,5) +
links7(g,5)+links8(h,5)+links9(i,5)+links10(j,5)+links11(k,5)+links12(l,5);
Trialcost=Time*CI(Arracft)+Fuel; %kg
if Trialcost<Cost
links13=Links.links{links12(l,1),links12(l,2),links12(l,3)};
for m=1:size(links13,1)
Time=(links1(a,4)+links2(b,4)+links3(c,4)+links4(d,4)+links5(e,4)+links6(f,4) +
links7(g,4)+links8(h,4)+links9(i,4)+links10(j,4)+links11(k,4)+links12(l,4) +
links13(m,4))/60;
if Av(links13(m,1),links13(m,2),links13(m,3))<t+60*Time
Fuel=links1(a,5)+links2(b,5)+links3(c,5)+links4(d,5)+links5(e,5)+links6(f,5) +
links7(g,5)+links8(h,5)+links9(i,5)+links10(j,5)+links11(k,5)+links12(l,5)+links13(m,5);
Trialcost=Time*CI(Arracft)+Fuel; %kg
if Trialcost<Cost
links14=Links.links{links13(m,1),links13(m,2),links13(m,3)};
for n=1:size(links14,1)
Time=(links1(a,4)+links2(b,4)+links3(c,4)+links4(d,4)+links5(e,4)+links6(f,4) +
links7(g,4)+links8(h,4)+links9(i,4)+links10(j,4)+links11(k,4)+links12(l,4) +
links13(m,4)+links14(n,4))/60; %min
if Av(links14(n,1),links14(n,2),links14(n,3))<t+60*Time
Fuel=links1(a,5)+links2(b,5)+links3(c,5)+links4(d,5)+links5(e,5)+links6(f,5) +
links7(g,5)+links8(h,5)+links9(i,5)+links10(j,5)+links11(k,5)+links12(l,5) +
links13(m,5)+links14(n,5); %kg
Trialcost=Time*CI(Arracft)+Fuel; %kg
if Trialcost<Cost
Trialtraj=[IP(1) links1(a,1) links2(b,1) links3(c,1) links4(d,1) links5(e,1) +
links6(f,1) links7(g,1) links8(h,1) links9(i,1) links10(j,1) links11(k,1)

```

```

links12(l,1) links13(m,1) links14(n,1);
IP(2) links1(a,2) links2(b,2) links3(c,2) links4(d,2) links5(e,2)
links6(f,2) links7(g,2) links8(h,2) links9(i,2) links10(j,2) links11(k,2)
links12(l,2) links13(m,2) links14(n,2);
IP(3) links1(a,3) links2(b,3) links3(c,3) links4(d,3) links5(e,3)
links6(f,3) links7(g,3) links8(h,3) links9(i,3) links10(j,3) links11(k,3)
links12(l,3) links13(m,3) links14(n,3)];
Cost=Trialcost;
Fuelcost=Fuel; %kg
Timecost=Time; %min
Timematrix(Arracft,:)=[0 links1(a,4) links2(b,4) links3(c,4) links4(d,4) links5(e,4)
links6(f,4) links7(g,4) links8(h,4) links9(i,4) links10(j,4) links11(k,4)
links12(l,4) links13(m,4) links14(n,4)];
Fuelmatrix(Arracft,:)=[0 links1(a,5) links2(b,5) links3(c,5) links4(d,5) links5(e,5)
links6(f,5) links7(g,5) links8(h,5) links9(i,5) links10(j,5) links11(k,5)
links12(l,5) links13(m,5) links14(n,5)];
end
end
end
clear('links14')
end
end
end
end
clear('links13')
end
end
end
end
clear('links12')
end
end
end
end
clear('links11')
end
end
end
end
clear('links10')
end
end
end
end
clear('links9')

```

```

        end
        end
    end
    clear('links8')
end
end
end
end
clear('links7')
end
end
end
end
clear('links6')
end
end
end
end
clear('links5')
end
end
end
end
clear('links4')
end
end
end
end
clear('links3')
end
end
end
end
clear('links2')
end
end
end
save(sprintf('%s%s', Path, 'Trialtrajectory'), 'Trialtraj');
end
clear('links1')

if exist('Trialtraj', 'var')
    Trajectories(:,:,:Arracft)=Trialtraj;
end

```

```

for m=1:length(Trialtraj)
    Blockingtime=sum(Timematrix(Arracft,1:m)); %s
    Av(Trialtraj(1,m),Trialtraj(2,m),Trialtraj(3,m))=Av(Trialtraj(1,m),Trialtraj(2,m),Trialtraj(3,m))+
    Blockingtime;
end
Av(Trialtraj(1,m),Trialtraj(2,m),Trialtraj(3,m))=Av(Trialtraj(1,m),Trialtraj(2,m),Trialtraj(3,m))+120;

Landingtime(Arracft)=t+sum(Timematrix(Arracft,:));
save(sprintf('%s%s%g%s%s',Path,'Optimal_trajectories_',Landed+1,'_',Acft),'Trajectories');
save(sprintf('%s%s%g%s%s',Path,'Fuel_burn',Landed+1,'_',Acft),'Fuelmatrix');
save(sprintf('%s%s%g%s%s',Path,'Descent_time',Landed+1,'_',Acft),'Timematrix');
save(sprintf('%s%s%g%s%s',Path,'Av_',Landed+1,'_',Acft),'Av');

Arracft=Arracft+1;
Landed=Landed+1;
end
t=t+1;
end

```